„Dunărea de Jos" University of Galaţi
Doctoral school of engineering

ABSTRACT OF DOCTORAL THESIS

RESEARCHES ON THE DESIGN AND GENERATION OF NON-CIRCULAR GEARS, WITH APPLICABILITY IN METALLURGICAL INDUSTRY

PhD student:

Eng. Niculescu Mircea

Scientific coordinator:

PhD. Prof. Eng. Andrei Laurenția

GALAŢI

2017

FOREWARD

The present papers offers modern and original solutions for solving practical problems within the metallurgical industry, namely in the field of wire products and hot rolling mill, where the author carries out his professional activity. Challenged by the current trend to substitute complex classical mechanisms and even the expensive electric motors with non-circular gears, the author proposes the introduction of these gears into the kinematics of machinery mechanisms in order to obtain variable movements and to improve the performance of the analyzed processes.

The research, based on multidisciplinary knowledge (machine parts, mechanisms, surface generation, informatics, graphic and computer-aided design) and on a solid practical experience in industry, is a significant contribution in the field of non-circular gearing, completing the current stage and generating new perspectives, with applications in various fields.

The research, carried out at the Faculty of Engineering of the "Dunărea de Jos" University from Galati, supporting the applications of SC LAMINORUL SA Braila, uses original variation laws of the non-circular gears transmission ratio, specific to the analyzed applications and develops own codes and approaches in the design and analytical generation of non-circular gears.

The author expresses his gratitude to the scientific leader of the papers, Professor Laurenţia Andrei, for his urge, to complete his practical experience with the research on the application of non-circular gears in the metallurgical industry and for the constant support given throughout the research.

Also, thanks are given to the members of the doctoral committee, to Professor Minodora Rîpă, Professor Viorel Păunoiu and Professor Nicolae Diaconu, for the given suggestions and for the constructive observations that contributed to the completion of the study.

Last but not least, the author expresses his gratitude and thanks to the family and to the ones closest to him, for the trust, understanding and support they have shown.

Galaţi, september 2017 Mircea Niculescu

CONTENTS
OF DOCTORAL THESIS

	Abstarct page	Thesis page
Key words; Introduction	1	-
Figures list	-	1
Tables list	-	7
1. THE CURRENT STATE OF RESEARCH IN THE FIELD.....	5	8
1.1. Introduction.....	5	8
1.2. Hypotheses and strategies for modeling non-circular centrodes	7	12
1.3. Hypotheses and methods for generating the teeth of non-circular gears	10	16
1.4. Industrial application of the non-circular gears.....	11	20
1.4.1. Modification of the crank-slider mechanism kinematics.....	11	20
1.4.2. Control of closing and adjustment elements	12	25
1.4.3. Optimizing of the resistant moments for the driving mechanisms	14	28
1.4.4. Mechanisms with intermittent movement.....	15	30
1.4.5. Various applications.....	-	36
1.5. Conclusions.....	16	36
2. DESIGNING AND GENERATION OF THE NON-CIRCULAR GEARS FOR THE MODIFICATION OF THE NAILS MACHINE KINEMATICS.....	17	37
2.1. Introduction.....	17	37
2.2. Modified kinematics of the nails machine.....	17	38
2.2.1. Analysis of the nails machine kinematics ……..	17	38
2.2.2. Modification of the crank-slider mechanism kinematics……	18	39
2.2.3. Comparative analysis of the slider kinematics ……	28	55
2.3. Non-circular gear for modifing the nails machine kinematics	29	56
2.3.1. Modeling of the non-circular centrodes.....	29	56
2.3.2. Generation of the non-circular gear teeth.....	30	58
2.3.3. Meshing analysis.....	32	64
2.4. Conclusions.....	41	83

3. DESIGNING AND GENERATION OF THE NON-CIRCULAR GEARS FOR THE MODIFICATION OF THE BILLETS HEATING FURNACE UNLOADING DOORS KINEMATICS 43 85

3.1. Introduction..... 43 85

3.2. Modified kinematics of the furnace doors driving mechanism..... 43 85

3.2.1. Analysis of the door driving mechanism kinematics 43 85

3.2.2. Modification of the door driving mechanism kinematics..... 44 88

3.2.3. Comparative analysis of the door kinematics..... 48 96

3.3. Non-circular gear for modifing the unloading doors kinematics 49 97

3.3.1. Modeling of the non-circular centrodes 49 97

3.3.2. Generation of the non-circular gear teeth 50 97

3.3.3. Meshing analysis 51 103

3.4. Conclusions..... 56 118

4. CONCLUSIONS AND PERSONAL CONTRIBUTIONS..... 58 120

4.1. Conclusions 58 120

4.2. Personal contributions..... 60 123

4.3. Perspectives for development..... 61 124

LIST OF PUBLISHED PAPERS 62 125

REFERENCES..... 63 126

ANNEXES ..... - 130

Annex 1. Generation of the non-circular gear centrodes, used for the nails machine ..... - 130

Annex 2. Generation of the non-circular gear teeth active flanks, used for the nails machine ..... - 135

Annex 3. Generation of the non-circular gear centrodes, used for the billets heating furnace unloading doors ..... - 147

Annex 4. Generation of the non-circular gear teeth active flanks, used for the billets heating furnace unloading doors ..... - 152

Annex 5. Graphs generation for the function of defining the transmission ratio, the driven wheel rotation angle and the crank-slider mechanism displacement .. - 158

KEY WORDS

Non-circular gears, non-circular centrodes, variable transmission ratio, multispeed gears, transmission ratio with trigonometric/polynomial variation, defining parameters of the transmission ratio, static contact between teeth, stress and strain distribution, modified kinematics of crank-slider mechanism, multiparameters hybrid function, divided working cycle.

INTRODUCTION

Due to the flexibility and to the offered advantges, the non-circular gears are an alternative to the classical mechanisms. The complexity of their kinematics and geometry, which limited the implementation of the designing standardized algorithms, along with certain technological limitations in the past, these non-circular gears were ocassionally used in industry, so far. The development of the simulation and modeling softwares and of the new processing technologies, enabled new aproaches to the non-circular gears designing and generation.

This paper presents two new applications of the non-circular gears, intended for metallurgical equipment. The applications advanced herewith contribute to the current state of the research in this field and at the same time, provide new perspectives for further developing the applicability of the non-circular gears.

THESIS OBJECTIVES

The research theme is the applicability of the non-circular gears, in two cases from the metallurgical industry domain, as follows:

i) inserting of a non-circular gears in the kinematics of a nails machine, in order to modify the crank-slider mechanism kinematics. The purpose of modifying the kinematics, is to improve the cold plastic deformation process, that take place during the nail head forming phase;

ii) inserting of a non-circular gears in the kinematics of the billets heating furnace unloading door driving mechanism, within the hot rolling mill line of the steel profiles. The purpose of modifying kinematics in this case is to increase the angular velocity of the unloading door, as long as the door does not seal, and to reduce heat loss while the door is open.

The designing of the two gears, consist of an own analytical route, proper to each application, considering the general recommendations from the literature. As a result, the first objective of the thesis is the **preliminary study of the research in the field,** focused on the designing hypotheses of the non-circular centrodes and on the teeth generation solutions, highlighting, the applications developed by the researchers from different approaches.

Making a synthesis of the known theoretical concepts, in order to solve the proposed applications, a similar theoretical study, with different starting dates, is pursued, to meet the following objectives:

- **adopting the variation laws of the non-circular gear transmission ratio, that lead to the desired variable kinematics**. Generally, the transmission ratio is considered a multiparameter function with multiple definition laws, corresponding to the phases of the work cycle. The analytical and geometric conditions regarding the existence of a positive, continuous, derivable and periodic transmission ratio, and of closed centrodes, allow the determination of the defining parameters of the transmission ratio, specific to each variation law and the study of their influence on kinematics; at the end of the analysis, it is possible to choose the appropriate

values of the parameters defining the transmission ratio, which correspond to the desired kinematics for each application. The analytical study was based on AutoLISP codes and graphical representations in AutoCAD.

- **generating the mated non-circular centrodes**, for each gear chosen to meet the kinematic and technological requirements of the applications concerned. The centrodes generation is based on the defined transmission ratio and the known distance between the axis of the wheels, and follows the rolling principle. Graphic representations and geometric investigation, were based on the features of AutoCAD application;
- **generation of non-circular gears tooth flanks and of the solid models,** using an analytical method that simulates the rolling of the standard generating rack, along the centrode, coordinate transformations and editations in AutoCAD graphics;
- **the analysis of meshing quality,** the analysis of the contact between the teeth and the analysis of the tensions and deformations state at the contact between the teeth, respectivelly, validate numerical choices/options and the correct development of the non-circular gears design algorithm. Teeth contact is analyzed, in static conditions, in AutoCAD environment, by "manual" rolling and dimensional investigations; the stress and deformation state is analyzed in AutoDesk Inventor, using the finite element method (FEM), both in static and dynamic conditions.

The research was carried out at the Faculty of Engineering at "Dunarea de Jos" University of Galati and at SC LAMINORUL SA in Braila, a metallurgical company, which produces hot-rolled steel profiles, where the research results can be actually implemented for the proposed applications.

THESIS STRUCTURE

Thesis is structured into four chapters, as follows:
i) the current state of research, with emphasis on industrial applications of non-circular gears; ii) designing and generating of the non-circular gears in order to modify the kinematics of the nails machine; iii) designing and generating of the non-circular gears in order to modify the kinematics of the billets heating furnace discharging door; (iv) conclusions and personal contributions.

Chapter 1 reviews the research published so far on the centrodes generation hypotheses and on the methods of non-circular gears teeth generation, as aproached by various researchers**.** The focus is on significant applications, published in specialized journals or patents, based on non-circular gears. The applications are grouped by destination and drive elements, resulting a diverse and efficient utility range of non-circular gears.

Chapter 2 presents the research on the kinematics modification of a crank-slider mechanism of a classic nails machine, using a non-circular gear, in order to improve the cold plastic deformation process, during the nail head forming phase. The kinematic modification aims to decrease the initial deformation velocity and to increase the time interval the deforming force is applied to.

Based on previous researches in the field, and considering the application requirements, several multiparameter functions are proposed for defining the transmission ratio, with cosine and polynomial variation laws, respectively, dividing the working cycle into two or three phases respectively. Following the above steps, the significant parameters that influence the kinematic of the crank-slider mechanism (the angles of delimitation of the working phases and the maximum and minimum values of the transmission ratio) are determined and their influence on the kinematics is studied. The analysis establishes that the cosine variation law of the

transmission ratio, with a working cycle in two or three phases, is the most appropriate and the desired values for the defining parameters are chosen.
Based on the fundamental principle of rolling and on an analytical method of determining the current points from the centrodes, the centrodes of the two gears, using original AutoLISP codes in the AutoCAD environment, are modeled.

The generation of the non-circular gears teeth flanks is based on the simulation of the tooth processing, with a single tooth of a standard rack, of a 20^0 pressure angle, following the positioning of the teeth under a constant curvature step.

The flank geometry is determined by an original analytical method, that follows the generation movements transferred to the rack and captures the point from the flank, located on the current meshing line. The non-circular gear teeth flanks, are automatically generated using AutoLISP original codes in the AutoCAD environment.

The performance of the non-circular gears meshing is evaluated by analyzing the static contact between the teeth and the stress and deformation states at the contact between the teeth considered critical, situated in the transition areas between the phases of the working cycle and on the areas where the dividing curves change their geometry.
The static contact spot and its distribution were highlighted using the AutoCAD application, based on an algorithm that makes use of the controlled initial interference in the areas adjacent to the transition teeth, performing the incremental "manual" rolling, and the listing of the data, automatically measured by the application. The analysis of the static contact spot results in a corresponding evolution of the contact spot, not interfering with the inactive flanks.

The state of stresses and deformations is analyzed in INVENTOR using the Finite Element Method (FEM), both in static and dynamic conditions. The analysis is performed at the same critical teeth. The study highlights the fact that the equivalent stresses fall within the permissible limits, with coverage safety coefficients, and that the kinematics of the non-circular gear complies with the initial conditions imposed.

Chapter 3 presents the research on the kinematics modification of the billets heating furnace unloading door by using a non-circular gear. The purpose of modifying kinematics is to reduce heat loss while the unloading door is opened by increasing the angular speed of the door.

In order to modify the door kinematics, it is proposed to insert a non-circular gear in the kinematical chain of the door driving mechanism, which divides the working cycle into two or three phases, that are carried out at different, variable speeds. The non-circular gear is designed based on an original transmission ratio, defined as a hybrid function: constant for small time, at the door opening and closing, and variable, according to a cosine law, for the rest of the cycle. The research goes through the same steps as the first application. As defining parameters that influence the variation of the transmission ratio, are chosen the angles of the driving gear that divide the working phases, and the maximum value of the transmission ratio. Studying the influence of these parameters on the door kinematics, it is concluded that, this is significantly influenced by the difference, between the working phases dividing angles.

The generation of centrodes and of the non-circular gears teeth flanks is based on the same principles and methods used in the first application, in two cases of the difference of the work phases delimitation angle, and for the three-phase working cycle considered more advantageous. The centrodes are open curves, taking account that, the rotation angle of the gears during the opening and closing of the doors is less than 360^0. Solid models generated in AutoCAD and imported into Inventor allow the analysis of the stress and deformation state at the teeth contact, by Finite Element Method (FEM). The analysis of three teeth, located in the area of the centrode, where the ray increases, in the second working phase, both static and

dynamic, in both cases, highlights that the equivalent stresses fall within the permissible limits, with coverings safety coefficients. At the same time, following the distribution of the contact patch, in these cases, a good quality meshing is obtained.

Chapter 4 presents the conclusions on the entire research work and highlights the personal contributions to the non-circular gears generation, based on the two applications approached.

The appendixes present the original AutoLISP codes created to generate the centrodes of non-circular gears and to generate their teeth.

CHAPTER 1

THE CURRENT STATE OF RESEARCHES IN THE FIELDS

1.1. INTRODUCTION

1.1.1. Brief history

The non-circular gears appeared since the 15th century. The first document, that marks the begining of the non-circular gears, was the sketch collection of Leonardo da Vinci named „Codex Madrid" [1] (Fig. 1.1.a, b). Here, is also mentioned the new idea of a wheel with non-circular outline and with self-intersecting centrode (Fig. 1.1c).

a) b) c)

Fig. 1.1. Non-circular gears sketched by Leonardo da Vinci [1]

The first prototypes of non-circular gears was used for the following application: clocks, musical instruments, automatic tools, machines for making keys, Geneva mechanisms and pumps [1].

Because they were not developed concrete methods to generate non-circular gears, researchers like Burmester [2], Glober [3] or Boyd [4], has focused on the possibilities of generating non-circular gears. At the same time, manufacturers have developed various methods for machining non-circular gears. Thus, in 1924, Fellows company, approached the processing of non-circular gears, by means of a stencil gear that meshes with a stencil rack (Fig. 1.2) [5].

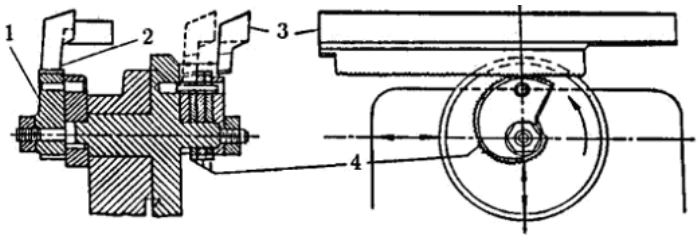

Fig. 1.2. Generation of a non-circular gear by rack [5]
1 – stencil gear; 2 – stencil rack; 3 – cutting tool; 4 – the wheel for machining

Bopp & Reuther in 1938 [6], starts from the meshing simulation of the non-circular worm gear with the mate worm, identical with worm mill (Fig. 1.3). Variable distance between the worm gear and worm is simulated using a cam mechanism. The disadvantage of both methods consists of fact that it had to made the stencil gear.

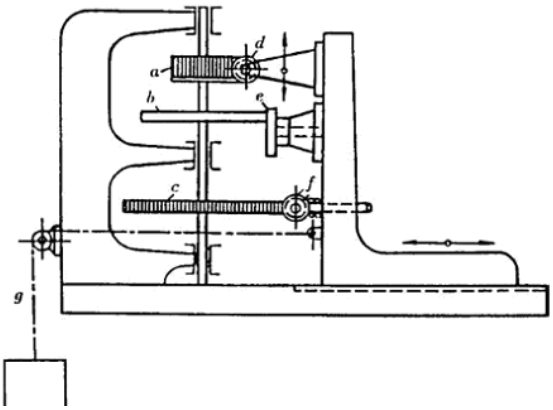

Fig. 1.3. Generation of a non-circular gear, by milling [6] a – gear to be generated; b – cam; c – stencil worm gear; d – worm mill; e – follower; f - worm

Revolutionizing of the non-circular gears generation, was carried out by Litvin, between 1949 - 1956, who approaches the flanks generation, as an envelope of surfaces family of the tool (rack cutter, worm mill or wheel cutter) [7], [8], [9].

The used method is shown in Fig. 1.4. and is based on the following principles: *i)* the non-circular gears are generated with the same tools used for circular gears, *ii)* the non-circular gears profiles are generated by rolling of the tool centrode, over the conjugate centrode of the gear and *iii)* the rolling is carried out in the same way as in the cutting process.

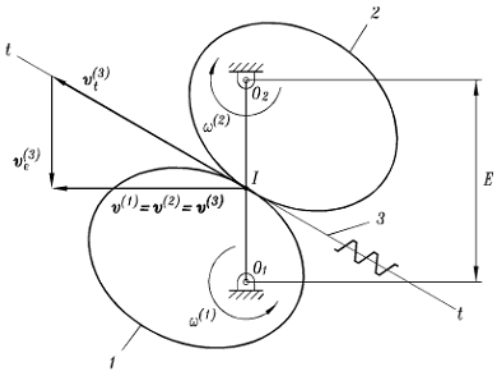

Fig. 1.4. Kinematics of the non-circular gears generation, with rack. [8]

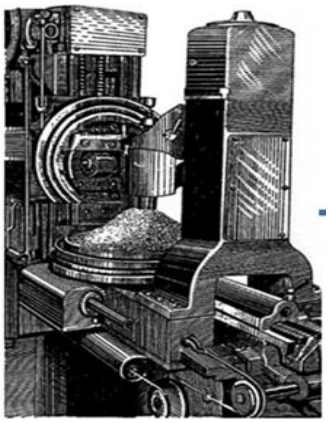

Fig. 1.5. Modified milling machine, for non-circular gear processing (1951) [8]

1.1.2. Overview. Benefits

Use of non-circular gears is justified and recommended by the following advantages:

- stability, rigidity and compact structure compared with cam mechanisms or transmission with belts or chain;
- high permissivity for motion variation, after given laws, compared to other mechanisms;
- high flexibility of the function for motion transmission/variation;
- cyclic, continuous, one-way motion, in comparison with the limited nature of the rectilinear, come-and-go motion of the cams;
- smooth crossing between motion and stationary phases, even at high speeds of lead elements;
- the outstanding dynamic performance, due to the constructive simplicity of mechanisms and reduced items, etc.

1.1.3. Non-circular gears types

Considering the main feature of the non-circular gear, i.e. the speed variation of the driven gear, it can be found the following types of non-circular gears:

- **Multispeed non-circular gears** (Fig. 1.6), where the driven gear has different speeds, constant on certain rotation angles of gear.

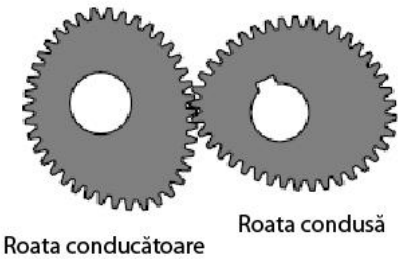

Fig. 1.6. Multisped non-circular gear, with two speed steps[10]

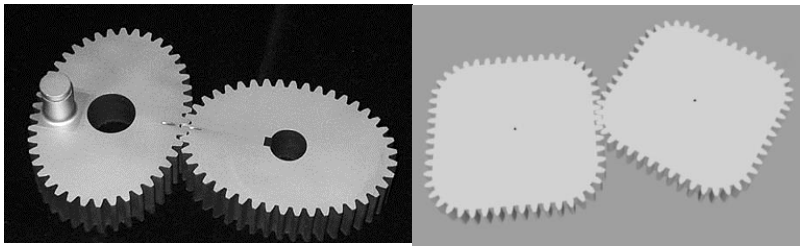

a) b)

Fig. 1.7. Elliptical (a) and square (b) non-circular gears [11]

- **Non-circular gears with continuous variation speed** (Fig.1.7) – are the most used, because the trasnsmission ratio follows a imposed law.
- **Non-circular gears that combine translation with rotation motion** (Fig. 1.8) – are used for the mechanisms of the packing and labeling machines and reproduce the irregular form of the product or part of the product.

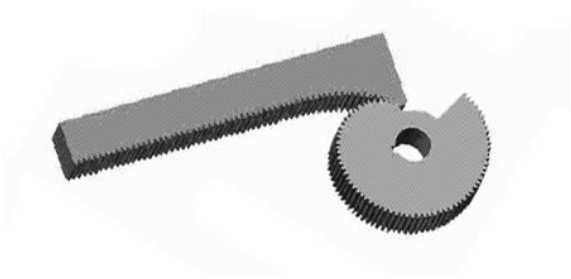

Fig.1.8. Non-circular gear-rack [12]

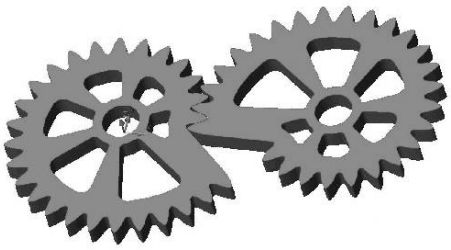

Fig. 1.9. Logarithmic non-circular gears [12]

Depending on the rotation angle of the non-circular gears (duration of the work cycle), the centrodes can be closed curves (Fig. 1.6 și Fig. 1.7) or open curves (Fig. 1.9), that transmit the motion only on one sector.

1.2. HYPOTHESES AND MODELING STRATEGIES OF THE NON-CIRCULAR CENTRODES

The defining element of a non-circular gear is the pitch curve / centrode, along which, the teeth are subsequently generated. The designing of the centrodes is based on the rolling principle, according to which, the centrodes are always tangent to the instant rotation center, rotate each other without slipping and any arch from a centrode is printed with the same length on the mate centrode. Depending on imposed input data, the designing of the centrodes starts from the hypotheses shown in Tab. 1.1.

Tabelul 1.1 The generation hypotheses of the non-circular centrodes

Nr.	Hypotheses	Input data	Result
1	Kinematic hypotheses of the transmission ratio	● Variation law of the transmission ratio, i_{21}=f(φ1) 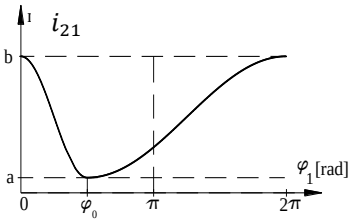 ● Distance between axes , A	● Geometry of the driving centrode: $r_1(\varphi_1) = \frac{A}{1 + i_{21}(\varphi_1)}$ ● Geometry of the driven centrode: $r_2(\varphi_1) = A\frac{i_{21}(\varphi_1)}{1 + i_{21}(\varphi_1)}$ ● Kinematics of the driven centrode: $\varphi_2(\varphi_1) = \int_0^{\varphi_1} \frac{d\varphi_1}{i_{21}(\varphi_1)}$
2	Hypotheses of the motion law	● Motion law of the driven element, $y = f(x), x_1 \le x \le x_2$ 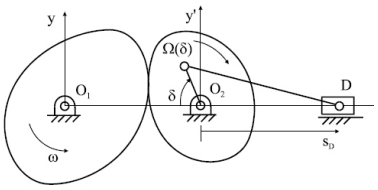 	● Kinematics of the driving centrode: $\varphi_1 = k_1 \cdot (x - x_1)$ ● Kinematic of the driven centrode $\varphi_2 = k_2 \cdot (f(x) - f(x_1))$; ● Instant transmission ratio: $i_{21} = \frac{d\varphi_1}{d\varphi_2} = \frac{k_1}{k_2 \cdot f'(x)}$ ● Geometry of the two centrodes: $r_2(\varphi_1)$ și $r_1(\varphi_1)$ (ip.1)
3	Geometrical hypotheses	● Driving centrode, $r_1(\varphi_1)$ 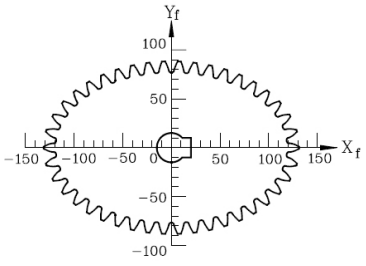 	● Distance between axes, A; ● Transmission ratio: $i_{21}(\varphi_1) = \frac{r_1(\varphi_1)}{A - r_1(\varphi_1)}$ ● Kinematics of the driven centrode: $r_2(\varphi_1) = A - r_1(\varphi_1)$; $\varphi_2(\varphi_1) = \int_0^{\varphi_1} \frac{d\varphi_1}{i_{21}(\varphi_1)}$

unde: i_{21} is the transmission ratio; φ_1 - rotation angle of the driving centrode; r_1- radius of the driving centrode; r_2- radius of the driven centrode; φ_2 - rotation angle of the driven centrode; A - distance between axes; x - displacement of the driven element; k_1, k_2 - scalar coefficients.

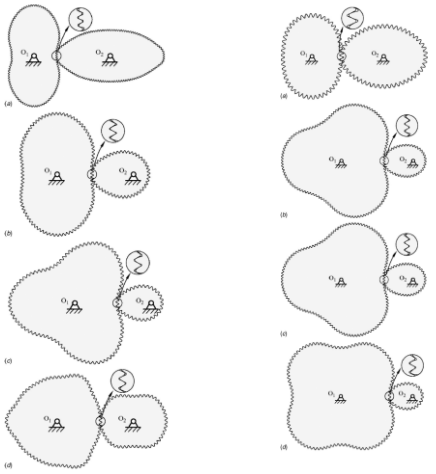

Fig. 1.10. Non-circular centrodes generated, based on Bezier curves [14]

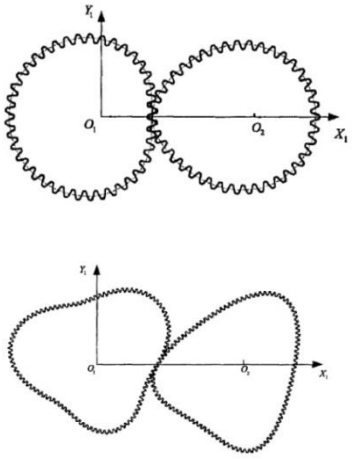

Fig. 1.11. Centrodes generated with Fourier series [15]

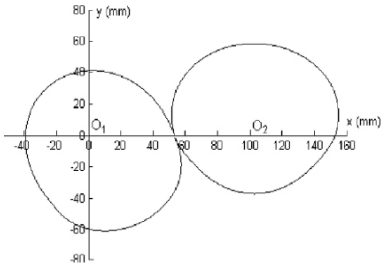

Fig. 1.13. Centrodes for pulsating motion of the crank-slider mechanism [17]

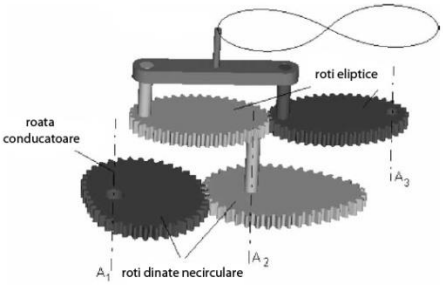

Fig. 1.15. Prototype of the non-circular gear transmission, for playing a trajectory in figure 8 [19]

a) b)

Fig. 1.14. Non-circular gears mechanisms for playing a exact trajectory [18] a) linear trajectory; b) imposed trajectory by 8 points

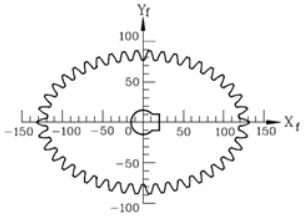

Fig. 1.17. Centrode generatd by Bair , by means Fourier series [21]

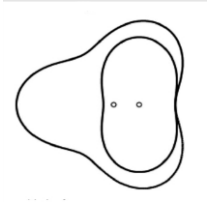

Fig. 1.18. Internal non-circular centrodes, remodeled [23]

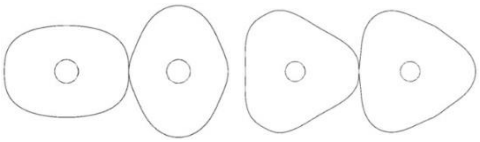

Fig. 1.19. Centrodes defined by the supershape equation [25]

1.3. HYPOTHESES AND GENERATION METHODS OF THE NON-CIRCULAR GEARS TEETH

Generation of the non-circular gears teeth, can't be approached in the same way as in the circular gears case, based on unwinding of the base circle [27] [28], due to the complex geometry of the teeth, from the first case. As a result, generation of the teeth flanks is done by means, special methodes, depending on local geometric features of the centrodes and on the rolling kinematics.

Analytical methods, based on the envelope theory **:**

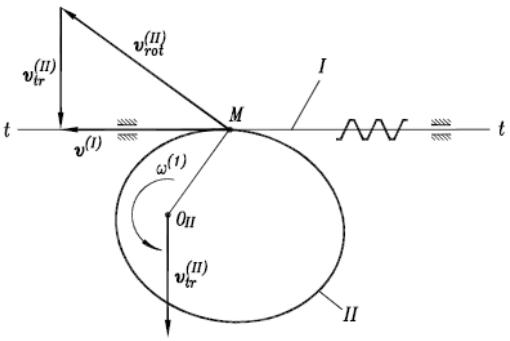

Fig. 1.20. Kinematics of the non-circular gears process, with rack [13]

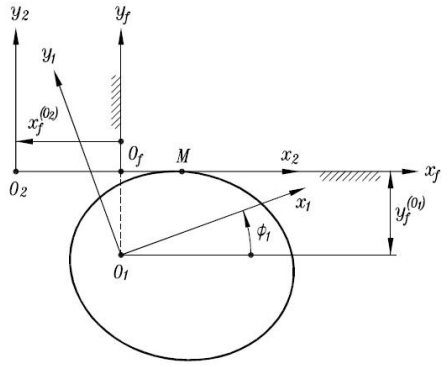

Fig. 1.21. Displacements representation for non-circular gears process, with rack [13]

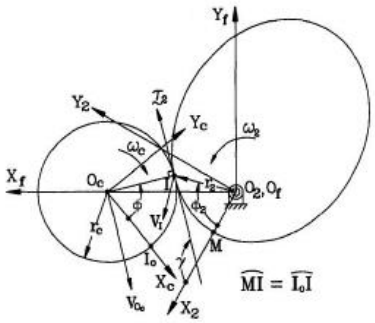

Fig. 1.23. Kinematics of the non-circular gears process, with cutting-wheel [31]

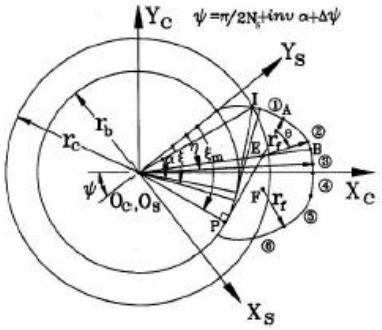

Fig. 1.24. Geometry of the cutting-wheel, proposed by Chang and Tsay [31]

Simulation process methods:

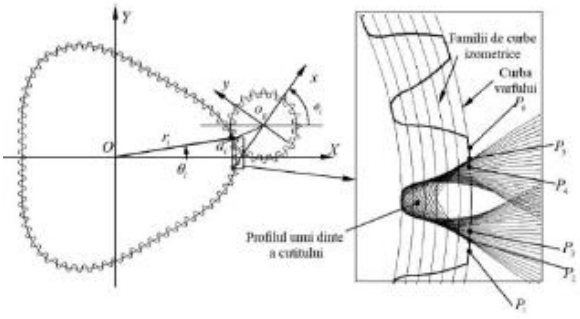

Fig. 1.28. Graphic simulation of the non-circular gear process, with cutting-wheel [38]

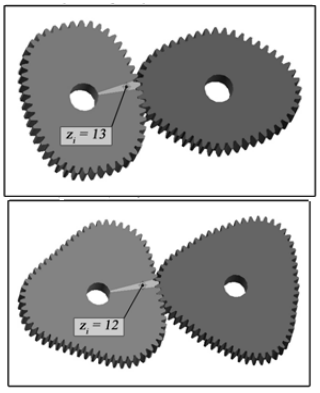

a)

b)

Fig. 1.29. Non-circular gears, with convex (a) and convex-concave (b) centrodes, generated by Vasie and Andrei [39], [40]

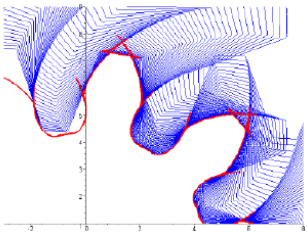

Fig. 1.32. Involute flanks generated by Lackzic [43]

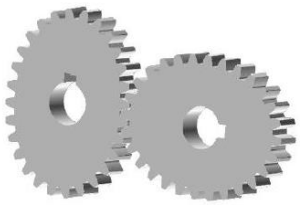

Fig. 1.33. Elliptical gears, generated by Gao [44]

1.4. INDUSTRIAL APPLICATIONS OF THE NON-CIRCULAR GEARS

1.4.1. Kinematics modification of the crank-slider mechanism

Many industrial applications, that use crank-slider mechanism, need to modify its conventional law of motion, in order to improve the applications performances. For this purpose, the use of the non-circular gears, it's a right solution for kinematics modification. Designing of the non-circular gears, for these applications, was performed either on the basis of the law of sliding movement [51], [52], [53] or, based on a required speed on certain phases of the operating cycle [54], [55].

1.4.1.1. Speed variation of the presses ram

An application found in literature, takes account the kinematics modification of a press, whose ram moves, following a optimized law by means a non-circular gear, coupled with a crank-slider mechanism [51].

For generation the non-circular gears centrodes, the motion law of the ram, s(t) is imposed. For following a optimized motion law, the ram has to get a modified cycle, comparison with conventional law. Starting from these considerations and from the simulation by means the Finite Element Method (FEM), Doege [52], [53] proposes a ram motion law as per Fig. 1.36

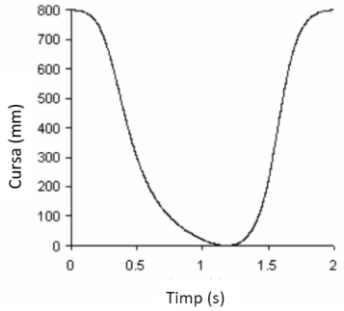

Fig. 1.36. Motion law of the press ram [51]

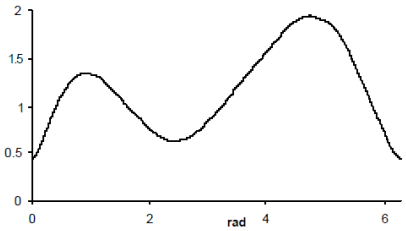

Fig 1.38. Law variation of the transmission ratio [51]

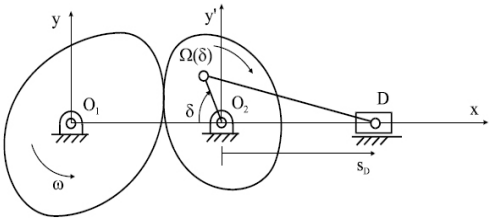

Fig.1.37. Scketch of the mechanism proposed by Doege [53]

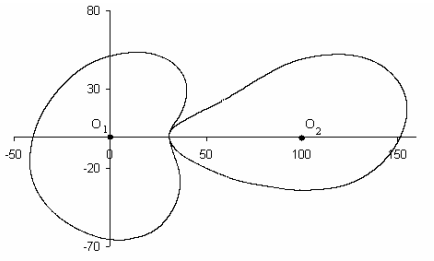

Fig 1.39. Generation of the centrodes, based on the optimized motion law [51]

The teeth profile determination, is made based on a mathematical model that describe the teeth evolution in meshing, maintaining constant pressure angle. In this way, are obtaining teeth with irregular profile, due to the variable radii of the centrodes (Fig.1.40). As a result, it propose a corection of t he pressure angle value.

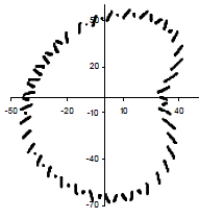

Fig. 1.40. Driving gear with constant pressure angle [51]

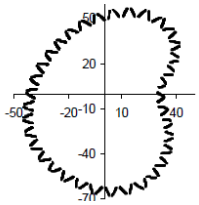

Fig. 1.41. Driving gear with variable pressure angle [51]

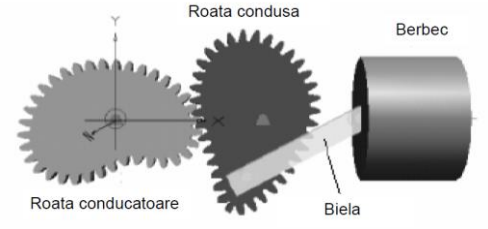

Fig. 1.43. Prototype of the driving mechanism [51]

Based on the above data, a CAD soft has generated, first, the non-circular gears model whose centrodes are represented in Fig.1.39 and then, the crank-slider mechanism driven by the non-circular gears pair.

1.4.1.2. Optimization of the working cycle at the internal combustion engine

An other application that introduce a non-circular gear to drive a crank-slider mechanism, is proposed by Quintero [55], for a internal combustion engine. The gear allows the piston speed to be adjusted over the entire cycle, so that, to improve the performance of the engine.

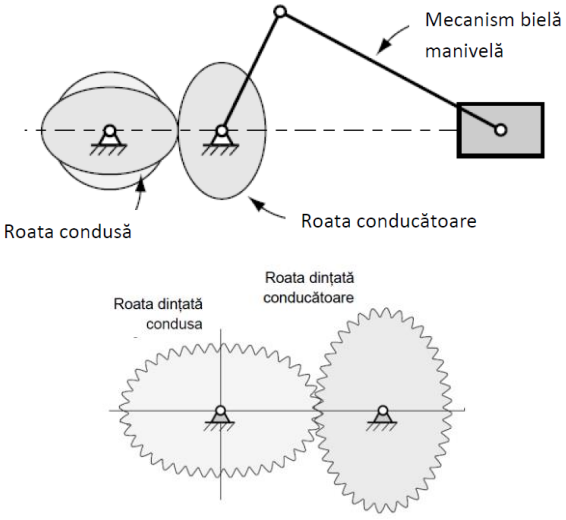

Fig. 1.44. Modified crank-slider mechanism [55]

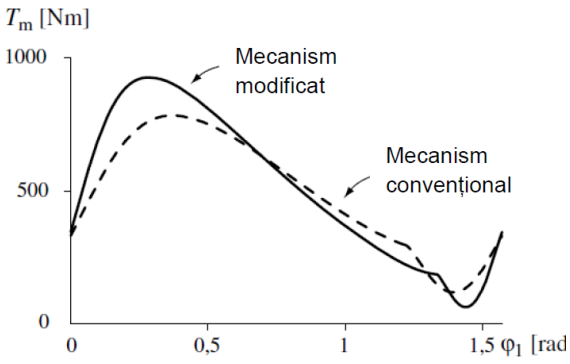

Fig. 1.48. Motor torque of the crank-slider mechanism [55]

1.4.2. Control of the closing/ regulation elements

In many applications that use closing or regulation elements (flaps, valves, doors, etc.), for technological reasons, is necessary either liniar motion transformation of the elements, in nonliniar motion following a imposed law [58], or transformation of nonliniar variation of a process parameters, in a liniar variation [59], [60].

1.4.2.1. Mechanism for driving the windows of motor vehicles

The application proposes the use of two non-circular gears to operate the variable speed door: lower, near the fully closed window position and raised on the rest of the window. Near the fully closed position, the variation of the transmission is small, that involves a lower window speed, easily controllable. Thus, a much easier control of the window opening is achieved, close to the fully closed position.

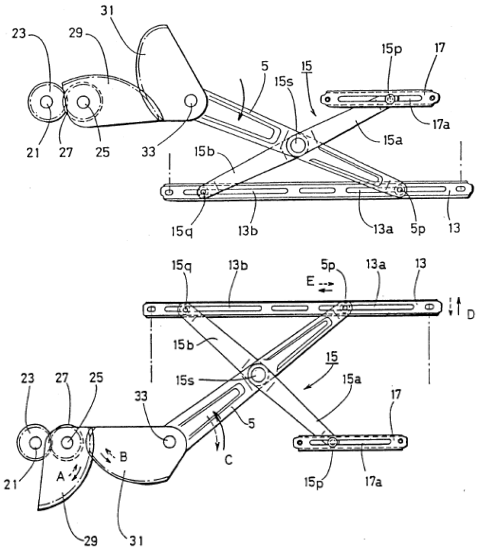

Fig. 1.51. Modified mechanism for driving the door window, in fully opened (a) and fully closed (b) position [58]

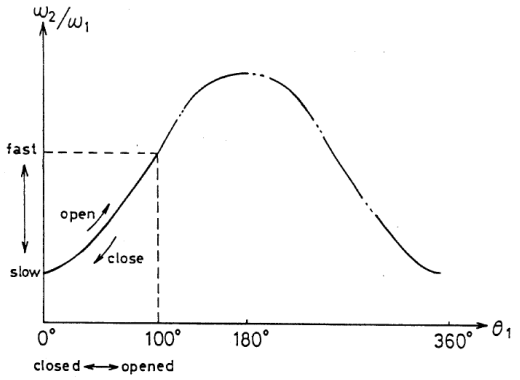

Fig. 1.52. Transmision ratio variation, depending on eccentric gear rotation angle [58]

1.4.2.2. Flap control speed regulation of the air conditioning control system of the vehicles

Maintaining a certain temperature inside a vehicle is done by dosing hot air and cold air through a throttle which, depending on its position, makes the mixture. Considering that, when rotating at constant throttle speed, the air passage section (and hence the air flow rate) does not vary linearly, the application [59] proposes an air flap mechanism control using a non-circular gear, which is capable of slowly rotating the flap at an imposed speed and at the same time constantly maintaining the total throttling time.

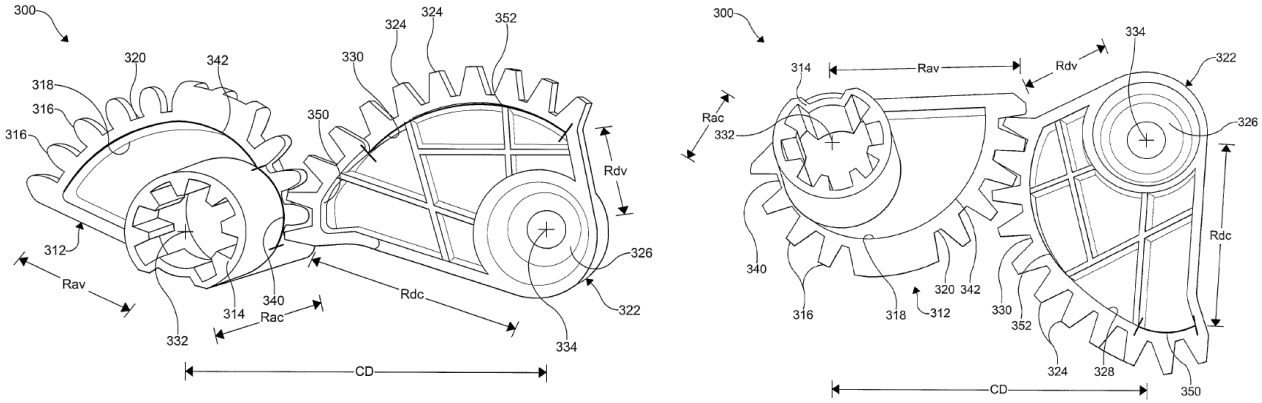

Fig 1.53. Non-circular gear used for driving the temperature control flap, in position fully closed – hot (a) and fully opened – cold (b) [59]

1.4.3. Optimization of the resistant moments to some driving mechanisms

In cases of the driving mechanisms, is necessary to reduce the force or the driving torque, to certain moments, or uniformization of the resistant torque. Considering that, this optimization is required only on certain phases of the working cycle the non-circular can successfully accomplish this goal. Thus, they are used to reduce the torque of the internal combustion engine [61], at the boat steering systems [62], [63], or at the mechanical pedal actuators [64].

1.4.3.1. Starting device for internal combustion engines

A starting device for engine [61] consist of a non-circular gears pair, which is interposed between the crankshaft and the toothed crown in the starting system with starter. When the rotational speed of a non-circular gear is maintained constant, the other wheel varies the angular speed in correspondence with the changing crankshaft torque, due to the engine characteristics.

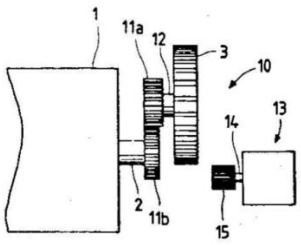

Fig. 1.54. Sketch of a engine starting device [61]

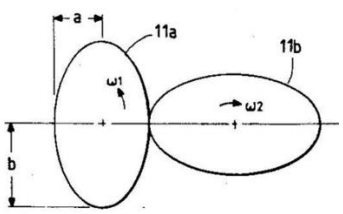

Fig. 1.55. Oval gear used on the starter [61]

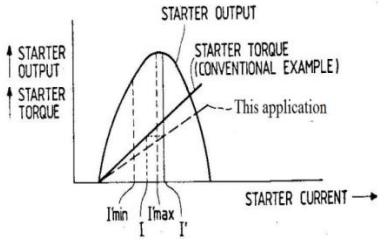

Fig. 1.57. Correlation between current, engine power and torque [61]

1.4.3.2. Watercraft steering system

A steering system particularly [62] suitable for watercraft wherein the input is non-linearly related to the output so that, when the watercraft is running on a straight course (Fig. 1.58), the steering is very sensitive operating at a low ratio input to output and when the watercraft is in full turn (Fig. 1.59), the steering is much less sensitive operating at a high ratio input to output.

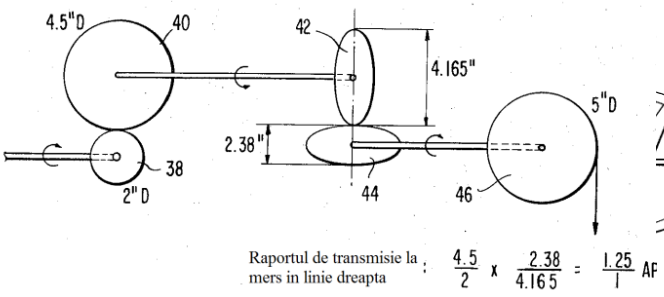

Fig. 1.58. Transmission sketh with non-circular gears in extreme position [62]

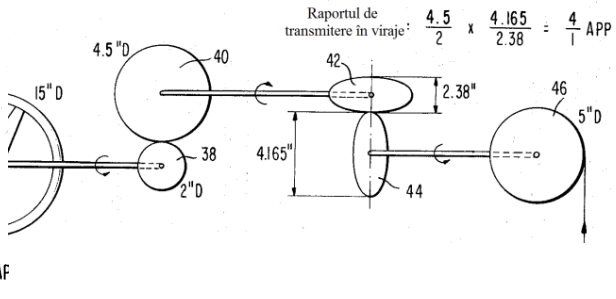

Fig. 1.59. Transmission sketch of non-circular gears in the opposite extreme position (90 ° rotary gear) [62]

1.4.4. Mechanism for intermittent motion

Non-circular gears, coupled with the planetary mechanisms or cams, can accomplish intermittent or reversal movement of the execution elements. This type of application removes the disadvantages of the conventional mechanisms for intermittent motion (Malta Cross, pawl mechanism, etc.)

1.4.4.1. Planetary mechanism for intermittent motion

This invention pertains to intermittent motion mechanisms of the type in which a continuous rotation applied to one member of a linkage produces an intermittent rotation of another member of that linkage. It used a circular gears and a non-circular gear.

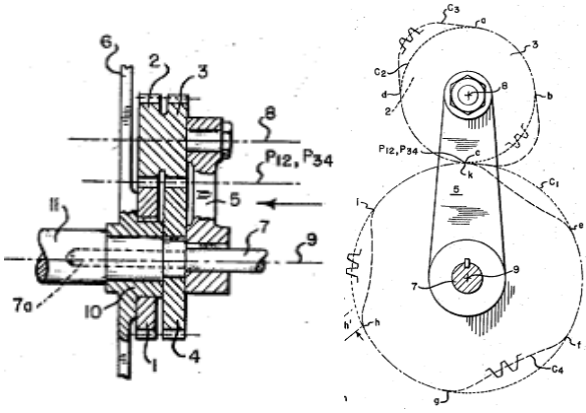

a) b)

Fig. 1.60. Meshing on circular sector, section (a) and lateral view (b) [65]

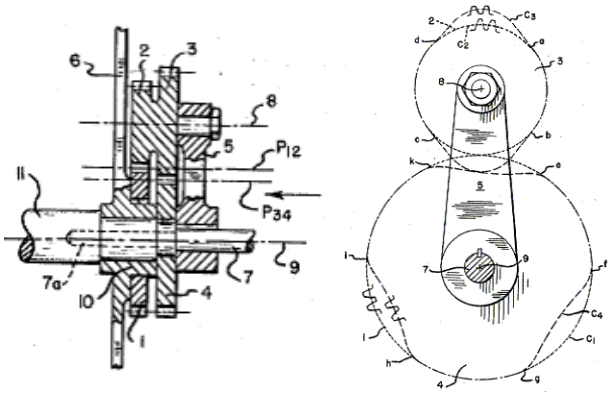

a) b)

Fig. 1.61. Meshing on non-circular sector, section (a) and lateral view (b)) [65]

1.4.4.2. Intermittent power supply mechanism

The proposed mechanism (Fig.1.62.) [66] provides an intermittent motion with precise control of the step motion, with no unwanted shocks at the beginning and end of the step movement, and very low abrasive wear. The presented mechanism [66] allows precise control of start and stop times without interruption, even at high speeds.

1.4.4.3. Machine for making wire coils

The wire feed is interrupted synchronously by means of a cam system, which interrupts, briefly, the contact between the feed rollers and the wire. This variable speed drive allows for a high duty cycle and also allows low feed speed (with feed rollers in contact), so that, wire deformation is minimal.

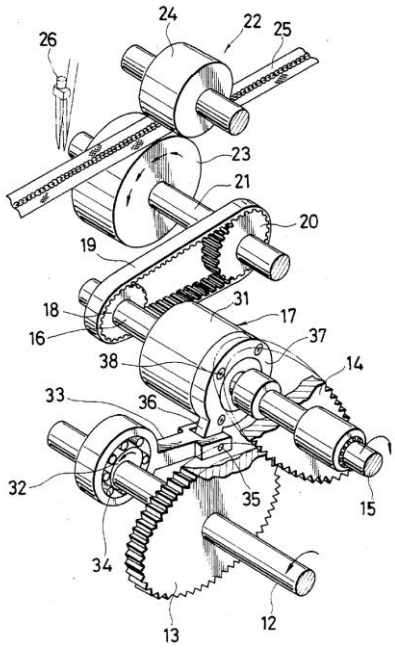

Fig. 1.62. Driving mechanism for intermittent motion [66]

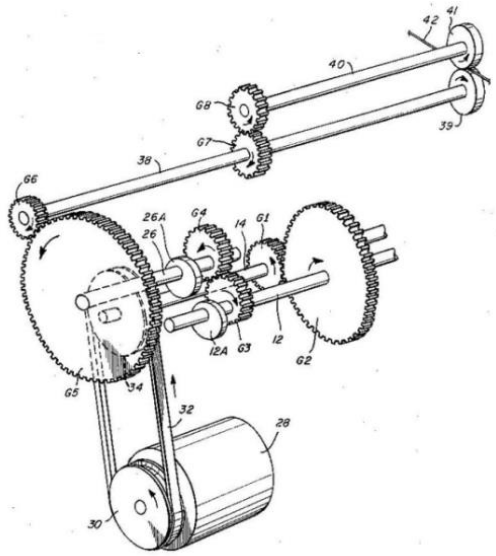

Fig. 1.63. Scketch of the machine for making wire coils [67]

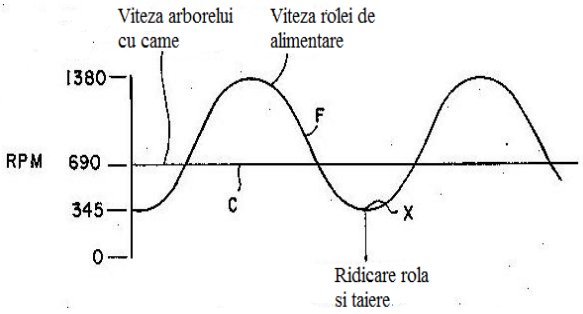

Fig.1.64. Feed rolls speed and camshaft diagram [67]

1.5. CONCLUSIONS

Due to the mechanical power transmitted, overload tolerance, high durability and low maintenance costs, in some technological operations, non-circular gears have been preferred to other types of mechanisms in different areas or in different stages of the technological process: automotive industry, agricultural industry, electronics, hydraulics, assembly, labeling, painting, grinding.

So far, many applications of non-circular gears have been limited to patents and have not been applied on a large scale, given the possibilities of processing and high costs. The development of modeling and simulation software, as well as the improvement of machining techniques, allowed new approaches and in-depth studies on the design of gears with variable transmission ratios.

The generation of non-circular centrodes has been approaches in three different ways, depending on the design data of each application. Regardless of the adopted hypothesis, the centrodes, can be, closed in the case of cyclical movements or open in the case of special movements, in which case the centrode has the form of predefined curves (logarithmic, exponential, etc.).

Generation of teeth was approached by specialists using different methods of involute building: analytical methods, methods of surface enveloping theory and methods of processing simulation.

So far, non-circular gears have been used, in particular, in the following applications: kinematics modification of classical mechanisms according to imposed requirements, variable speed control of locking / adjusting elements within certain installations or drive mechanisms, optimizing moments resistant to some actuation mechanisms or obtaining intermittent movements using classical mechanisms.

Chapter 2

NON-CIRCULAR GEARS FOR KINEMATICS MODIFICATION OF THE NAILS MACHINE

2.1. INTRODUCTION

A classic nails machine is an automatic machine that performs all the operations necessary to make the nails from wire, piece by piece. The working cycle, consists of performing the following operations: nail head forming, wire advance, wire cutting to the length of the nail rod and removing the nail. All operations are performed successively, during a complete rotation of the shaft, according to the diagram from Fig. 2.1 The characteristics of the machine for which the analysis was made are shown in Tab.2.1

Tabel 2.1. *Characteristics of the nails machine, type MCC 337 [71]*

Diameters range	3,5 – 6 mm
Nails lenght range	50 – 180 mm
Productivity	180 pcs /min
Course of the slider	300 mm
Driving motor	11 kw ; 750 rot/min
Power supply	380 V ; 50 Hz
Dimensions	3150 x 1950 x 1095 mm
Weight	4730 kg

In order to improve the performance of the machine, it is proposed to modify the working cycle of the crank-slider mechanism of the main movement, by decreasing the working speed, during the nail head forming and maintaining it at a relatively constant value. For this, it is proposed to drive the main shaft by means of a non-circular gear, so that at the moment of deformation the ram has a lower speed and the return motion is made at a high speed. Thus, besides improving the plastic deformation conditions of the head, without affecting the working cycle of the other mechanisms and the productivity of the machine, there are several other advantages, such as: increasing the deformation force application time, improving product quality, making larger nails on classic nails machines, increasing tool reliability, increasing process stability, reducing noise and increasing the machine capacity in case of conventional head nails.

2.2. MODIFIED KINEMATICS OF THE NAILS MACHINE

2.2.1. Kinematic analysis of the nails machine

As is shown in the kinematic scheme in Fig. 2.2, the MCC 337 [71] nails machine is composed of several mechanisms corresponding to each operation.

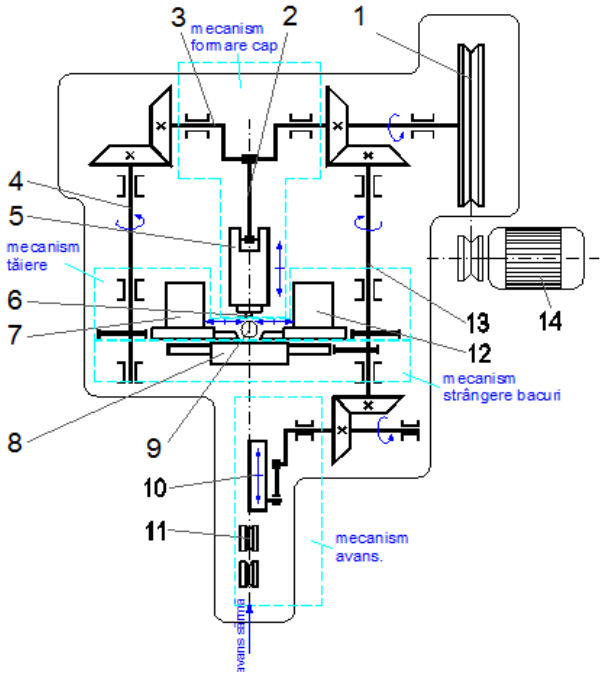

Fig. 2.2. Kinematic scheme of MCC 337 nails machine [71]

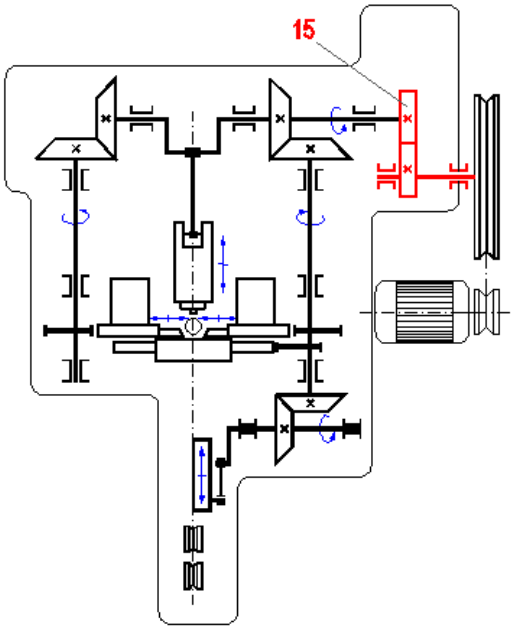

Fig. 2.3. Modified kinematic scheme of MCC 337 nails machine

1 - handwheel / flywheel; 2 – connecting rod; 3 - crankshaft; 4 – left shaft; 5 - slider; 6-ram; 7- left cutter support; 8 - dies box; 9 - nails removing; 10 – advance device; 11 – straightening rolls; 12 – right cutter support; 13 – right shaft; 14 – motor; 15 – non-circular gear

2.2.2. Kinematics modification of the crank-slider mechanism

Often, when making nails with larger head or when the wire has a high degree of hardening, there are cracks on the nail head or other defects. At the same time, due to the very high wire deformation speed, correlated with the high frequency of beatings, the produced noise exceeds the permissible limit. To eliminate these undesirable effects, it is proposed to drive the main shaft by means of a non-circular gear (Figure 2.3) so that, at the moment of deformation, the head former has a lower speed and the returning is made at high speed. In this way, only the kinematic of the crank-slider mechanism changes, without significantly affecting the other movements or characteristics of the machine.

Conventionally, variation laws of displacement and sliding speed are represented by curves *1* and *1 '*, respectively, in Fig. 2.4. As can be seen in Fig. 2.4a, the head formation takes place at the end of the sliding stroke, on the distance *s'*, in the angle range *df'*, the rest of the stroke not being important for the deformation process. In this interval, the velocity is decreasing from *v'* to 0, the interval dφ being generally within [*7π / 9π*], depending on the type of nail.

To improve the nail head formation process, as described above, is proposed that, on the distance s', the slide moves according to a law similar to curve 2, and the speed varies according to a law similar with curve *2'*. In this case, it can see that the interval *dφ''* in which plastic deformation occurs is much greater than *dφ'* and the velocity from which the deformation process starts *v''< v'*, resulting in a significantly lower acceleration. In order to not change the working cycle, it is necessary, for the rest of stroke and during the returning stroke, the ram speed to be higher, this fact doesn't affect the processes that take place during the rest of the cycle.

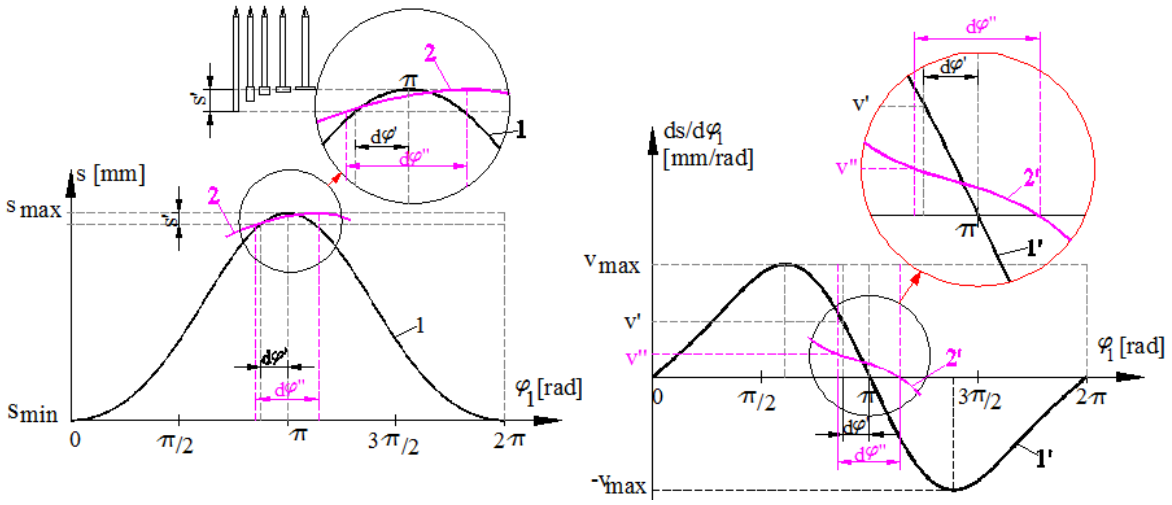

a) b)

Fig.2.4. Comparison between the displacement variation law (a), and relative speed (b) of the slider, in the conventional case and in the modified law case

2.2.2.1. Two-phases working cycle with trigonometric variation of transmission ratio

It is considered that the working cycle of the crank-slider mechanism, with the same duration as the rotational movement of the non-circular gear (2π), is divided into two phases. For the motion specific to these phases, following the proposals of other researchers ([51], [52]), the transmission ratio is defined by function (Figure 2.5):

$$i_{21}(\varphi_1) = \begin{cases} c_1 + c_2 \cdot \cos(c_3 \cdot \varphi_1 + c_4), \text{dacă } \varphi_1 \in [0, \varphi_0] \\ c_5 + c_6 \cdot \cos(c_7 \cdot \varphi_1 + c_8), \text{dacă } \varphi_1 \in [\varphi_0, 2\pi] \end{cases}, \quad (2.1)$$

where: φ_0 is the rotation angle of the pinion, that divide the working phases;
c_1 ...c_8 – constants that assure the defining of a correct tansmission ratio,

The rotation angle of the driven gear, calculated with the relation:

$$\varphi_2(\varphi_1) = \int_0^{2\pi} i_{21}(\varphi) d\varphi \quad , \quad (2.6)$$

becomes:

$$\varphi_2(\varphi_1) = \begin{cases} c_1 \cdot \varphi_1 + \frac{c_2}{c_3} \cdot \sin(c_3 \cdot \varphi_1 + c_4) + ct_1, \text{dacă} \varphi_1 \in [0, \varphi_0] \\ c_5 \cdot \varphi_1 + \frac{c_6}{c_7} \cdot \sin(c_7 \cdot \varphi_1 + c_8) + ct_2, \text{dacă} \varphi_1 \in [\varphi_0, 2\pi] \end{cases}, \quad (2.7)$$

where ct_1, ct_2 are constants integration.

The constants c_1 ... c_8, ct_1, ct_2 are determined by imposing the following conditions:

- The transmission ratio is between a minimum and a maximum limit ⇒ $a < i_{21} < b$
- The function that defining the variation of the transmission ratio (ec.2.1) is periodic ⇒ $i_{21}(0) = i_{21}(2\pi) = b$, $i_{21}(\varphi_0) = a$ (2.2)
- The variation of the transmission ratio (ec.2.1) is a continuous and derivable function at point $\varphi_1 = \varphi_0$. ⇒ $i'_{21}(0) = i'_{21}(\varphi_0) = i'_{21}(2\pi) = 0$ (2.4)

● The tangents to the function graph at the points $\varphi_1 \in \{0, \varphi_0, 2\pi\}$,are parallel to the abscissa

● Function $\varphi_2(\varphi_1)$ is continuous, monotonically increasing in the range [0, 2π] and derivable

● Closed centrodes

$$\Rightarrow \quad \varphi_{2s}(\varphi_0) = \varphi_{2d}(\varphi_0); \quad \varphi_2'_s(\varphi_0) = \varphi_2'_d(\varphi_0) . \tag{2.8}$$

$$\Rightarrow \quad \varphi_2(0) = 0,\ \varphi_2(2\pi) = 2\pi \tag{2.10}$$

$$\Rightarrow \quad a+b = 2 \tag{2.11}$$

It results the following values of the constants that defining the transmission ratio and the rotation angle of the driven gear (Table 2.2):

Tabel 2.2. *The defining constants of the non-circular gear kinematics with two phases of the working cycle and with trigonometric variation transmission ratio*

$c_1 = \frac{a+b}{2}$	$c_2 = \frac{(b-a)}{2}$	$c_3 = \frac{\pi}{\varphi_0}$	$c_4 = 0$	$ct_1 = 0$
$c_5 = \frac{a+b}{2}$	$c_6 = -\frac{(b-a)}{2}$	$c_7 = \frac{\pi}{2\pi-\varphi_0}$	$c_8 = -\frac{\pi \cdot \varphi_0}{2\pi-\varphi_0}$	$ct_2 = 0$

From Tab. 2.2 and relation (2.11) result that the non-circular gear kinematics ca be varies by means of two parameters, respectively the angle that divides the working phases φ_0 and the extrem value of the transmision ratio *a* (or *b)*. The figures 2.6 and 2.7 show teh influence of the defining parameters of the transmission ratio on gear kinematics

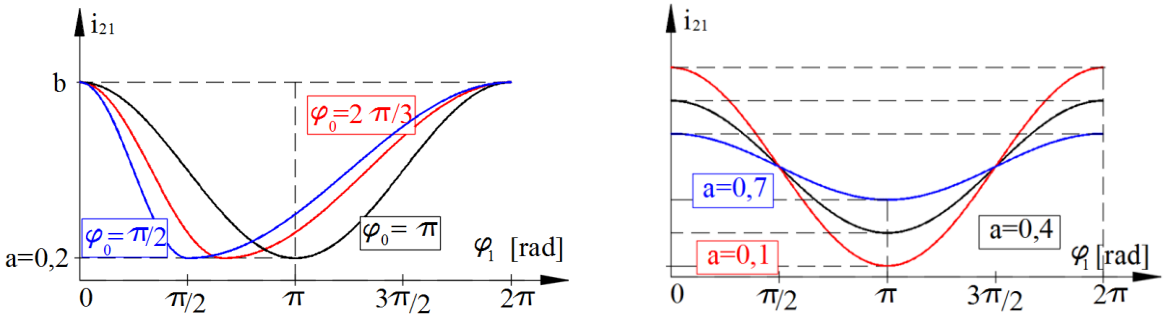

a) a = 0,2 b) φ_0 = 5π/6

Fig. 2.6. Influence of the angle φ_0 (a) and of the minimum value *a* (b) on the transmission ratio – two phases working cycle, trigonometric variation of the transmission ratio

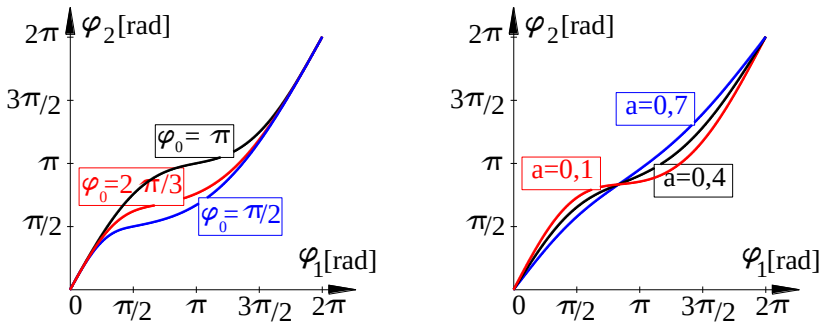

a) a = 0,2 b) φ_0 = 5π/6

Fig. 2.7. Influence of the angle φ_0 (a) and of the minimum value *a* (b) on the rotation angle of the driven gear – two phases working cycle, trigonometric variation of the transmission ratio

The transmission of the nonuniform motion from the driven wheel of the non-circular gear to the crank causes a non-uniform translational motion of the slider, whose stroke is defined by the relation:

$$s(\varphi_2) = -r \cdot \cos\varphi_2 + \sqrt{l^2 - r^2 \cdot sin^2\varphi_2}\ , \tag{2.12}$$

where r is the crank length; l – conecting road length (Fig. 2.8).

Figure 2.9 shows the diagram of the composite function $s(\varphi_2(\varphi_1))$, in the hypothesis of the sinusoidal variation of the transmission ratio and Fig. 2.10 shows the variation of the relative slide speed $ds / d\varphi_1$.

.

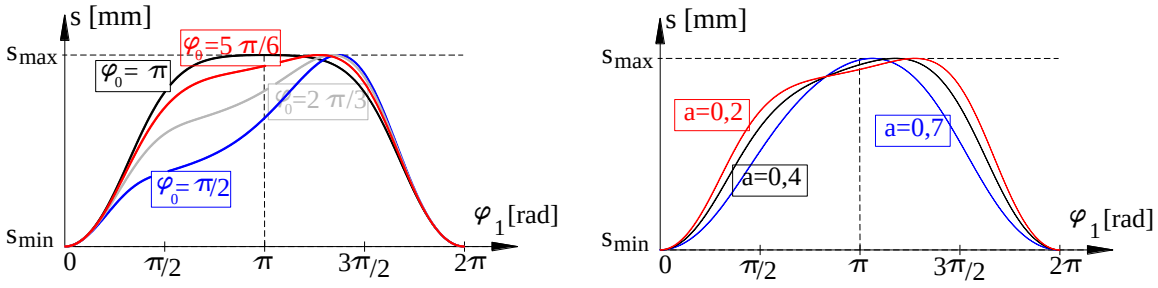

a) a = 0,2 b) φ_0= 5π/6

Fig. 2.9. Influence of the angle φ_0 (a) and of the minimum value a (b) on the slide displacement – two phases working cycle, trigonometric variation of the transmission ratio

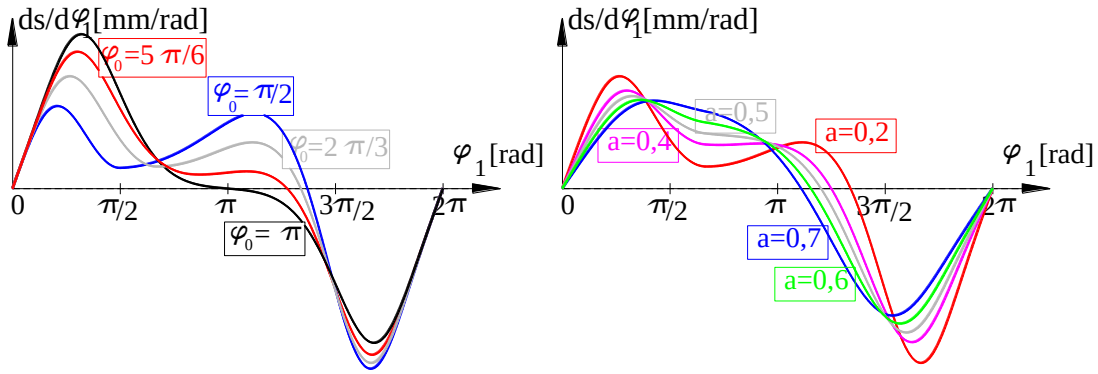

a) a = 0,2 b) φ_0= 5π/6

Fig. 2.10. Influence of the angle φ_0 (a) and of the minimum value a (b) on the relative speed of the slide – two phases working cycle, trigonometric variation of the transmission ratio

Following the analysis of the above graphs, it is considered that a convenient variant of the kinematics is obtained for the following values of the parameters that influence the process: $\boldsymbol{\varphi_0 = 8\pi/9}$ **;** $\boldsymbol{a = 0,4}$.

2.2.2.2. Two-phases working cycle with polynomial variation of transmission ratio

Another function proposed for the non-circular gear ratio transmission, assuming the two-phase division of the rotation period of the motion, is defined by:

$$i_{21}(\varphi_1) = \begin{cases} c_1 \cdot \varphi_1^3 + c_2 \cdot \varphi_1^2 + c_3 \cdot \varphi_1 + c_4, \text{daca } \varphi_1 \in [0, \varphi_0] \\ c_5 \cdot \varphi_1^3 + c_6 \cdot \varphi_1^2 + c_7 \cdot \varphi_1 + c_8, \text{daca } \varphi_1 \in [\varphi_0, 2\pi]\ . \end{cases} \tag{2.13}$$

The angle of driving gear rotation in this hypothesis is:

$$\varphi_2(\varphi_1) = \begin{cases} \frac{1}{4}c_1 \cdot \varphi_1^4 + \frac{1}{3}c_2 \cdot \varphi_1^3 + \frac{1}{2}c_3 \cdot \varphi_1^2 + c_4 \cdot \varphi_1 + ct_1, \text{dacă} \varphi_1 \in [0, \varphi_0] \\ \frac{1}{4}c_5 \cdot \varphi_1^4 + \frac{1}{3}c_6 \cdot \varphi_1^3 + \frac{1}{2}c_7 \cdot \varphi_1^2 + c_8 \cdot \varphi_1 + ct_2, \text{dacă} \varphi_1 \in [\varphi_0, 2\pi] \end{cases} . \quad (2.16)$$

Imposing the same conditions as in chapter 2.2.2.1, the following values for constants c_1 ... c_8 , ct_1, ct_2 :

Tabel 2.3. *The defining constants of the non-circular gear kinematics - two phases working cycle, and polynomial variation of the transmission ratio*

$c_1 = \frac{2(b-a)}{\varphi_0^3}$	$c_2 = \frac{-3(b-a)}{\varphi_0^2}$	$c_3 = 0$	$c_4 = b$	$ct_1 = 0$
$c_5 = \frac{-2(b-a)}{(2\pi-\varphi_0)^3}$	$c_6 = \frac{3(b-a)(2\pi+\varphi_0)}{(2\pi-\varphi_0)^3}$	$c_7 = \frac{-12\pi(b-a)\cdot\varphi_0}{(2\pi-\varphi_0)^3}$		$a + b = 2$
$c_8 = \frac{8a\pi^3 - 12a\pi\varphi_0 + 6b\pi\varphi_0^2 - b\varphi_0^3}{(2\pi-\varphi_0)^3}$		$ct_2 = \frac{\pi(b-a)\varphi_0(4\pi^2 - 6\pi\varphi_0 + \varphi_0^2)}{(2\pi-\varphi_0)^3}$		

It studying the influence of the defining parameters (φ_0 and a) of the transmission ratio, on the non-circular gear kinematics variation (Fig. 2.11, 2.12), and on the displacement and relative speed of the slide (Fig. 2.13, 2.14).

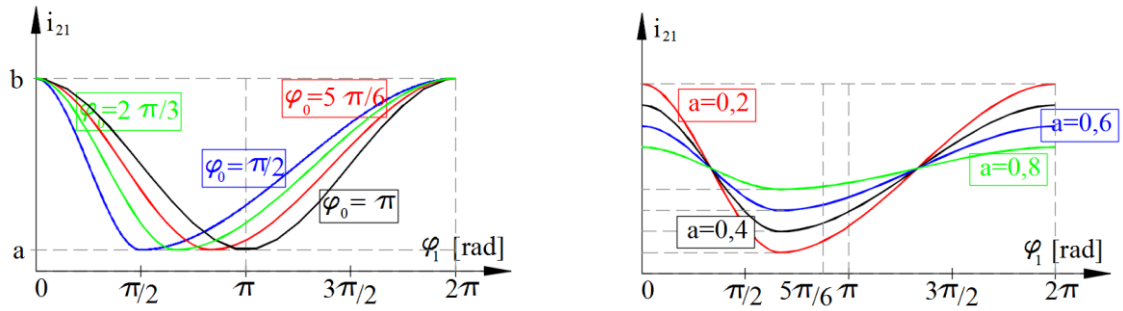

a) a = 0,2 b) φ_0= 5π/6

Fig. 2.11. Influence of the angle φ_0 (a) and of the minimum value a (b) on the slide displacement – two phases working cycle, polynomial variation of the transmission ratio

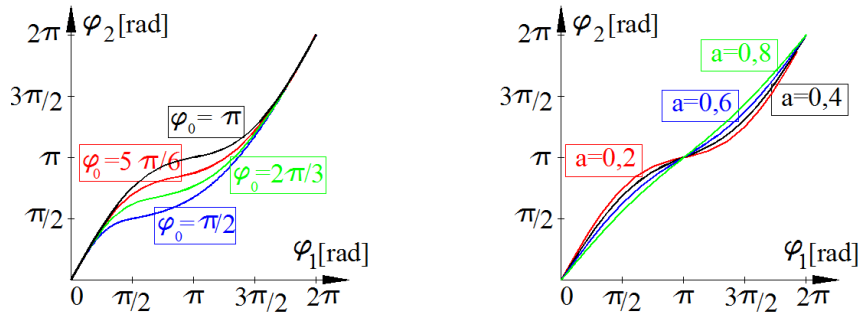

a) a = 0,2 b) φ_0= 5π/6

Fig. 2.12. Influence of the angle φ_0 (a) and of the minimum value a (b) on the rotation angle of the driven gear – two phases working cycle, polynomial variation of the transmission ratio

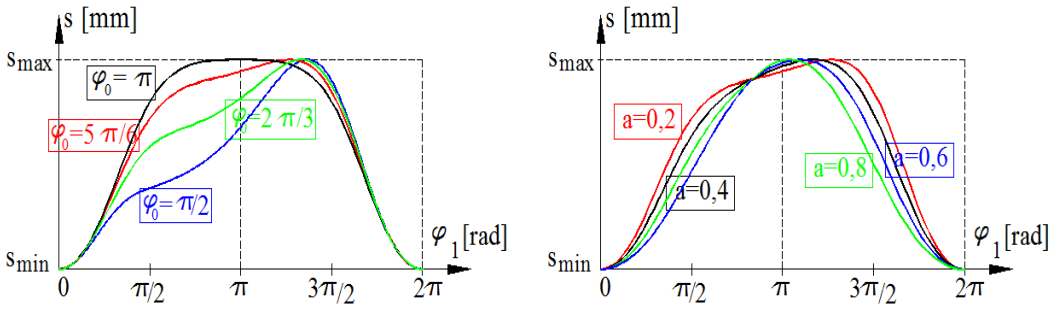

a) a = 0,2 b) φ_0= 5π/6

Fig. 2.13. Influence of the angle φ_0 (a) and of the minimum value a (b) on the slide displacement – two phases working cycle, polynomial variation of the transmission ratio

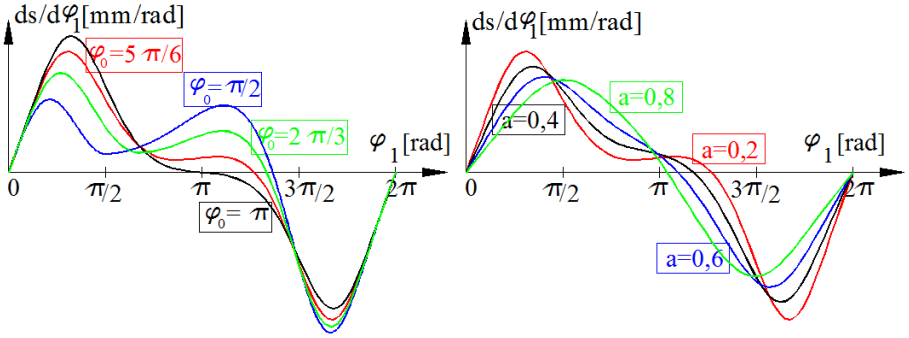

a) a = 0,2 b) φ_0= 5π/6

Fig. 2.14. Influence of the angle φ_0 (a) and of the minimum value a (b) on the relative speed of the slide – two phases working cycle, polynomial variation of the transmission ratio

The values of the parameters are also proposed as a convenient variant $\boldsymbol{\varphi_0 = 8\pi/9}$ and $\boldsymbol{a}$ **= 0,4**, the differences from the previous case being insignificant.

2.2.2.3. Three-phases working cycle with trigonometric variation of transmission ratio

Another approach consider that, the working cycle of the crank-slider mechanism, with the same duration as the rotational movement of the non-circular gear (2π), is divided into three phases: fast-forward phase, working phase, in which the slide speed is gradually reduced, and fast returning phase. For the motion specific to these phases, the transmission ratio will be defined by three functions. As in the two-phases working cycle case, two hypotheses will be analyzed: trigonometric variation and polynomial variation of the transmission ratio.

The following definition law is proposed for the transmission ratio:

$$i_{21}(\varphi_1) = \begin{cases} c_1 + c_2 \cdot \cos(c_3 \cdot \varphi_1 + c_4), \text{daca} \varphi_1 \in [0, \varphi_{1a}] \\ c_5 + c_6 \cdot \cos(c_7 \cdot \varphi_1 + c_8), \text{daca} \varphi_1 \in [\varphi_{1a}, \varphi_{1r}] \\ c_9 + c_{10} \cdot \cos(c_{11} \cdot \varphi_1 + c_{12}), \text{daca} \varphi_1 \in [\varphi_{1r}, 2\pi] \end{cases}, \quad (2.17)$$

where φ_{1a} is the rotation angle of the driving gear that marks the advance phase end and the working phase begining; φ_{1r} - rotation angle of the driving gear that marks the working phase end and the returning phase begining; c_1 ... c_{12} – constants that assure a correct kinematics and geometry.

The rotation angle of driven gear is defined by:

$$\varphi_2(\varphi_1) = \begin{cases} c_1 \cdot \varphi_1 + \dfrac{c_2}{c_3} \cdot \sin(c_3 \cdot \varphi_1 + c_4) + ct_1, \text{dacă} \varphi_1 \in [0, \varphi_{1a}] \\ c_5 \cdot \varphi_1 + \dfrac{c_6}{c_7} \cdot \sin(c_7 \cdot \varphi_1 + c_8) + ct_2, \text{dacă} \varphi_1 \in [\varphi_{1a}, \varphi_{1r}] \\ c_9 \cdot \varphi_1 + \dfrac{c_{10}}{c_{11}} \cdot \sin(c_{11} \cdot \varphi_1 + c_{12}) + ct_3, \text{dacă} \varphi_1 \in [\varphi_{1r}, 2\pi] \end{cases}, \quad (2.20)$$

where ct_1, ct_2, ct_3 are integration constants,

The followings condition are imposed to functions $i_2(\varphi_1)$ and $\varphi_2(\varphi_1)$,

- The transmission ratio is between a minimum and a maximum limit ➡ $a < i_{21} < b$
- The function defining the variation of the transmission ratio (ec.2.1) is periodic ➡ $i_{21}(0) = i_{21}(2\pi) = b$, $i_{21}(\varphi_{1a}) = a$, $i_{21}(\varphi_{1r}) = i_i$ (2.18)
- The variation of the transmission ratio is a continuous and derivable function in points $\varphi_1 = \varphi_{1a}$ și $\varphi_1 = \varphi_{1a}$ ➡ $i'_{21}(0) = i'_{21}(\varphi_{1a}) = i'_{21}(\varphi_{1r}) = i'_{21}(2\pi) = 0$ (2.19)
- Tangents to the function graph in points $\varphi_1 \in \{0, \varphi_{1a}, \varphi_{1r}, 2\pi\}$, are parallel to the abscissa
- The function $\varphi_2(\varphi_1)$ is continuous, monotonically increasing in range $[0, 2\pi]$ and derivable ➡ $\varphi_{2s}(\varphi_{1a}) = \varphi_{2d}(\varphi_{1a})$; $\varphi'_{2s}(\varphi_{1a}) = \varphi'_{2d}(\varphi_{1a})$ $\varphi_{2s}(\varphi_{1a}) = \varphi_{2d}(\varphi_{1a})$; $\varphi'_{2s}(\varphi_{1a}) = \varphi'_{2d}(\varphi_{1a})$

where i_i is the intermediate value of the transmission ratio at the transition between the working and return phases. Thus, results the following values of the constants defining the transmission ratio and the rotation angle of the driven gear (Tab.2.4).

Tabel 2.4. *The defining constants of the non-circular gear kinematics - three phases working cycle and trigonometric variation of the transmission ratio*

$c_1 = \dfrac{a+b}{2}$	$c_2 = \dfrac{b-a}{2}$	$c_3 = \dfrac{\pi}{\varphi_{1a}}$	$c_4 = 0$	$ct_1 = 0$
$c_5 = \dfrac{a+i_i}{2}$	$c_6 = \dfrac{a-i_i}{2}$	$c_7 = \dfrac{\pi}{\varphi_{1r}-\varphi_{1a}}$	$c_8 = -\dfrac{\pi \cdot \varphi_{1a}}{\varphi_{1r}-\varphi_{1a}}$	
$ct_2 = \dfrac{b-i_i}{2} \cdot \varphi_{1a}$	$c_9 = \dfrac{b+i_i}{2}$	$c_{10} = \dfrac{i_i-b}{2}$	$c_{11} = \dfrac{\pi}{2\pi-\varphi_{1r}}$	
$c_{12} = -\dfrac{\pi \cdot \varphi_{1r}}{2\pi-\varphi_{1r}}$		$ct_3 = \dfrac{a-b}{2} \cdot \varphi_{1r} + \dfrac{b-i_i}{2} \cdot \varphi_{1a}$		

In order to obtain closed centrodes, the condition (2.10) is required, which leads to the interdependence of the significant values of the parameters that define the transmission ratio, respectively the minimum value a, the intermediate value i_i and the maximum value b:

$$b \cdot [2\pi - (\varphi_{1r} - \varphi_{1a})] + i_i \cdot (2\pi - \varphi_{1a}) + a \cdot \varphi_{1r} = 4\pi \ . \quad (2.22)$$

As an intermediate value, i_i satisfies the relation:

$$a < i_i < b \quad , \tag{2.23}$$

causing restrictions of the extreme value variation of the transmission ratio

Thus, the kinematic of the non-circular gear can be varied by means of four parameters: *a*, φ_{1a}, φ_{1r} și *b*.

Figures 2.16 to 2.19 show the influence of the defining parameters of the transmission ratio on gear kinematics variation.

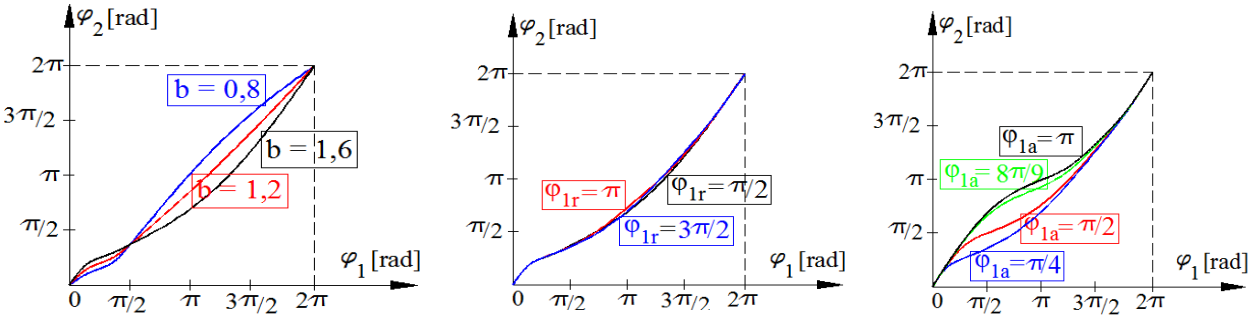

a) a = 0,4; $\varphi_{1a} = \pi/4$; $\varphi_{1r} = \pi/2$ b) a =0,4 ; $\varphi_{1a} = \pi/4$; b = 1,6 c) a = 0,4 ;$\varphi_{1r} = 3\pi/2$; b = 1,6

Fig. 2.17 Influence of the maximum transmission ratio *b* (a), angle φ_{1r} (b) and angle φ_{1a} (c) on the rotation angle of the driven gear

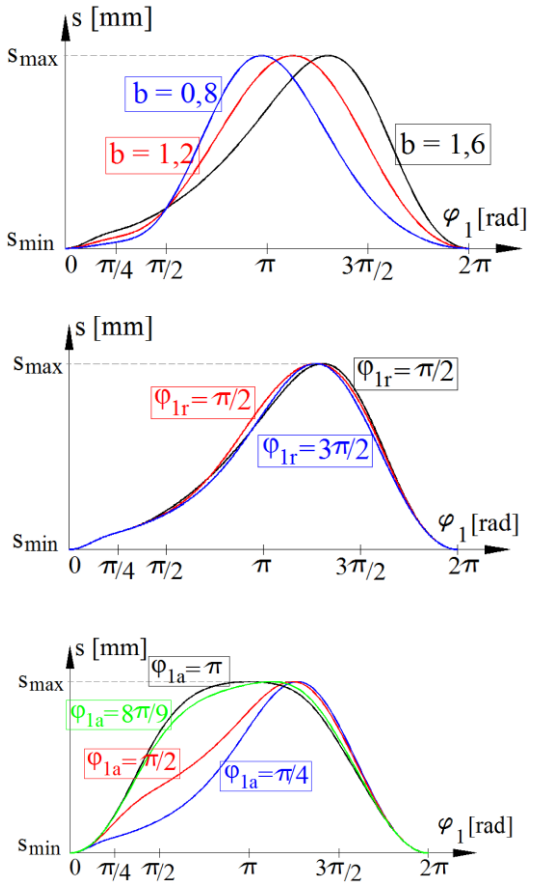

a)

a = 0,4
$\varphi_{1a} = \pi/4$
$\varphi_{1r} = \pi/2$

b)

a = 0,4
$\varphi_{1a} = \pi/4$
b = 1,6

c)

a = 0,4
$\varphi_{1r} = 3\pi/2$
b = 1,6

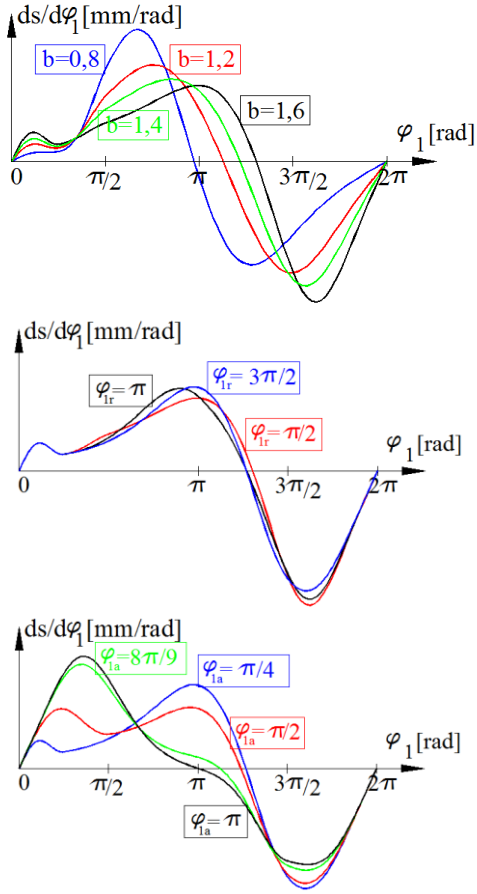

Fig. 2.18. Influence of the maximum transmission ratio *b* (a), angle φ_{1r} (b) and angle φ_{1a} (c) on the slide displacement

Fig. 2.19. Influence of the maximum transmission ratio *b* (a), angle φ_{1r} (b), and angled φ_{1a} (c) , on the slide speed

Studying the variation of kinematics of the crank-slider mechanism on the interval where the nail head is formed, the following combination is proposed as a desired version: ***a* = 0,4; *b* = 1,6; $\varphi_{1a} = 8\pi/9$; $\varphi_{1r} = 3\pi/2$**.

2.2.2.4. Three-phases working cycle with polynomial variation of transmission ratio

Another function that defines the transmission ratio of non-circular gear, in the hypothesis of the three-phase division of the rotation period of the movement, is:

$$i_{21}(\varphi_1) = \begin{cases} c_1 \cdot \varphi_1^3 + c_2 \cdot \varphi_1^2 + c_3 \cdot \varphi_1 + c_4, & \text{dacă } \varphi_1 \in [0, \varphi_{1a}] \\ c_5 \cdot \varphi_1^2 + c_6 \cdot \varphi_1 + c_7, & \text{dacă } \varphi_1 \in [\varphi_{1a}, \varphi_{1r}] \\ c_8 \cdot \varphi_1^2 + c_9 \cdot \varphi_1 + c_{10}, & \text{dacă } \varphi_1 \in [\varphi_{1r}, 2\pi]\,. \end{cases} \quad (2.25)$$

In order to achieve the desired variation for the transmission ratio, the same conditions are required, obtaining the values of the constants according to Table 2.6.

Figures 2.20 to 2.23 show the influence of the defining parameters of the transmission ratio, on the gear kinematics variation

Tabel 2.6. *The defining constants of the non-circular gear kinematics - three phases working cycle and polynomial variation of the transmission ratio*

$c_1 = \frac{2(b-a)}{\varphi_{1a}^3}$	$c_2 = \frac{-3(b-a)}{\varphi_{1a}^2}$	$c_3 = 0$	$c_4 = b$
$c_5 = \frac{p}{2(\varphi_{1r} - \varphi_{1a})}$	$c_6 = \frac{-p\varphi_{1a}}{\varphi_{1r} - \varphi_{1a}}$	$c_7 = a + \frac{p\varphi_{1a}^2}{2(\varphi_{1r} - \varphi_{1a})}$	
$c_8 = \frac{-p}{2(2\pi - \varphi_{1r})}$	$c_9 = \frac{2p\pi}{2\pi - \varphi_{1r}}$	$c_{10} = b - \frac{2p\pi^2}{2\pi - \varphi_{1r}}$	
$i_i = a + \frac{p}{2}(\varphi_{1r} - \varphi_{1a})$		$b = a + \frac{p}{2}(2\pi - \varphi_{1a})$	
$ct_1 = 0$	$ct_2 = \frac{1}{4}{\varphi_{1a}}^4 c_1 + \frac{1}{3}{\varphi_{1a}}^3(c_2 - c_5) + \frac{1}{2}{\varphi_{1a}}^2(c_3 - c_6) + \varphi_{1a}(c_4 - c_7) + ct1$		
$ct_3 = \frac{1}{3}{\varphi_{1r}}^3(c_5 - c_8) + \frac{1}{2}{\varphi_{1r}}^2(c_6 - c_9) + \varphi_{1r}(c_7 - c_{10}) + ct2$			
$p = \frac{24\pi(1-a)}{16\pi^2 - 4\pi\varphi_{1r} + 2\varphi_{1a}\varphi_{1r} - 6\pi\varphi_{1a} - \varphi_{1a}^2}$			

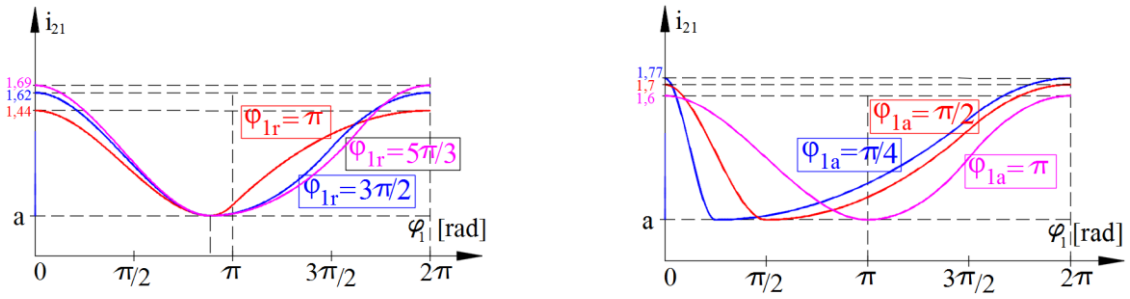

a) a = 0,4 ; $\varphi_{1a} = 8\pi/9$ b) a = 0,4 ; $\varphi_{1r} = 3\pi/2$

Fig. 2.20. Influence of the angle φ_{1r} (a) and angle φ_{1a} (b) on the transmission ratio

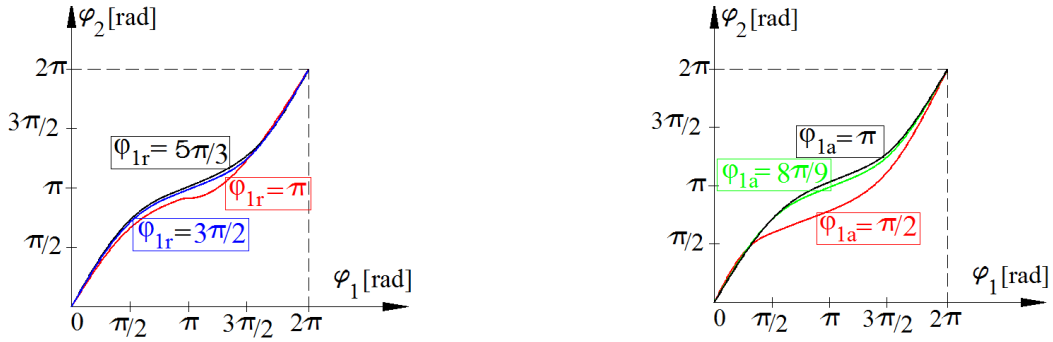

a) a = 0,4 ; $\varphi_{1a} = 8\pi/9$ b) a = 0,4 ; $\varphi_{1r} = 3\pi/2$

Fig. 2.21. Influence of the angle φ_{1r} (a) and angle φ_{1a} (b) on driven gear rotation angle

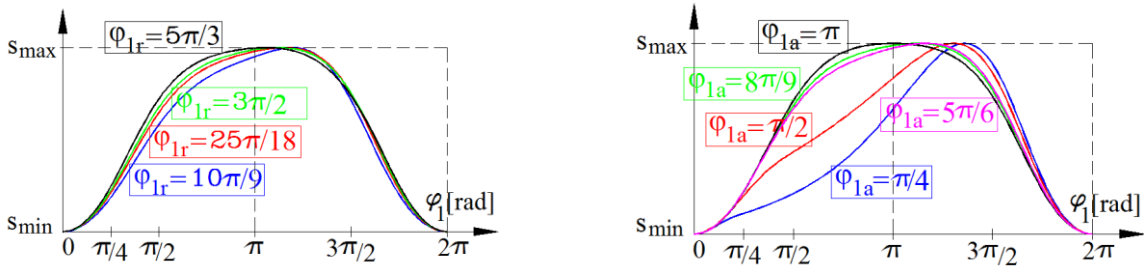

a) a = 0,4 ; $\varphi_{1a} = 8\pi/9$ b) a = 0,4 ; $\varphi_{1r} = 3\pi/2$

Fig. 2.22. Influence of the angle φ_{1r} (a) and angle φ_{1a} (b) on the slide displacement

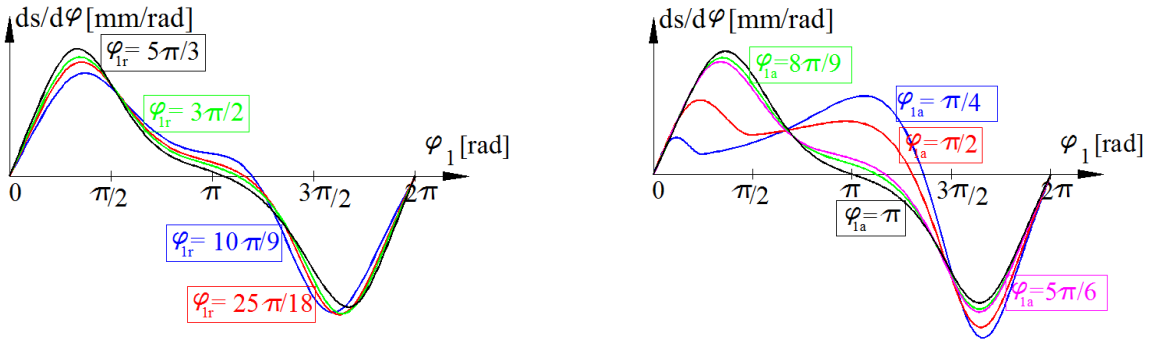

a) a = 0,4 ; $\varphi_{1a} = 8\pi/9$ b) a = 0,4 ; $\varphi_{1r} = 3\pi/2$

Fig. 2.23. Influence of the angle φ_{1r} (a) and angle φ_{1a} (b) on the slide relative speed

2.2.3. Comparative analysis of slide kinematics

In order to find the best solution for the slide kinematics, on the mentioned interval, was considered the variant chosen for each case studied and applied in case of nails type ϕ4 x 50 mm with a head diameter of 13 mm.

The defining parameters of the transmission ratio are: for the two-phases working cycle $\boldsymbol{\varphi_0 = 8\pi/9}$, $\boldsymbol{a = 0,4}$, $\boldsymbol{b = 1,6}$, and for the three-phases working cycle $\boldsymbol{\varphi_{1a} = 8\pi/9}$; $\boldsymbol{\varphi_{1r} = 3\pi/2}$, $\boldsymbol{b = 1,62}$; these parameters, as how results from the analysis from section 2.2, induce the desired kinematics for the forming process, resulting the nail head.

In Fig. 2.24 are shown the graphs of variation laws for the transmission ratio, i_{21}, slide displacement, s and slide relative speed, $ds/d\varphi$, in the four cases, for the above parameters. As can be seen, in case of the two-phase working cycle, the graphs of the two laws, trigonometric and polynomial, overlap almost completely, the differences being insignificant.

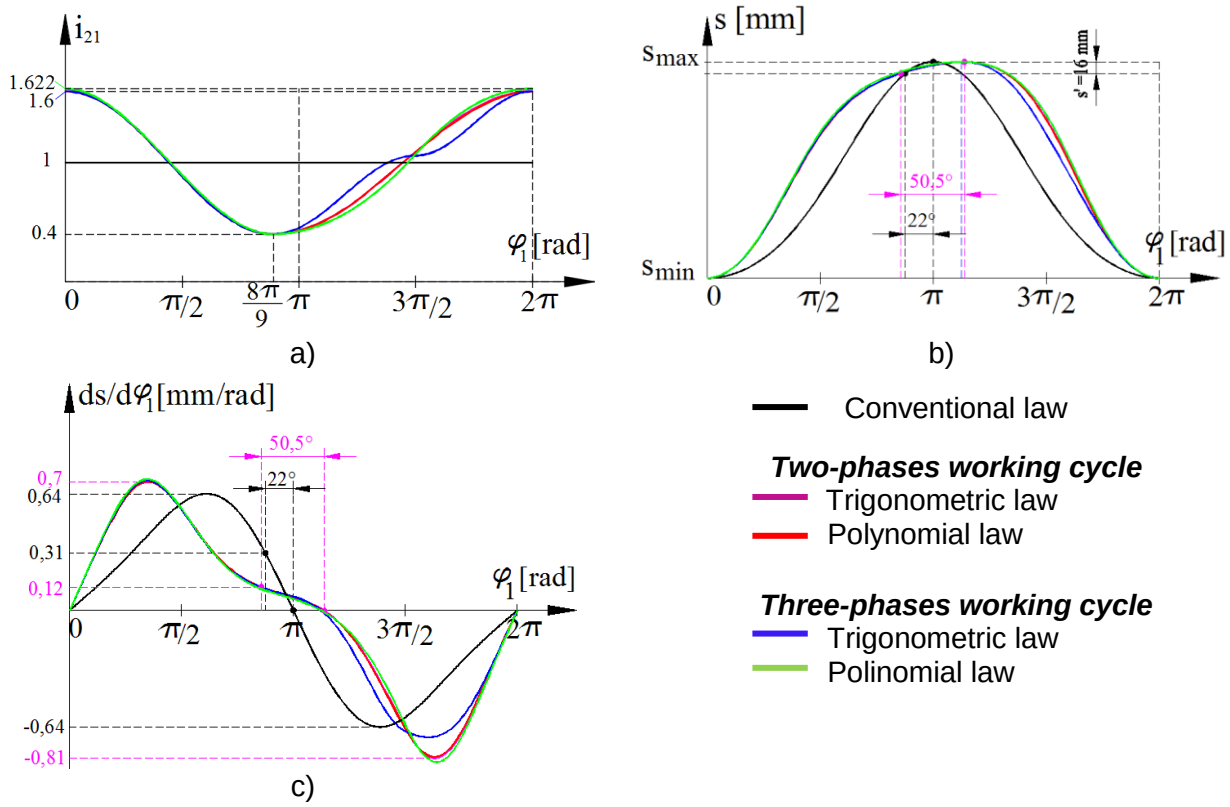

Fig. 2.24. Comparative analysis of the transmission ratio i_{21} (a), displacement s (b) and speed $ds/d\varphi$ (c) variation laws, for the parameters $\varphi_0 = 8\pi/9$; $a = 0,4$; $b = 1,6$; $\varphi_{1a} = 8\pi/9$; $\varphi_{1r} = 3\pi/2$

Comparing the proposed movement graphs with conventional motion graph, the advantages are obvious: the relative velocity at the beginning of the deformation decreases from $v' = 0,31$ mm/rad to $v'' = 0,12$ mm/rad, and the interval in which deformation occurs, increases from $d\varphi' = 22°$ to $d\varphi'' = 50,5°$, resulting accelerations of 6 times smaller. Regarding the slider motion outside of the studied range, there can be noticed increases of maximum speeds, more important on the two-phases working cycle, and increases of accelerations on the first half of the stroke, respectively on the second half of the return motion.

2.3. NON-CIRCULAR GEAR FOR MODIFICATION OF THE NAILS MACHINE KINEMATICS

2.3.1. Non-circular centrodes modeling

In the particular case of the non-circular gears that modify the kinematics of the crank-slider mechanism, determination of the centrodes / pitch curves of the gears is based on the hypothesis of the transmission ratio definition. In this case, according to the literature [1], if the variation law of the transmission ratio, i_{21}, and the distance between the centers of rotation, A, are known, defining the transmission ratio

$$i_{21}(\varphi_1) = \frac{d\varphi_2}{d\varphi_1} = \frac{r_1}{r_2} = \frac{r_1}{A - r_1}\ , \tag{2.28}$$

the following expression is obtained for the radius of the driving centrode:

$$r_1(\varphi_1) = \frac{A}{1 + i_{21}(\varphi_1)}\ , \tag{2.29}$$

where r_1, φ_1 are the polar coordinates of the current point from the centrode (Fig. 2.25).

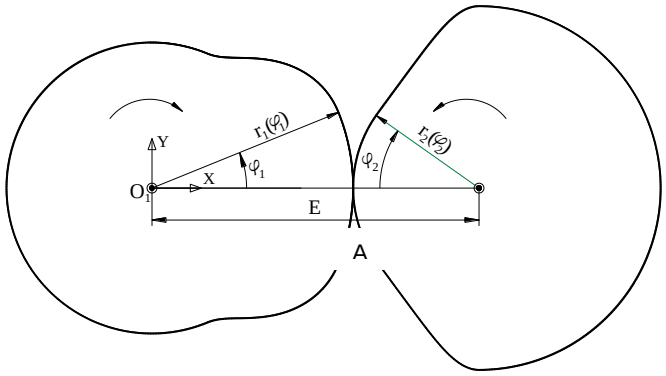

Fig. 2.25. Rolling of the mate non-circular centrodes [72]

The driven centrode is defined by the equation:

$$r_2(\varphi_2) = A\frac{i_{21}(\varphi_1)}{1 + i_{21}(\varphi_1)} \tag{2.30}$$

where φ_2 is the polar angle of the centrode, calculated with relation (2.6).

Starting from the variation of the transmission ratio and analysis from section 2.2.2, equations (2.29) and (2.30) will define the centrodes / pitch curves of the non-circular gears proposed in the kinematics of the MCC 337 nails machine. Figure 2.26 shows the pitch curves obtained for the variation of the transmission ratio, i_{21}, following a trigonometric law (2.9), and two-phases, respectively three-phases working cycle.

The modeling process of the centrodes was carried out in the graphical environment of AutoCAD, based on an original AutoLISP code (Appendix 1).

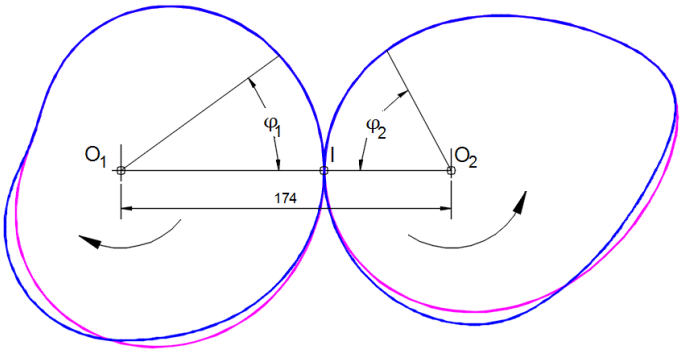

Two-phases working cycle, trigonometric law, φ_0 = **8π/9; *a* = 0,4; *b* = 1,6**

Three-phases working cycle, trigonometric law, ***a* = 0,4; *b* = 1,6; φ_{1a} = 8π/9; φ_{1r} = 3π/2**

Fig. 2.26. Non-circular centrodes for crank-slider driving mechanism

2.3.2. Non-circular gears teeth generation

To generate the teeth flanks, the rolling method, described in an analytical way, was applied [73]; it consider the local geometry of the centrodes and a tooth of the generating rack with standard geometry, running on the non-circular pitch curve. The tooth flank is defined as a set of intersection points between the instantaneous meshing line and the active flank of the rack tooth.

The gear teeth are disposed by considering a constant pitch on the curve (the length of the curve is divided by the number of teeth); as a result, due to the complex geometry of the curve, the teeth module is a real, non-standardized number, irrelevant in later processing of the gears, by unconventional technologies.

To generate the tooth flank, all the rolling movements are transferred to the tooth of the generating rack. The point from the tooth flank results as the intersection between meshing line $(la)_{ij}$ and rack tooth flank. Figure 2.27 details the generation of the gear tooth flank and allows the tooth flank coordinates to be expressed relative to the coordinate system attached to the driving gear, $O_1x_1y_1$:

The top area of the tooth active flank is the geometric location of the points F_{ij}, whose coordinates are expressed by (Figure 2.27 b):

$$\begin{aligned} x_{1ij} &= r_1(\varphi_{1ij}) \cdot \cos\varphi_{1ij} - s_{ij} \cdot \cos\alpha \cdot \cos(\mu_{ij} + \alpha + \varphi_{1ij}) \\ y_{1ij} &= r_1(\varphi_{1ij}) \cdot \sin\varphi_{1ij} + s_{ij} \cdot \cos\alpha \cdot \sin(\mu_{ij} + \alpha + \varphi_{1ij}) \,, \end{aligned} \tag{2.34}$$

where r_{1ij}, φ_{1ij} are the polar coordinates of the instantaneous rotation center P_{ij}, s_{ij} - the rolling distance along the tangent $(tg)_{ij}$, μ_{ij} - the angle between the current tangent and the position vector O_1P_{ij} ; α - standard pressure angle (20^o).

A same algorithm allows expressing the root segment of the active tooth flank as a locus of the points F_{ij}, defined by:

$$\begin{aligned} x_{1ij} &= r_1(\varphi_{1ij}) \cdot \cos\varphi_{1ij} + s_{ij} \cdot \cos\alpha \cdot \cos(\mu_{ij} + \alpha + \varphi_{1ij}) \\ y_{1ij} &= r_1(\varphi_{1ij}) \cdot \sin\varphi_{1ij} + s_{ij} \cdot \cos\alpha \cdot \sin(\mu_{ij} + \alpha + \varphi_{1ij}) \,. \end{aligned} \tag{2.35}$$

To define the inactive flank of the tooth, repeat the previous procedure considering that the generation will be with the other flank of the rack tooth, and the rolling changes its meaning.

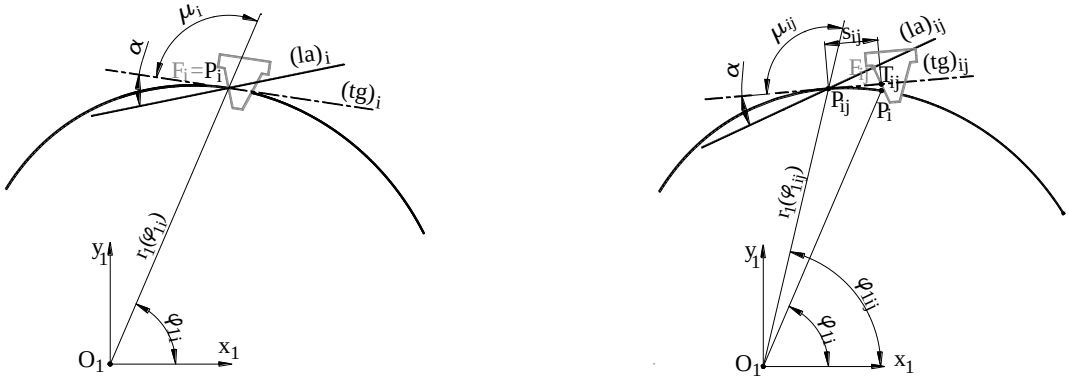

a) Initial generation position b) Generation of the top tooth - active flank

Fig. 2.27. Generating the tooth of the driving gear

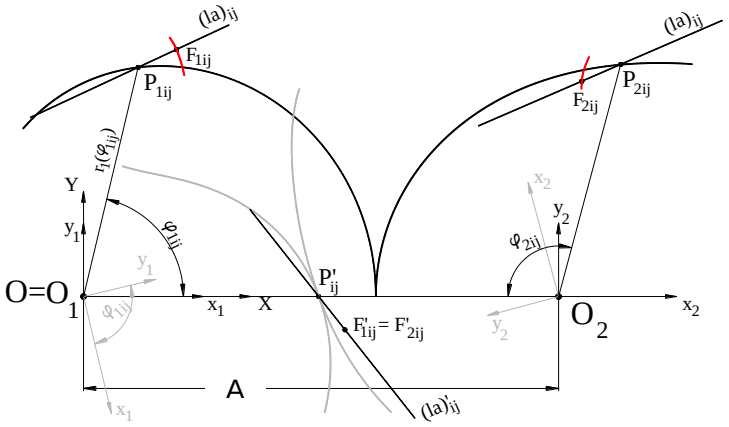

Fig. 2.28. Generation of the driven gear tooth flank

Starting from the profile of the driving gear tooth flank, the mating profile of the driven gear tooth is analytically expressed, considering the meshing of the gears [13] and the coordinate transformations by rotation and translation, respectively. Thus, the coordinates of the current points F'_{2ij} from the driven gear tooth flank, are:

$$\begin{bmatrix} x_{2ij} \\ y_{2ij} \end{bmatrix} = \begin{bmatrix} \cos\varphi_{2ij} & \sin\varphi_{2ij} \\ -\sin\varphi_{2ij} & \cos\varphi_{2ij} \end{bmatrix} \cdot \left(\begin{bmatrix} -A \\ 0 \end{bmatrix} + \begin{bmatrix} \cos\varphi_{1ij} & \sin\varphi_{1ij} \\ -\sin\varphi_{1ij} & \cos\varphi_{1ij} \end{bmatrix} \cdot \begin{bmatrix} x_{1ij} \\ y_{1ij} \end{bmatrix} \right), \quad (2.38)$$

where φ_{2ij} is the angle of rotation corresponding to the driven gear; A – distance between axes.

An original AutoLISP code (Appendix 2) automatically generates the profile of the non-circular gears tooth flanks, with a number of teeth $z_1 = z_2 = 36$, within a predetermined rolling distance, chosen to ensure full flank generation.

The transverse sections of the wheels (Figure 2.29), by extrusion, allow the solid gear model to be generated (Figure 2.31). A comparison of the teeth profiles in the two cases is shown in Fig.2.30. Note that, the teeth are similar as profile shape, due to the fact that the centrodes, in the two cases, differ only on the return stroke of the slide.

The virtual models of the gears are shown in Fig. 2.31. The width of the wheels is set to B = 50 mm.

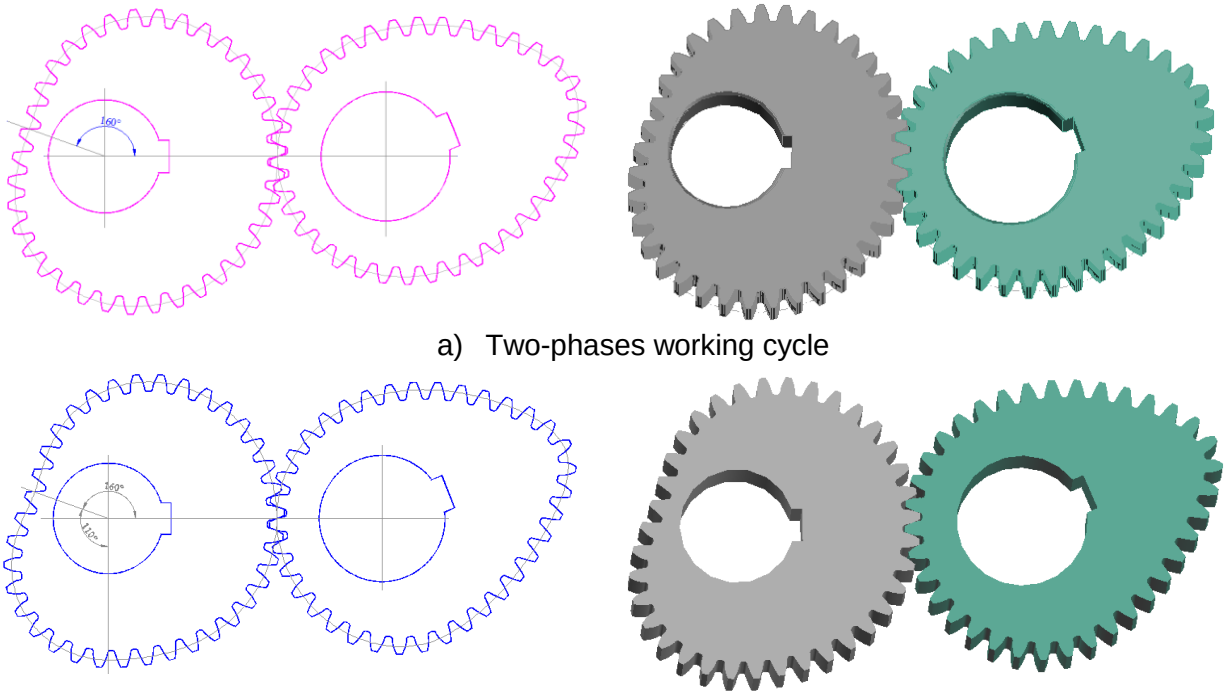

a) Two-phases working cycle

b) Three-phases working cycle

Fig.2.29. Cross section of non-circular gears with trigonometric variation of the transmission ratio

Fig. 2.31. Models of the non-circular gear with trigonometric variation of the transmission ratio, for the crank-slider mechanism

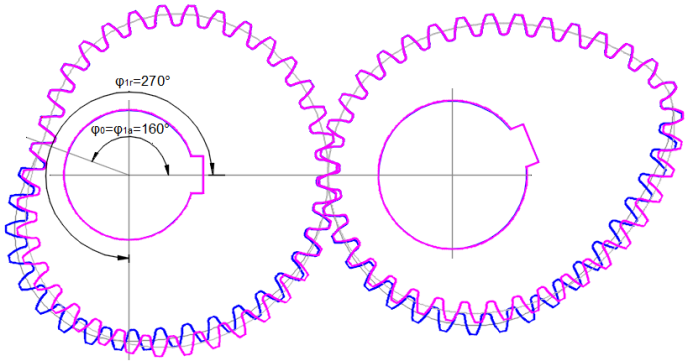

Fig. 2.30. Comparison of teeth in the two-phases and three-phases work cycle, respectively: Two-phases working cycle; Threee-phases working cycle

2.3.3. Meshing analysis

2.3.3.1. Analysis of teeth contact

The analysis of the static contact surface between the teeth, was done in each of the two cases (trigonometric law, working cycle with two and three-phases) for the D1 and D27 teeth pair, respectively (Figure 2.32), these teeth being located in the areas of the centrodes that modify their geometry, according to the defining laws of transmission ratio in phases 3 and 1, respectively 2 and 3. The analysis also extended to the neighboring teeth, highlighting the contact surfaces between the teeth that mashe in the same time. Fig. 2.32 shows the non-circular gears areas aimed in meshing.

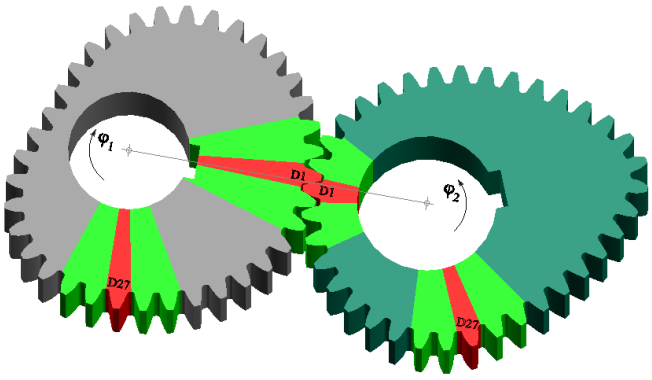

Fig. 2.32. Highlighting analyzed teeth as respect to contact

Illustration of the contact patch and its distribution pattern was obtained using solid gear models in AutoCAD graphical environment, following the algorithm (Fig. 2.33) [74]:

a) The considered teeth pair was put in meshing, on the centers line, rotating the driving gear with angle $\boldsymbol{\varphi}_1$ and the driven gear with the angle $\boldsymbol{\varphi}_2$, calculated with realation (2.20) (Fig. 2.33a);
b) The driving gear has been rotated at an angle of 0.005 ° to create a minimum torque so that the contact patch appears. (Fig. 2.33b);
c) The driving gear has been rotated incrementally in increments of 1° and the driven gear with the corresponding angles calculated so that the rolling is made over the entire length of the considered tooth pair active flanks. Figure 2.33c illustrates particular positions of meshing;
d) Intersecting every time the gears solid models, results the static contact patch, and the number of teeth pair, that are simultaneous in meshing.

Using AutoCAD facilities, they were gathered the data on the contact area, as the area of the solid resulting as a intersection between the solid models of the two wheels, for each

individual position. Based of these data, and using EXCEL soft, were generated the graphs of the size and distribution of the contact patch in the analyzed cases.

Fig. 2.34- 2.37 illustrates the evolution and size of the contact patch on the driving wheel for the two pairs of teeth, D1 and D27, and in the two design hypotheses.

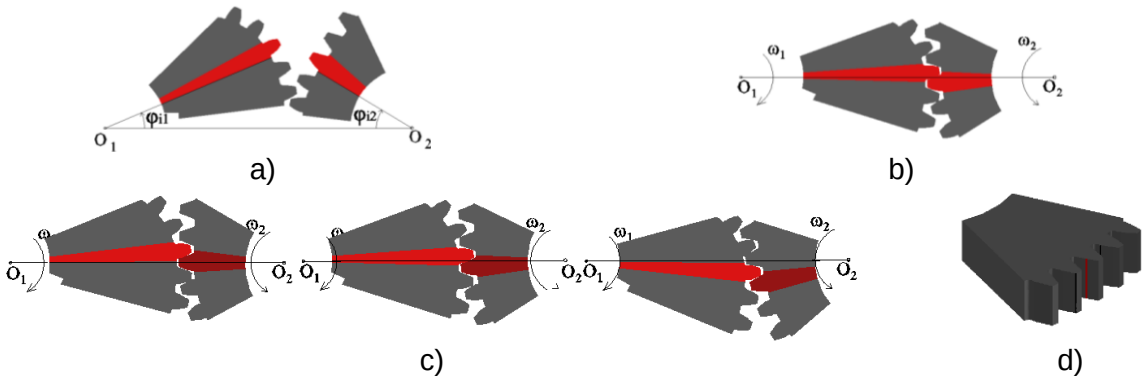

Fig 2.33. Algorithm for studying the static contact patch of non-circular gears [74]

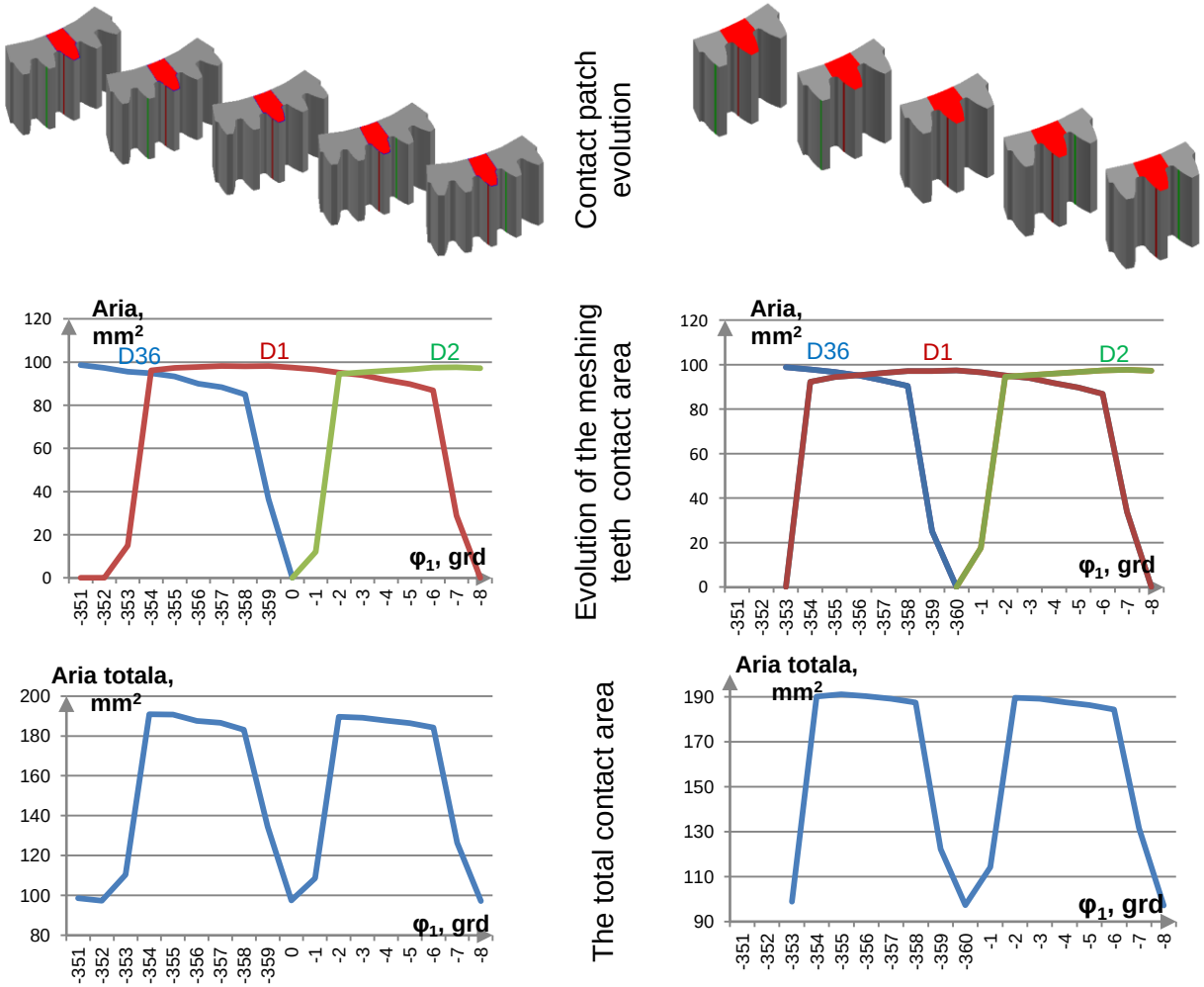

Fig. 2.34. Contact patch for D1 teeeth pair in case of the two-phase working cycle and trigonometric variation of the transmission ratio

Fig. 2.35. Contact patch for D1 teeeth pair in case of the three-phase working cycle and trigonometric variation of the transmission ratio

Analysing the above graphs, the following can be observe:
- the distribution and size of the contact patch is similar in both cases. On the entire meshing of the tooth D1, there are two teeth in contact, excepting the case, when center of rotation is on the center line, in which case the tooth D1 is meshing alone and takes up the entire load;
- the contact patch area is uniformly distributed over each of the three teeth, the total area having a minimum point at the point where the tooth D1 is single in mashing;
- with respect to the meshing start time of the D1 pair, a difference of about 1 ° can be seen due to the different position of the root of tooth D1;
- no interference has occurred during meshing, which confirm the correct generation of gear tooth.

Considering the above analysis, it can be concluded that there are no significant differences between the two cases, the quality of meshing being neither qualitatively nor quantitatively influenced.

In the same way, was performed the contact patch analysis, for the D27 and adjacent teeth pairs, in the two cases. Considering the meshing of the D27 teeth pair and the adjacent teeth, the situation is different from the case of the meshing the D1 teeth pair. If, in the case of the two-phases working cycle, the graphs are similar to the previous situation, in the case of the three-phases working cycle, the situation changes, both the distribution and the size of the patch being variable. For a correct comparison and better differentiation, the graphs obtained above for the D27 teeth pair and the adjacent pairs, were overlapped (Fig. 2.38).

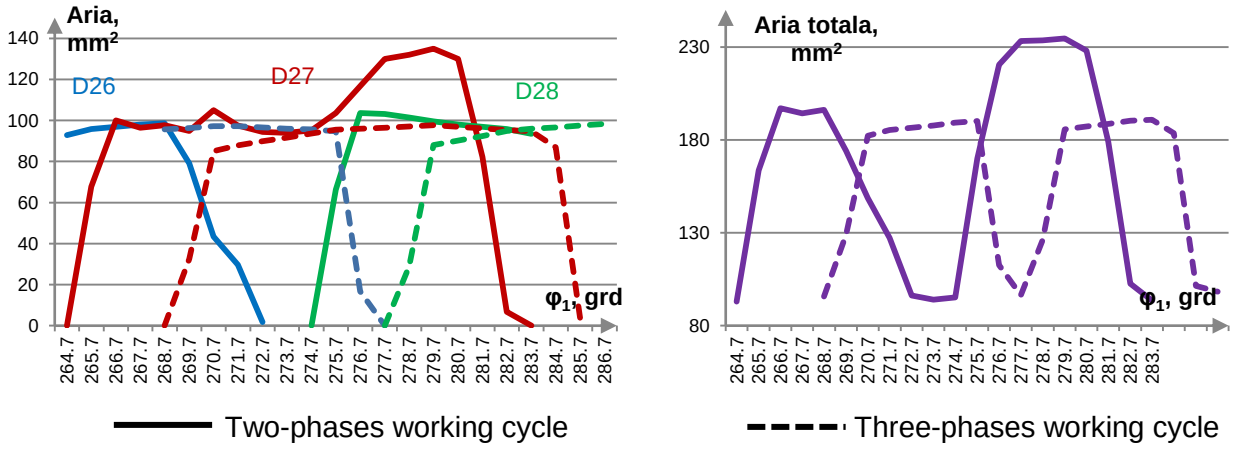

Fig. 2.38. Comparative analysis of the contact area, during the meshing of the D26, D27 și D28 teeth

2.3.3.2. Static analysis of stress and strain distribution

Since, non-circular gears are complex machine parts, with variable geometry, the approach of the stress and strain distribution can't be achieved by standardized methods, the finite element method (FEA) being the only solution.

The study will be performed in AutoDesk Inventor [75], [76], [77] on solid models imported from AutoCAD [78], [79] taking into account the characteristics of the virtual environment used:: stress and strain are directly proportional with the load, and force application is static, without taking into account the effects of dynamic loads (inertia forces, weight, etc.).

The static analysis of stress and strain distribution is performed for each of the two cases presented in Section 2.3.2, i.e. trigonometric variation of the transmission ratio, with a working cycle divided in two and three phases, repectively. The study highlights the influence of the

centrode shape on the stress and strain distribution that occurs in the driving gear during the nail head forming phase.

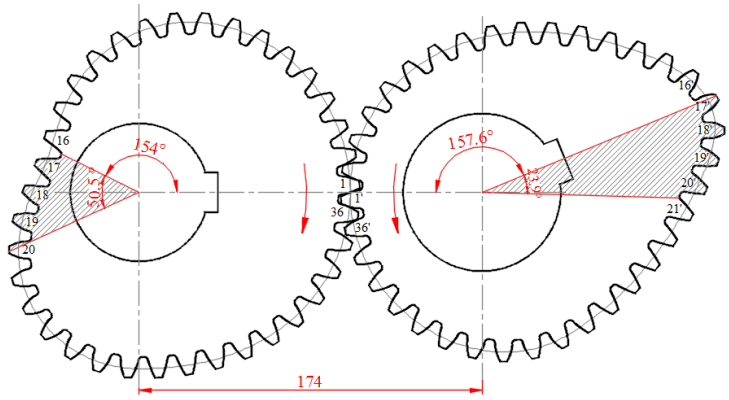

Fig. 2.39. Highlighting the area corresponding to the nail head forming phase

The FEA simulation is performed on a driving gear tooth, positioned on the non-circular area of centrode, in the area corresponding to the wire cold heading phase (Fig.2.39), where the meshing forces are maximum.. As can be seen in Fig. 2.39, the cold forming of the material takes place during the rotation of the driving gear with an angle of approximately 50.5 ° and the driven gear with an angle of 23.9°. Taking account that the radius of the driving gear is minimal at the begining of the phase, so the meshing force is maximum, will analyse the tooth no. 18.

In the AutoDesk Inventor working environment, FEA analysis involves the following steps:

1. Importing, from Inventor, of the driving gear cross section, edited in AutoCAD (Figure 2.29), and solid model generation (Figure 2.40);

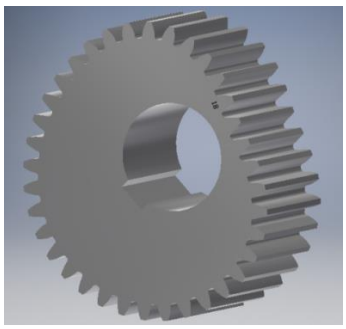

Fig. 2.40. Solid model of the driving gear generated in AutoDesk Inventor

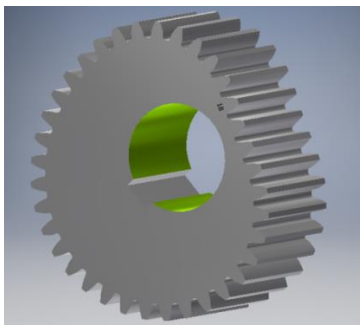

Fig. 2.41. Constraint of the gear hub

2. Choosing the gear material. An alloy steel was chosen with a flow limit of 350 MPa and a stress limit of 420 Mpa;

3. Establishing the constraints and the degrees of freedom. The gear hub is set (Fig. 2.41) with a single degree of freedom: rotation around the Ox axis (rotation axis);

4. Determining the structure of the finite elements (Fig 2.42):

- Number of nodes: 778114, number of finite elements: 498993;
- The average size of the finite element (as fraction of the framing space): 0,1;
- The minimum size of the finite element (as fraction of the average aize): 0,2 ;
- Maximum rotation angle of the element: 60°;

5. Positioning the force, on the crown of the studied tooth (Figure 2.43), normal on the surface of the tooth, in the direction of the meshing line, and acting on the entire width of the tooth;

6. Simulation of meshing, generation and retrieval of Von Misses stress distribution, strain field, and safety factor distribution (Figures 2.46, 2.47).

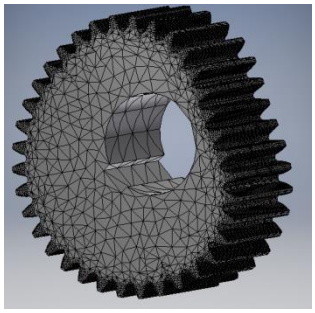

Fig. 2.42. Partition of the model into finite elements

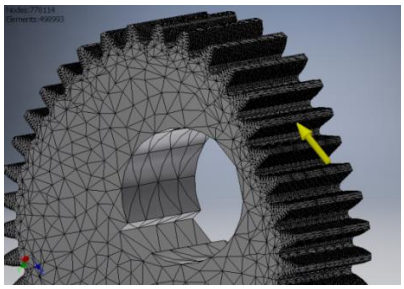

Fig. 2.43. Force positioning during meshing, assuming uniparous meshing

For the calculation of the force applied on the tooth, it was considered, for the first time, the maximum force required to cold-heading, for material forming, with formula [82], [83]:

$$F_{max} = k \cdot a \left(1 + \frac{\mu D}{3 H}\right) \cdot A \cdot R_{def} \quad \text{[N]} \ , \tag{2.39}$$

where (Fig. 2.44) *k* is a coefficient that depends on the complexity of the piece shape (*k* = 1,1....1,3), *a* – coefficient which takes into account the mechanical forming scheme (*a* = 1,25...1,75), *D* – diameter of cold-headed head [mm], *H* – high of cold-headed head [mm], *A* – cross section of the cold-headed head [mm], *μ* – friction coefficient of the blank in the active die area (μ = 0,1 ...0,15), R_{def} - forming resistance of the processed material [N/mm^2].

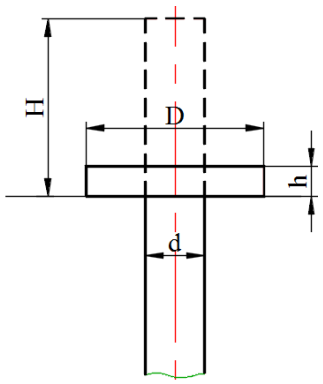

Fig. 2.44. Schema procesului de refulare, în cazul formării capului cuiului [82]

It choose the nail type Ø4 x 100 for which, according to GOST 4028-63, the diameter of the nail shank is d = 4 mm, the diameter of the nail head is D = 7.5 mm and the head height is h = 1.5 mm. With these elements, according to the law of volume constancy in the case of cold-heading [84], [85], [86], the height H = 5,27 mm is calculated. Having these elements and adopting the following values for coefficients: k = 1,1; a = 1.25; μ = 0,1 and for R_{def} = 500 N / mm^2, the maximum forming force value is obtained, F_{max} = 35435 N. Knowing the constructive elements of the crank-slider mechanism [50], results the following values for crank force and torque: ***F_t* = 15768,5 N** ; ***M_t* = 2365275 Nmm.** The calculated torque required for the driven non-circular gear $M_{t2} = M_t$, corresponds to a torque at the driving gear ***M_{t1}* = 1031260 Nmm**, considering that at the meshing time of teeth 18 - 18 ', the transmission ratio of the non-circular gear is i_{21} = 0.436. Thus, results the following values for the force applied on the tooth (Tab.2.7):

Tabelul 2.7. *The value of the force applied on the driving gear tooth no.18*

Place of application	Two-phases working cycle	Three-phases working cycle
Midle of the tooth	20016,7 N	19531,4 N
Top of the tooth	18220,1 N	17780,3 N

In Fig. 2.46 and 2.47 are shown the results of the FEA simulation in the two cases of the working cycle: three or two phases.

In order to compare the analyzed cases, in Fig. 2.48 ÷ 2.50 are shown the graphs of the maximum values of the analyzed parameters, according to Tab. 2.8

Tabelul 2.8. *The extreme values of the analyzed parameters, by FEA, - no.18 -18 ' tooth meshing*

Working cycle	Place of meshing 18 – 18’	Maximum Von Misses stress, [MPa]	Maximum displacement, [mm]	Minimum safety factor
Three-phases	midle	198,9	0,006609	1,76
Two-phases		205,9	0,007091	1,7
Three-phases	top	205,4	0,0148	1,7
Two-phases		216,8	0,0155	1,61

Comparing the maximum Von Mises stress, it can conclude that, they are higher in the case of the two-phase working cycle, this is explained by the shape of the centrode in the analyzed area, which has larger radii. Higher stres values are also recorded at the top of the tooth compared to the middle area but without significant differences.

After the static analysis of stress and strain distribution, it can conclude that, in the two design hypotheses, the gear has similar behaviors, a slight advantage being recorded in the case of the three-phases working cycle.

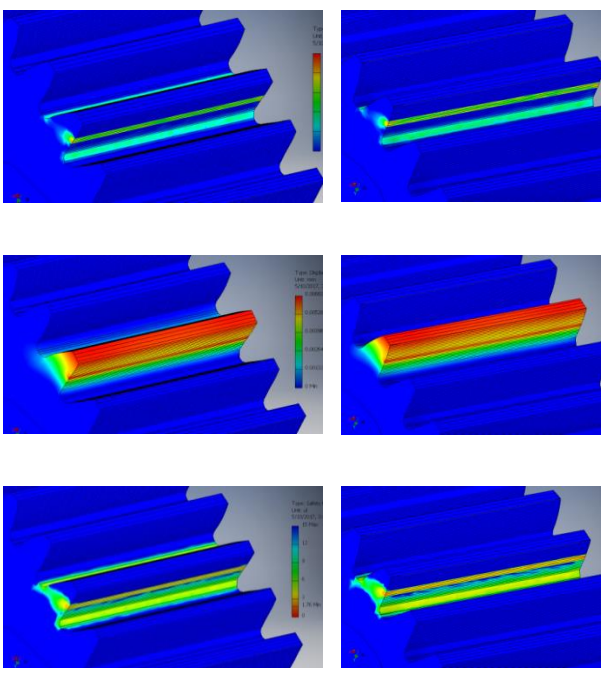

a) Three-phases working cycle

b) Two-phases working cycle

Fig 2.46. Von Mises stress, displacement and safety factor distribution, in case of meshing on the no. 18 tooth middle.

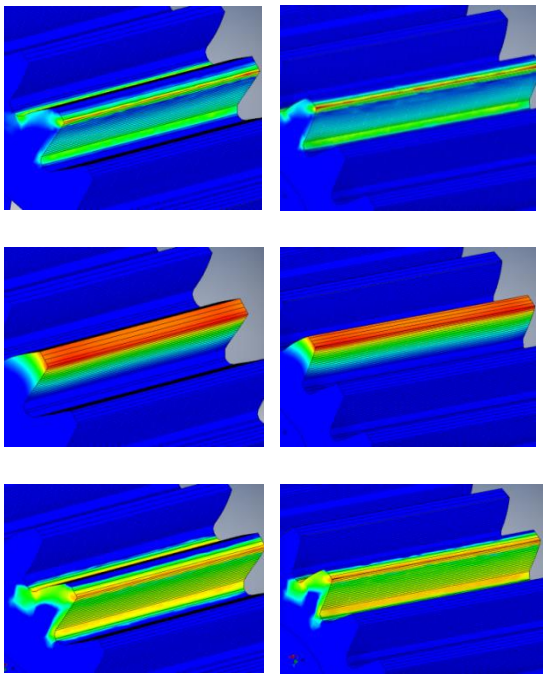

a) Three-phases working cycle

b) Two-phases working cycle

Fig 2.47. Von Mises stress, displacement and safety factor distribution, in case of meshing on the no. 18 tooth top

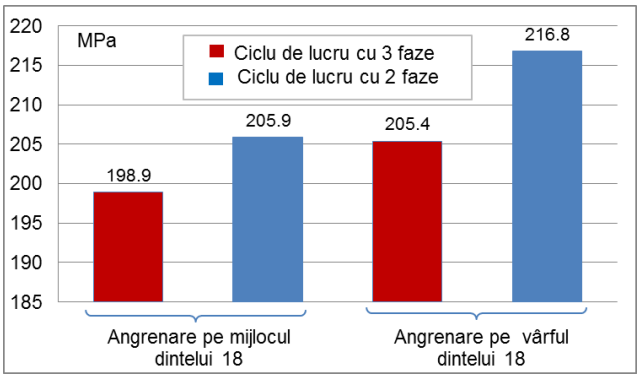

Fig 2.48. Comparison of the maximum Von Mises equivalent stress (static analysis)

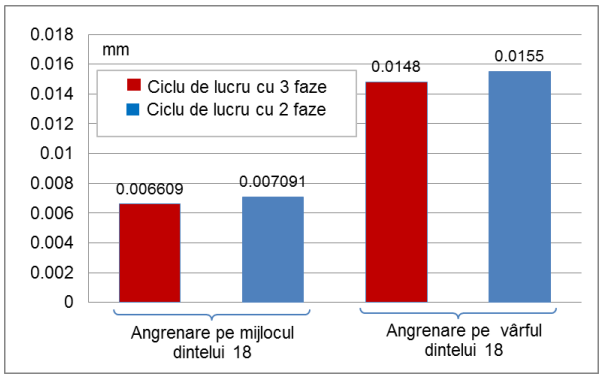

Fig. 2.49. Comparison of the maximum displacements (static analysis)

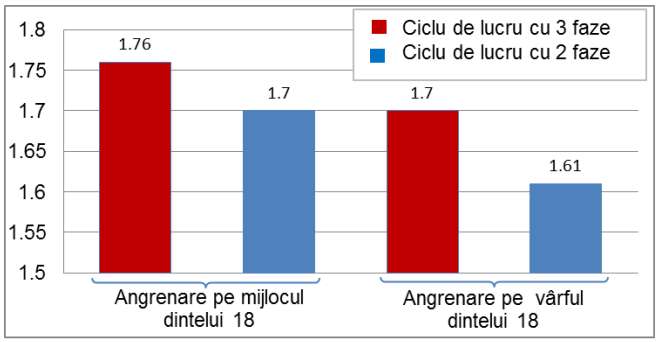

Fig 2.50. Comparison of the minimum safety factor (static analysis)

2.3.3.3. Dynamic analysis of the stress and strain distribution

In contrast with the static stress and strain analysis by the FEM method, the dynamic simulation eliminates the errors that may occur in the first case, as a result of the correctness of the hypothesis seted for defining the calculation model. Thus, the dynamic simulation created in Inventor takes into account the joints defined by the designer to determine interactions between components but also kinematic constraints such as [87]: gravitational force, inertia forces, interaction forces between components, friction forces, imposed forces, torsional moments, etc. The analysis of the performance of non-circular gears meshing by dynamic simulation is performed based on the following algorithm:

- Build the assembly to achieve dynamic simulation in Inventor (Fig. 2.51);
- Imposing the mechanical constraints on the components: the casing is fixed, without any degree of freedom, the shafts have a single degree of freedom - the rotation around their own axis, and the gears are fixed on the shafts without any degree of freedom from them;
- To perform the simulation, a resistant torque to the driven shaft and a driving torque on the driving shaft, both equal to 1031260 Nmm, are added.
- Performing the dynamic simulation and analysis of the results based on the output specific to the movement: the position of the gears (Fig 2.52), the variation of the rotation speeds (Fig 2.53) and the variation of the two gears accelerations (Fig 2.54);
- Data obtained from dynamic simulation is exported for FEA analysis.

The dynamic simulation was performed in the case of the three-phases non-circular gears whose transmission ratio varies according to the law defined above (ec. 2.21).

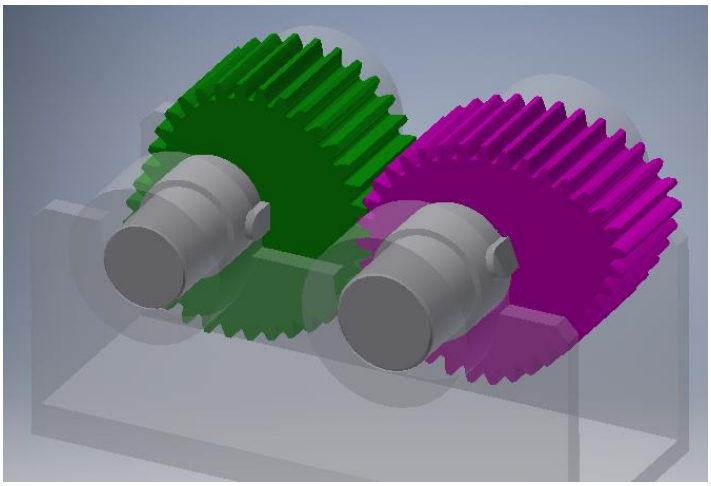

Fig. 2.51. The assembly used to perform dynamic simulation in Inventor

Analyzing the graphs of angular speeds (Fig.2.53) and accelerations (Fig.2.54), it can be noticed that, following the dynamic simulation for the three-phases working cycle, the same kinematics data as the required data, was obtained. This, confirms the correctness of the design of non-circular gears, whose kinematics corresponds to the conditions initially imposed.

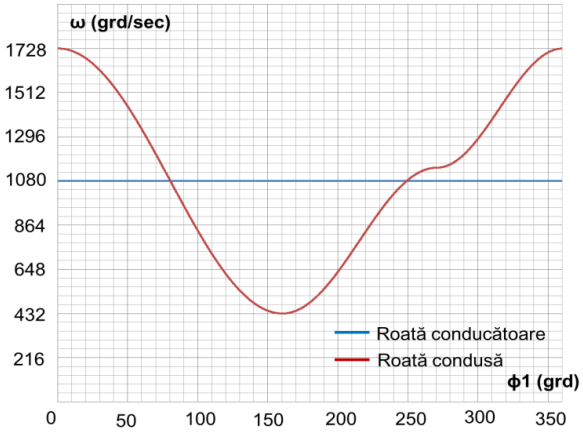

Fig. 2.53. Variation of angular speeds obtained by dynamic simulation in Inventor for the three-phases working cycle

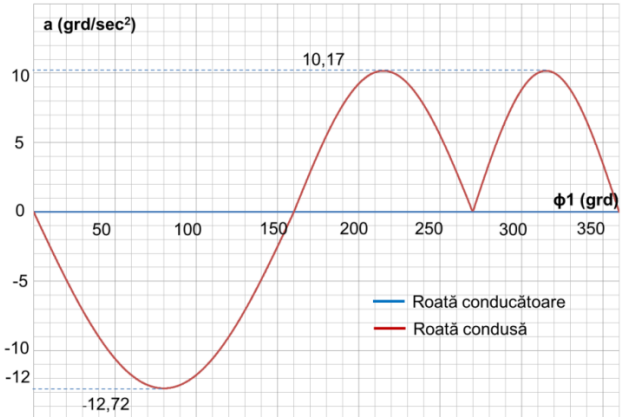

Fig. 2.54. Variation of acceleration obtained by dynamic simulation in Inventor for the three-phase work cycle

FEM analysis was performed in two cases: meshing on the middle of the tooth 18 and on the top of he tooth 18, respectively, on each of the two wheels (Fig. 2.56, 2.58). After the analysis, it can be concluded that the meshing is correct, variations occurring on the height of the tooth, with maxims in the middle area where the meshing is uniparous. .

Based on the maximum values of the analyzed parameters (Table 2.9), the comparative graphs from Fig. 2.59, 2.60 and 2.61, were drawn. Their analysis leads to the conclusion that, on the analyzed area, the driving gear is the most stressed with a minimum safety factor of low value.

The results obtained with the dynamic analysis of stress and strain distribution differ from those obtained with static analysis. It is obvious that dynamic simulation delivers high precision results because it takes into account both the meshing mode and the other forces involved in the interaction between the two gears.

Tabelul 2.9. *The extreme values of the parameters analyzed by FEA, using the data obtained from the dynamic simulation in the case of the 18-18' tooth meshing*

Analysed parameters	Tooth no.18	Tooth no. 18'
Meshing on the middle of the tooth no.18 (uniparous meshing)		
Maximum Von Mises stress,[MPa]	246,6	158,6
Minimum safety factor	1,42	2,21
Maximum displacements, [mm]	0,04335	0,01752
Meshing on the top of the tooth no.18 (biparous meshing)		
Maximum Von Mises stress,[MPa]	109,9	145,6
Minimum safety factor	3,18	2,4
Maximum displacements, [mm]	0,0512	0,0216

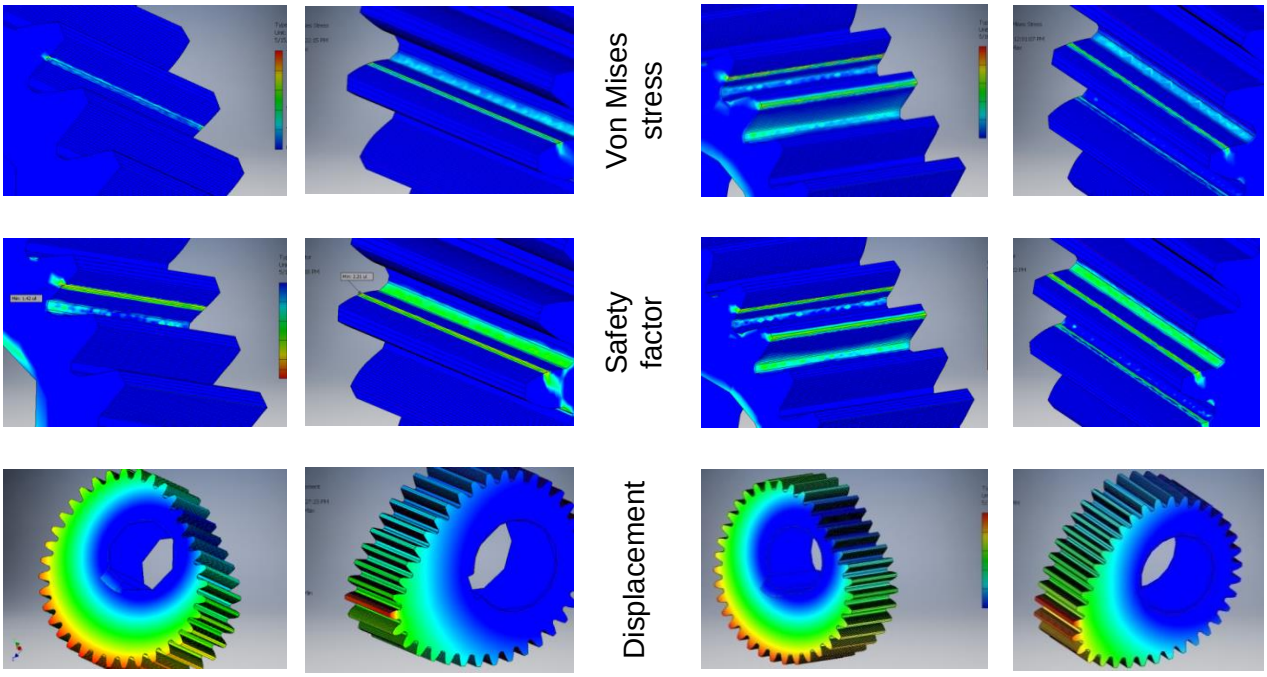

a) Driving gear b) Driven gear

Fig 2.56. FEM Dynamic Analysis, in case of meshing on the middle of the driving gear tooth no.18

a) Driving gear b) Driven gear

Fig. 2.58. FEM Dynamic Analysis, in case of meshing on top of the driving gear tooth no.18

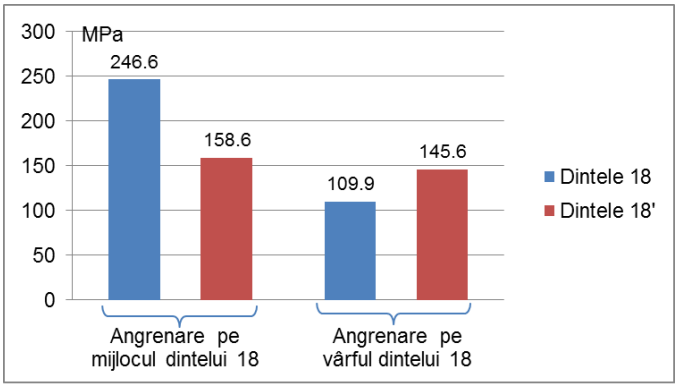

Fig 2.59. Comparison of the maximum Von Mises equivalent stress (dynamic analysis)

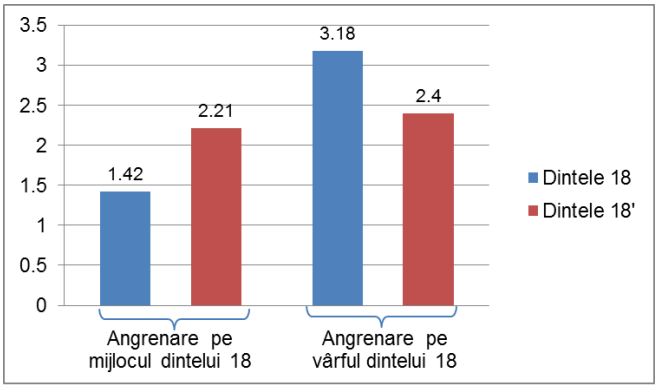

Fig. 2.60. Comparison of the minimum safety factor (dynamic analysis)

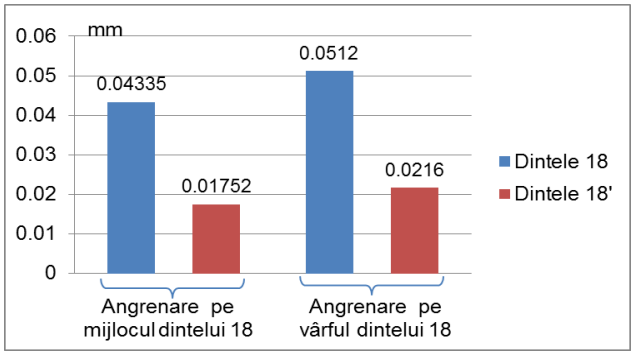

Fig 2.61. Comparison of the maximum displacements (dynamic analysis)

2.4. CONCLUSIONS

Chapter 2 presents the results of the research on the modification of the crank-slider kinematics for a classic nails machine using a non-circular gear in order to improve the cold plastic deformation process, during the nails head forming phase**.** The modified kinematics aims the decreasing of the initial deformation velocity and increasing the time interval in which the deforming force is applied.

The proposed modifications are aimed at achieving the following advantages: low degree of the wire hardening, which offers the possibility of extending the range of nails dimensions made on the machine, increasing the capacity of the machine for normal nails, better product quality and eliminating scrap, increased reliability of tools, increased stability of the plastic deformation process and noise reduction.

There were considered two laws of transmission ratio variation: trigonometric and polynomial, dividing the working cycle into two, respectively three phases. Four designing hypotheses were thus obtained. Starting from the proposed definition laws of the transmission ratio, significant parameters have been set, that alter the kinematics of the crank-slider mechanism: the rotation angles of the driving gear, which delimit the working phases (φ_0, φ_{1a}, φ_{1r}) and the minimum transmission ratio (*a)*, studying the influence of these parameters on the displacement and on the relative speed of the mechanism. It founded that, with increasing the value of the working phases dividing angle through the median value π, convenient values of the slide displacement and speed are obtained. It is also desirable to have as little as possible minimum transmission ratio, but, for constructive reasons, it can not be greatly reduced.

Following the analysis, convenient values were chosen for the defining parameters of the transmission ratio ($\varphi_0 = 8\pi/9$; $\varphi_{1a} = 8\pi/9$; $\varphi_{1r} = 3\pi/2$; $a = 0{,}4$) which modifies the kinematics of the process in the phase of the nail head forming, without substantially affecting the kinematics of the other movements in the working cycle.

Studying the charts of the displacement and the relative speed variation of the slide, it was concluded that in the case of the two-phases working cycle, variations in displacement and velocity, according to trigonometric law, are similar to variations according to the polynomial law, and in the case of the working cycle in three phases, the law of trigonometric variation leads to lower maximum speeds of the slide. In addition, the polynomial variation law of the transmission ratio implies a more laborious procedure. As a result, the designing of the non-circular gear has

further considered the case of the trigonometric variation laws of the transmission ratio, with two and three phases working cycle, respectively.

Once the optimal parameters and the transmission ratio variation laws were seted, the pitch curves for each gear have been modeled using the AutoCAD application and the AutoLISP programming language. The analysis of the pitch curves in the two cases (two-phase and three-phases working cycle) confirms a favorable geometry for centroids, generally composed of convex arches, except for a small concave portion on the driving gear. This form of centrodes allows for subsequent generation of the gear teeth.

To generate the flanks of the driving gear teeth, the rolling method was applied and an analytical method was developed to track the tooth of the generating rack on the non-circular centrode. The positioning and rolling movements required to generate the tooth flank were transferred to the tooth of the generating rack with standard geometry. The arrangement of the teeth on the gear pitch curve, considered a constant circular step, different in the two designing hypothesis, due to the different lengths of the division curves. The mated flanks of the driven gear teeth were generated by the coordinate transformation method, following the meshing of the teeth. The automatic generation of the teeth flank profiles was based on original AutoLISP codes, and the completion of the gears representation was accomplished by additional editing operations in AutoCAD. A comparison of the tooth profiles generated in the two cases, showed that the teeth are similar as the flanks profile shape, differences being recorded in the quadrant 4 of the gear, with a geometry specific to the slide return kinematics.

Considering the complex geometry of the non-circular gear, where the behavior of the teeth meshing is difficult to determine, the quality of the meshing, according to the static contact patch criterion, was studied as a first qualitative parameter of the meshing. The highlighting of the contact patch and its distribution was made using solid gear models and by means of AutoCAD software, in the case of teeth located at the transition between the dividing arcs defined by different laws. Thus, the contact patch in the areas adjacent to the "transition teeth" were analyzed, where the variation law of the transmission ratio, the geometry of the pitch curve and the tooth profiles, was modified. Using the features provided by AutoCAD, data on contact patch area and its distribution were collected. The analysis of the static contact patch showed that its evolution was properly, and there were no interferences on the inactive flanks. Differences between the characteristics of the contact patch appear on the transition teeth, in the two cases; in the case of the three-phases working cycle, the patch distribution is not as favorable as in the two-phases working cycle, but the dividing of the working cycle in three phases, is useful for the kinematics of the crank-slider mechanism.

To analyze the stress and strain distribution, that occur in the gear, the Finite Element (FEA) method was used in the Autodesk Inventor work environment. The stress and stain distribution analysis was performed on the 18-18' teeth pair, located in the area corresponding to the nail head-forming phase, where the meshing forces are maximum. The analysis was performed both statically and using the results of dynamic meshing simulation, situation very close to real operating conditions. The study highlighted that the equivalent stresses fall within the permissible limits, with coverage coefficients, and that the gear kinematics respects the initial conditions imposed.

Capitolul 3

NON-CIRCULAR GEARS FOR THE FURNACE UNLOADING DOOR KINEMATICS MODIFICATION

3.1. INTRODUCTION

In the process of profiles hot-rolling, the first operation in the rolling flow is the heating of the billets (raw material) at a temperature of 1250° C in the specialized furnace. The furnace has a capacity of 70 t/h and is feeded with billets, one by one, by means the pushing machine.The exit of the billets from the furnace is made through the front of the furnace, simultaneously with the feeding, so that, when a billet is introduced into the furnace through one end of the furnace, the first billet located next to the discharge door at the other end is thrown on the roller table. Further, the billets follow the technological flow. The billets unloading rhythm is approximately one billets every 2-3 minutes; each time, the unloading door opens and closes to allow billets to fall on the roller table. Considering that the actual billets discharge time is very low (about 1 to 2 seconds) compared to the time of opening and closing the door (12 seconds), a large amount of heat is lost through the open space. The door speed is uniform throughout the billets discharge, resulting in energy losses, additional methane gas consumption and, respectively, increases in production costs.

In order to reduce these heat losses, it is proposed to modify the kinematics of the door driving mechanism by using a non-circular gears; the speed of the unloading door can be varied so that, at closing and opening, the speed remains the initial speed and in the rest of the stroke the speed increases, reducing the time that the door is opened and in consequence the heat losses.

3.2. MODIFIED KINEMATICS OF THE FURNACE DOORS DRIVING MECHANISM

3.2.1. Kinematics analysis of the furnace unloading doors driving mechanism

The furnace unloading doors is driven by an asynchronous electric motor (1) via a worm gear reducer (2) and a chain drive (4) according to Fig. 3.1 - 3.2 [88]. The door (8) is raised by means of chains (7) that is winding onto the wheels (6).

The total transmission ratio is 140, so the door lifting speed is about 0.08 m / s. This low speed is required when closing and opening the door in order to avoid mechanical shocks on the structure on the front of the furnace. The door is opened by turning the motor in one direction, and the closing is done by reversing the direction of rotation. Limiting the door stroke is done electrically through a controller.

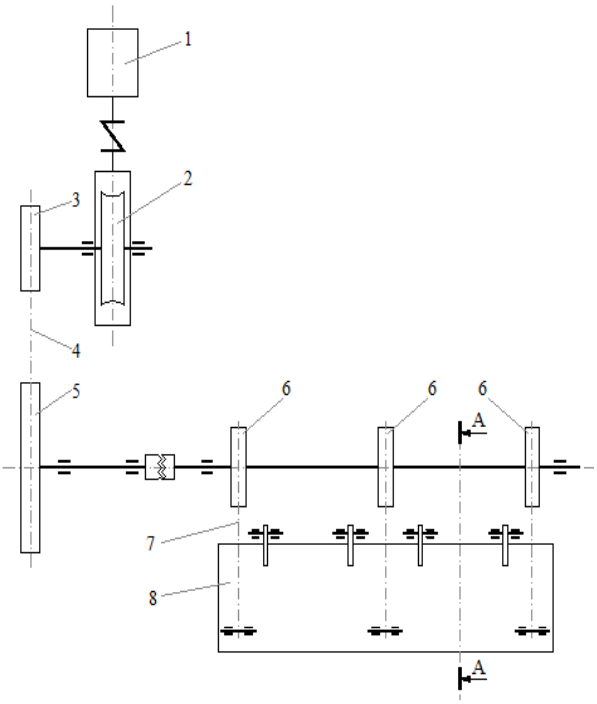

Fig. 3.1. The unloading door driving kinematics [88]

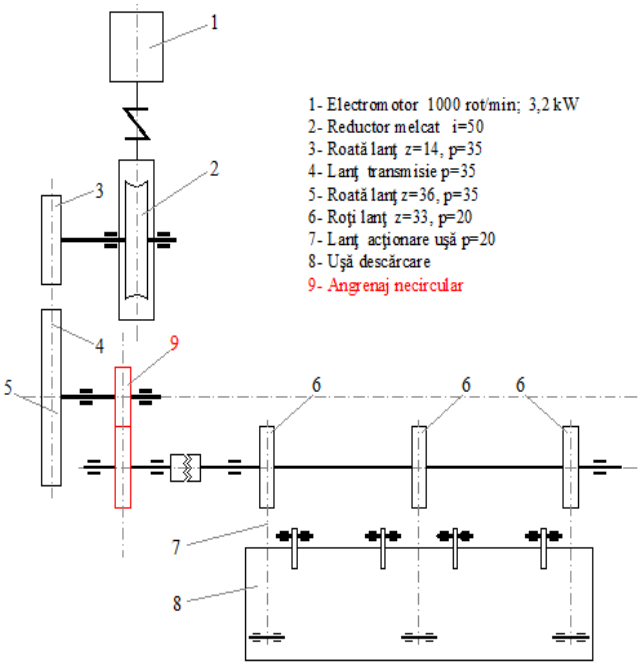

Fig. 3.3. The driving of the unloading door using non-circular gears.

3.2.2. The modified kinematics of the door driving mechanism

In order to increase the angular speed of the door, it is proposed to introduce a non-circular gear (Fig. 3.4) into the door kinematics, between the chain transmission (4) and the wheel drive shaft (6). The non-circular gears (9) perform less than one rotation and have circular (θ_2, θ_2') and non-circular (θ_1, θ_1') portions, as in Fig. 3.4. The overall rotation angle of the driven gear is θ_1' + θ_2' = 308.3° (corresponding to a door opening at 45°), the transmission ratio progressively increasing from 1:1 to 2:1.

On the portion defined by angle θ_1', the door speed increases from the initial speed v_1 = 0,08 m/s to v_2, proportional to the radius. On the angle portion θ_2', the velocity $v_2 > v_1$ remains constant, the unloading door opening at high speed. Reversing the motor rotation, the door is close at the same speed v_2, near to the moment of sealing, when the speed drops back to the initial value v_1 = 0.08 m/s, closing the door slowly.

In order to modify the kinematics of the discharge door mechanism, a multi-variable transmission ratio with variable parameters is defined for the non-circular gear.

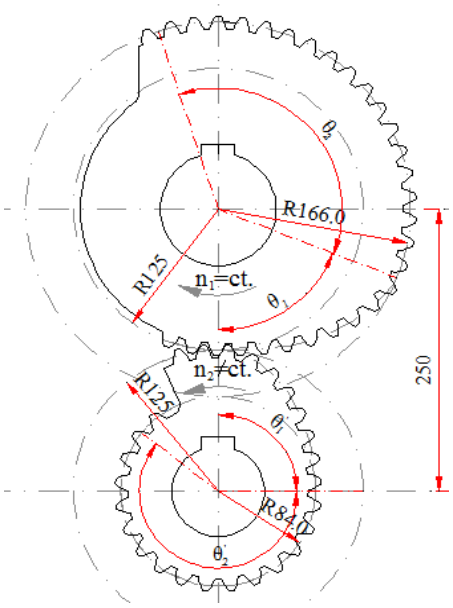

Fig. 3.4. Non-circular gear proposed for unloading door driving

3.2.2.1.Two-phases working cycle

To divide the work cycle into two phases, the following definition function of the non-circular gear transmission ratio is proposed::

$$i_{21}(\varphi_1) = \begin{cases} 1 + \mathrm{a} \cdot \sin b\varphi_1 , & \text{daca } \varphi_1 \in [0, \varphi_\mathrm{v}] \\ \mathrm{i_{max}}, & \text{daca } \varphi_1 \in [\varphi_\mathrm{v},\ \varphi_{1\mathrm{t}}] , \end{cases} \tag{3.1}$$

where: φ_v is the rotation angle of the driving gear, which delimits the range at which the speed decreases; *a, b* – constants that ensure the definition of a correct transmission ratio, respectively the subsequent generation of mated non-circular centrodes; i_{max} – maximum value of the transmission ratio ; φ_{1t} – driving gear rotation angle that corresponding to a driven gear rotation with 308,3°, angle required to open the furnace door with 45 °.

Driving gear rotation angle, calculated with:

$$\varphi_2(\varphi_1) = \int_0^{2\pi} i_{21}(\varphi_1) d\varphi \ , \tag{3.3}$$

becomes:

$$\varphi_2(\varphi_1) = \begin{cases} \varphi_1 - \dfrac{a}{b} \cdot \cos b\varphi_1 + ct_1, & \text{dacă} \varphi_1 \in [0, \varphi_v] \\ i_{max} \cdot \varphi_1 + ct_2, & \text{dacă } \varphi_1 \in [\varphi_v, \varphi_{1t}] \ . \end{cases} \tag{3.4}$$

The followings condition are required:

- i_{21} pozitive and continuous function $\Rightarrow$ $1 + a \cdot \sin b\varphi_1 = i_{max}$; (3.5)
- i_{21} derivable function $\Rightarrow$ $\cos b\varphi_1 = 0$; $b\varphi_1 = \pi/2$; (3.6)
- $\varphi_2\,(\varphi_1)$ continuous function $\Rightarrow$ $\varphi_v + ct_1 = i_{max} \cdot \varphi_v + ct_2$; (3.7)
- $\varphi_2(\varphi_{1t}) = \varphi_{2t} = 308{,}3°$ $\Rightarrow$ $i_{max} \cdot \varphi_{1t} + ct_2 = 308{,}3°$; (3.8)
- $\varphi_2(0) = 0$ $\Rightarrow$ $-\dfrac{a}{b} + ct_1 = 0$. (3.9)

Solving the above equation systems, results:

$$\mathrm{a} = i_{max} - 1 \ , \tag{3.10}$$

$$b = \frac{\pi}{2\varphi_v} \tag{3.11}$$

Considering as initial data i_{max} și φ_v, it can calculate $\varphi_{1\mathrm{t}}$:

$$\varphi_{1t} = \frac{(\pi - 2) \cdot (i_{max} - 1) \cdot \varphi_v + \pi \cdot \varphi_{2t}}{\pi i_{max}} \ . \tag{3.12}$$

Fig. 3.5 ÷ 3.7 show the influence of the defining parameters i_{max} and φ_v on the centrodes kinematics

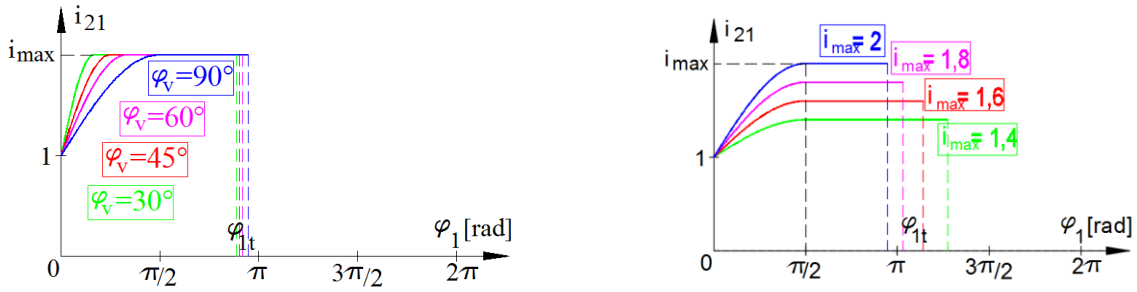

a) i_{max} = 2 b) φ_v = 90°

Fig. 3.5. The influence of the angle φ_v (a) and maximum value i_{max} (b) on the transmission ratio

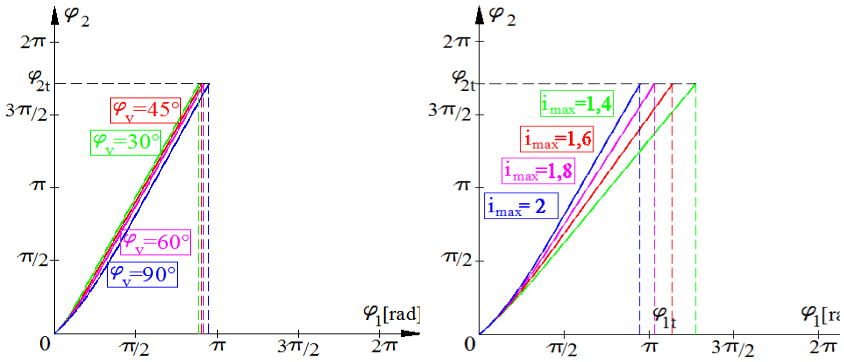

a) i_{max} = 2 b) φ_v =90°

Fig. 3.6. The influence of the angle φ_v (a) and maximum value i_{max} (b) on the driven gear rotation angle

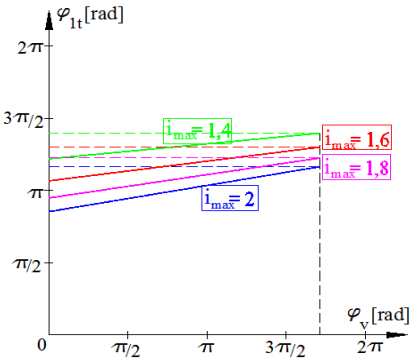

Fig. 3.7. The influence of the maximum value i_{max} on the total rotation angle of the driving gear

3.2.2.2. Three-phases working cycle

To divide the working cycle into three phases, the following definition law is proposed for the transmission ratio:

$$i_{21}(\varphi_1) = \begin{cases} 1, & \text{dacă } \varphi_1 \in [0, \varphi_u] \\ a + b \cdot \sin(c \cdot \varphi_1 + d), & \text{dacă } \varphi_1 \in [\varphi_u, \varphi_{v,}] \\ i_{max}, & \text{dacă } \varphi_1 \in [\varphi_v, \varphi_{1t}], \end{cases} \tag{3.14}$$

where φ_u, φ_v are the rotation angles driving gear, that delimit the interval where the lowering of the door speed occurs; *a, b* – constants that ensure the definition of a correct transmission ratio, respectively the subsequent generation of mated non-circular centrodes; φ_{1t} – driving gear rotation angle that corresponding to a driven gear rotation with 308,3°.

The driven gear rotation angle:

$$\varphi_2(\varphi_1) = \begin{cases} \varphi_1 + ct_1, & \varphi_1 \in [0, \varphi_u] \\ a\varphi_1 - \frac{b}{c} \cdot \cos(c\varphi_1 + d) + ct_2, & \varphi_1 \in [\varphi_u, \varphi_{v,}] \\ i_{max}\varphi_1 + ct_3, & \varphi_1 \in [\varphi_{v,}\varphi_{1t}]. \end{cases} \tag{3.16}$$

The following condition are required:

- i_{21} pozitive function $\Rightarrow$ $a > b$; (3.17)

- i_{21} continuous function $\Rightarrow$ $\begin{cases} 1 = a + b \cdot \sin(c\varphi_u + d) \\ a + b \cdot \sin(c\varphi_v + d) = i_{max} \end{cases}$; (3.18)

- i_{21} derivable function $\Rightarrow$ $\begin{cases} \cos(c\varphi_u + d) = 0 \quad \Rightarrow \quad c\varphi_u + d = \pi/2 \\ \cos(c\varphi_v + d) = 0 \quad \Rightarrow \quad c\varphi_v + d = \pi/2 \end{cases}$; (3.19)

- $\varphi_2(0) = 0$ $\Rightarrow$ $ct_1 = 0$; (3.20)

- $\varphi_2(\varphi_1)$ continuous function $\Rightarrow$ $\begin{cases} \varphi_u = a\varphi_u + ct2 \\ a\varphi_v + ct_2 = i_{max} \cdot \varphi_v + ct_3 \end{cases}$; (3.21)

- $\varphi_2(\varphi_{1t}) = \varphi_{2\,t} = 308{,}3°$ $\Rightarrow$ $i_{max} \cdot \varphi_{1t} + ct_3 = \varphi_{2t} = 308{,}3°$. (3.22)

Solving the above equations, results the followings values of the constants:

$$c = \frac{\pi}{\varphi_v - \varphi_u} \quad , \qquad d = \frac{\pi(\varphi_v - 3\varphi_u)}{2(\varphi_v - \varphi_u)} \; . \tag{3.23}$$

$$a = \frac{i_{max} + 1}{2} \; , \qquad b = \frac{1 - i_{max}}{2} \; . \tag{3.24}$$

$$ct_1 = 0 \; , \qquad ct_2 = \frac{1 - i_{max}}{2} \cdot \varphi_u \; , \qquad ct_3 = \frac{1 - i_{max}}{2} \cdot (\varphi_u + \varphi_v) \; . \tag{3.25}$$

Considering the parameters $i_{max,}$ φ_u și φ_v as defining data, the driving gear rotation angle will be:

$$\varphi_{1t} = \frac{\varphi_{2t}}{i_{max}} + \frac{i_{max} - 1}{2i_{max}} \cdot (\varphi_u + \varphi_v) \; . \tag{3.26}$$

The figures 3.8 ÷ 3.10 show the influence of the defining parameter, on the centrodes geometry and kinematics.

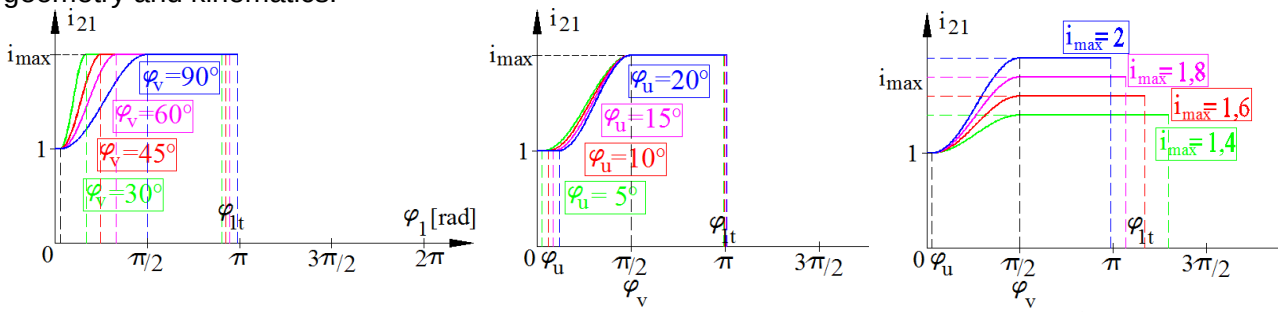

a) $i_{max} = 2$; $\varphi_u = 5°$ b) $i_{max} = 2$; $\varphi_v = 90°$ c) $\varphi_u = 5^0$; $\varphi_v = 90°$ d)

Fig. 3.8. Influence of the angles φ_v (a), φ_u (b) and maximum transmission ratio i_{max} (c) on the transmission ratio

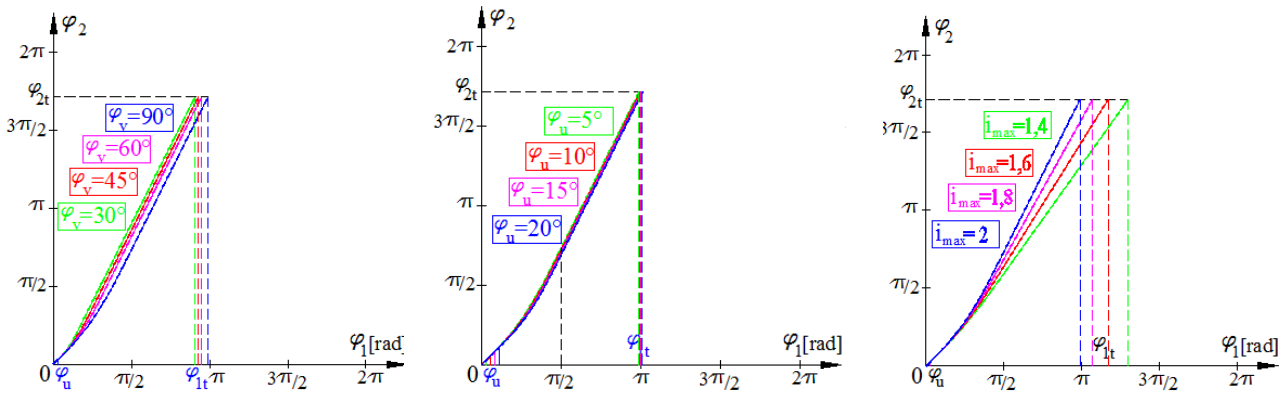

a) i_{max} = 2 ; φ_u = 5° b) i_{max} = 2 ; φ_v = 90° c) φ_u = 5° ; φ_v = 90°

Fig. 3.9. Influence of the angles φ_v (a), φ_u (b) and maximum transmission ratio i_{max} (c) on the driven gear rotation angle

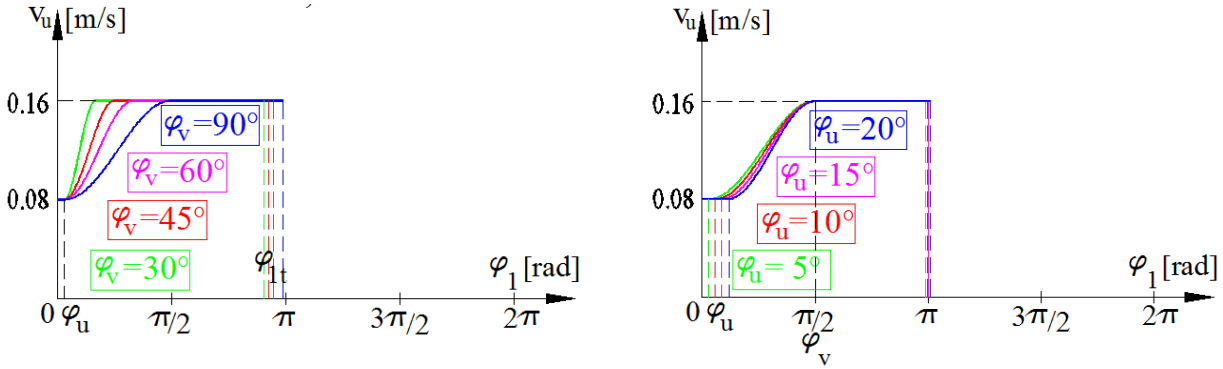

a) i_{max} = 2 ; φ_u = 5° b) i_{max} = 2 ; φ_v = 90°

Fig 3.10. Influence of the angles φ_v (a) and φ_u (b) on the door lifting speed

Analysing the graphs from Fig.3.8, it can observe that the transmission ratio i_{21} is influenced in the same way as in the previous case by the parameters i_{max} and φ_v. In adition, increasing the start angle φ_u, leads to the increase of the slope of the variation curve of the transmission ratio in the second phase, in the same way as φ_v. Combining the influence of the angle φ_v and φ_u on the ratio i_{21}, it results that the significant influence on the slope of the transmission ratio variation curve is given by the difference φ_v - φ_u, in the direction of the slope increasing with the decreasing of the difference between the two angles.

3.2.3. Comparison of the door kinematics

In order to find a convenient variant of the transmission ratio variation law, a comparison was made between the two-phase variation law, for the case i_{max} = 2 and φ_v = 90°, an the three-phases variation law, for the case i_{max} = 2, φ_u = 20° and φ_v in three variantes: 90°, 110° and 130° (Fig 3.11).

As a result of the transmission ratio variation analysis, it is chosen as a convenient variant for both technological and cinematic purposes, the three-phase working cycle with the lowest value of the angle φ_u and a difference (φ_v - φ_u) ∈ [50°, 80°].

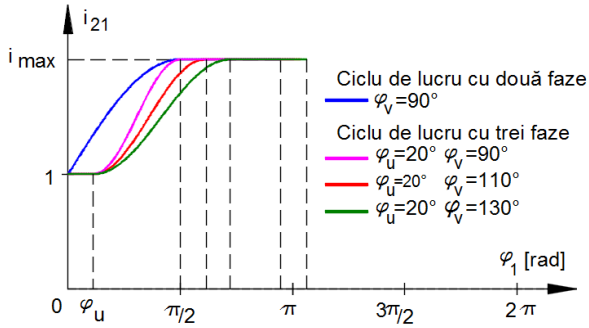

Fig. 3.11. Comparative analysis of the transmission ratio variation laws for i_{min}= 1 and i_{max} = 2, for a different number of phases and different defining parameters

3.3. NON-CIRCULAR GEAR FOR MODIFYING THE DOOR DRIVING MECHANISM KINEMATICS

3.3.1. Non-circular centrodes modeling

The modeling of non-circular centrodes is based on the fundamental principle of rolling and the hypothesis mentioned in Chapter 2 (section 2.3). In the particular case of the non-circular gears that modify the kinematics of the door driving mechanism, the determination of the centrodes / pirch curve is based on the hypothesis of the transmission ratio definition.

Starting from the variation of transmission ratio and analysis from section 3.2.2, equations (2.28) and (2.29) allow the generation of centtrodes / pitch curves of non-circular gears.

By means of initial parameters i_{max}, φ_u and φ_v and considering a three phases working cycle, the centrodes of the two gears were modeled. Figure 3.12 shows, comparatively, the shape of centrode for the various analyzed cases. The process of modeling the pitch curves was carried out in the graphical environment of AutoCAD, based on an original AutoLISP code (Appendix 3).

The centrodes analysis confirms, once again, the necessity to chose small angle values φ_u and the fact that the variation of the maximum transmission ratio i_{max} , influences significantly only the total angle φ_{1t}.

For generating the non-circular gears, the following parameters are considered:**i_{max} = 2**, **φ_u = 10°** and two cases for **φ_v**: **φ_v = 60°** respectively **φ_v = 90°**.

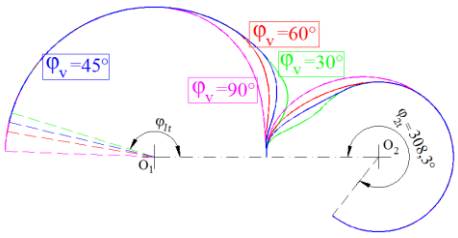

i_{max} = 2 ; φ_u = 5°

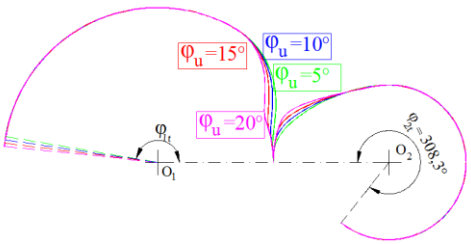

i_{max} = 2 ; φ_v =90°

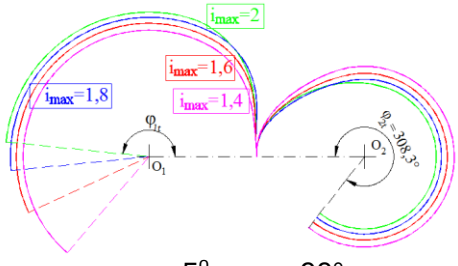

φ_u = 5° ; φ_v = 90°

Fig. 3.12. Comparison of the non-circular centrodes

3.3.2. Non circular gear teeth generation

For the generation of the teeth flanks, the rolling method described in Chapter 2 (section 2.3.2) was applied, where all the movements related to the rolling are transferred to the tooth of the generating rack.

Starting from the equations (2.34) ÷ (2.38) that defining the profiles of the driving and driven gear teeth, an original AutoLISP code (Annex 4) automatically generates the profile of the tooth flanks with a number of teeth $z_1 = z_2 = 29$, within a predefined rolling distance, chosen to ensure complete flank generation (Figure 3.13). The cross sections of the gears, by extrusion, allow the solid model to be generated (Figure 3.16). Fig. 3.14 shows the cross-sections of the two non-circular gears in the two hypotheses: $\varphi_v = 90°$, $\varphi_u = 10°$ (Fig. 3.14 a) and $\varphi_v = 60°$, $\varphi_u = 10°$ (Fig. 3.14 b).

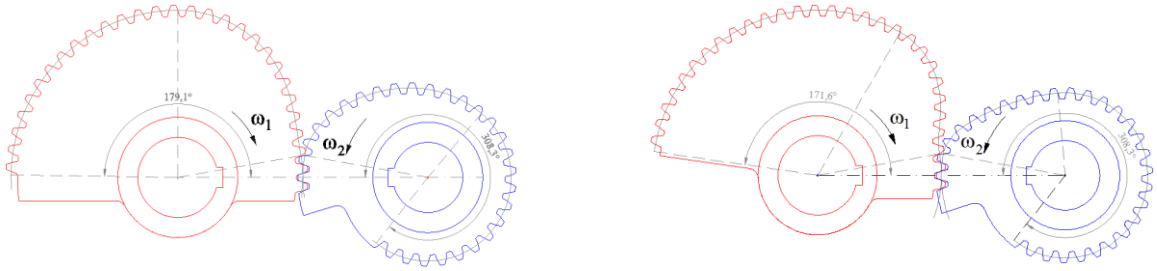

a) $i_{max} = 2$, $\varphi_u = 10°$, $\varphi_v = 90°$ *b)* $i_{max} = 2$, $\varphi_u = 10°$, $\varphi_v = 60°$

Fig 3.14. Cross section of the non-circular gears

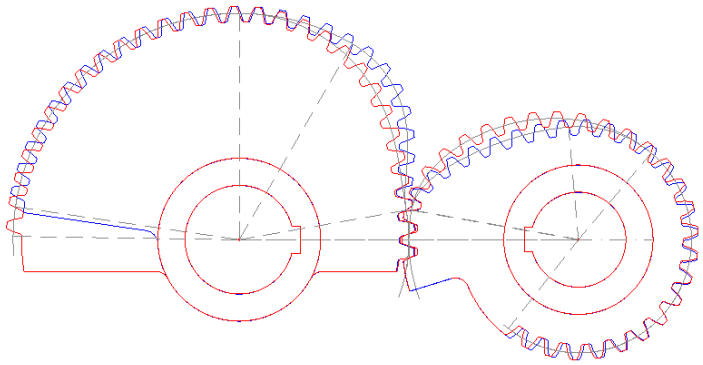

Fig 3.15. Comparison of the teeth profile

hypothesis1: $i_{max} = 2$, $\varphi_u = 10°$, $\varphi_v = 60°$

hypothesis 2: $i_{max} = 2$, $\varphi_u = 10°$, $\varphi_v = 90$

A comparison of the teeth profiles in both cases is shown in Fig. 3.15. It can be seen that the teeth are similar as profile shape, due to the fact that the centrodes in the two cases differ only in the passing area from the $i_{min} = 1$ transmission ratio to the $i_{max} = 2$ transmission ratio.

The virtual models of the gears are shown in Fig. 3.16. The width of the wheels is set to B = 50 mm.

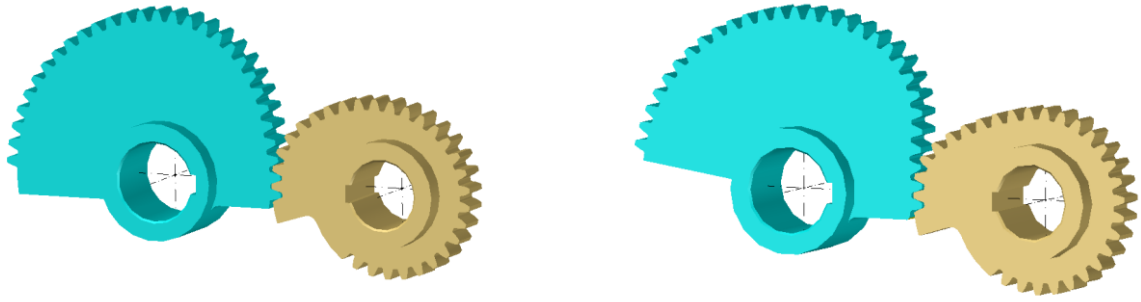

a) $i_{max} = 2$, $\varphi_u = 10°$, $\varphi_v = 90°$ a) $i_{max} = 2$, $\varphi_u = 10°$, $\varphi_v = 60°$ b)

Fig 3.16. Non-circular gears solid model

3.3.3. Meshing analysis

3.3.3.1. Static analysis of the stress and strain distribution

The static analysis of the stress and strain distribution is performed in the Autodesk Inventor graphical environment by the Finite Element Method (FEA) for each of the two cases resulting from Section 3.3.2 : $\varphi_v - \varphi_u = 50°$, respectively $\varphi_v - \varphi_u = 80°$. The study highlights the influence of the difference ($\varphi_v - \varphi_u$) on stress and strain distribution that occur in driving gear. The static analysis is made on three teeth of the driving gear, located in its non-circular portion, teeth no. 4, 7 and 10. Tooth no. 4 is located in the concave area of the centrode, and the teeth no.7 and 10 are located in the middle and in the end of the centrode, from the second zone of the working cycle (Fig 3.18).

In the same way, it go through the same steps, as it shown in chapter 2 (section 2.3.3.2). The forces were calculated considering a constant torque of 1000 Nm, corresponding to the mass of the furnace discharge door, m = 1000kg. This resulted in the force applied to the tooth (Tab. 3.1);

Tabelul 3.1 Values of the forces applied to the analyzed teeth

$\varphi_v - \varphi_u$	**Tooth no. 4**	**Tooth no. 7**	**Tooth no. 10**
50°	7479,4 N	6361,3 N	5851,4 N
80°	7589,5 N	6800,4 N	6169,0 N

In Fig. 3.22 ÷ 3.24, the results of the FEA simulation are shown in the two cases: $\varphi_v - \varphi_u = 50°$ and $(\varphi_v - \varphi_u) = 80°$.

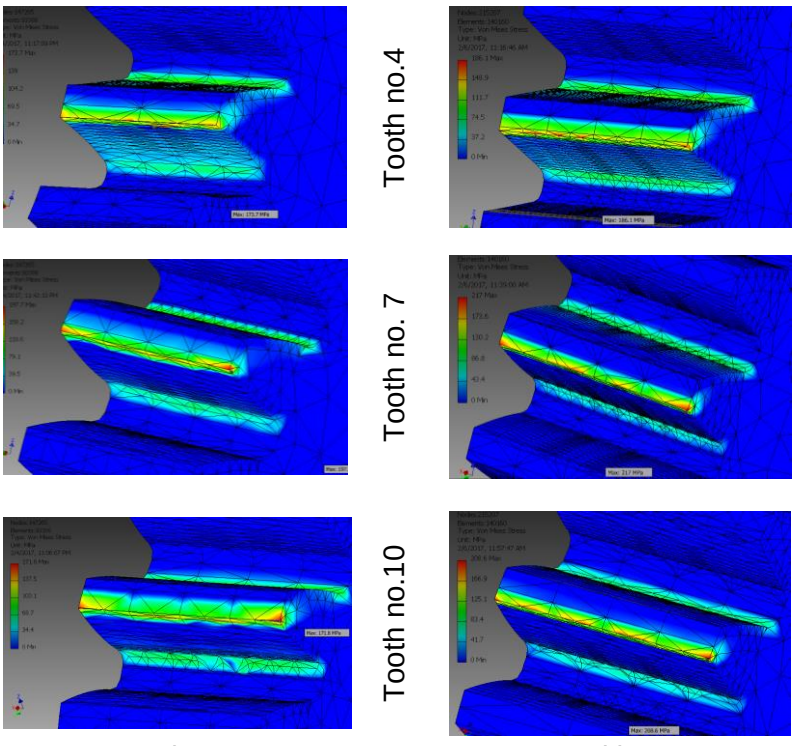

Fig. 3.22. Distributions of Von Mises equivalent stresses for $\varphi_v - \varphi_u = 50°$ (a) and $\varphi_v - \varphi_u = 80°$ (b)

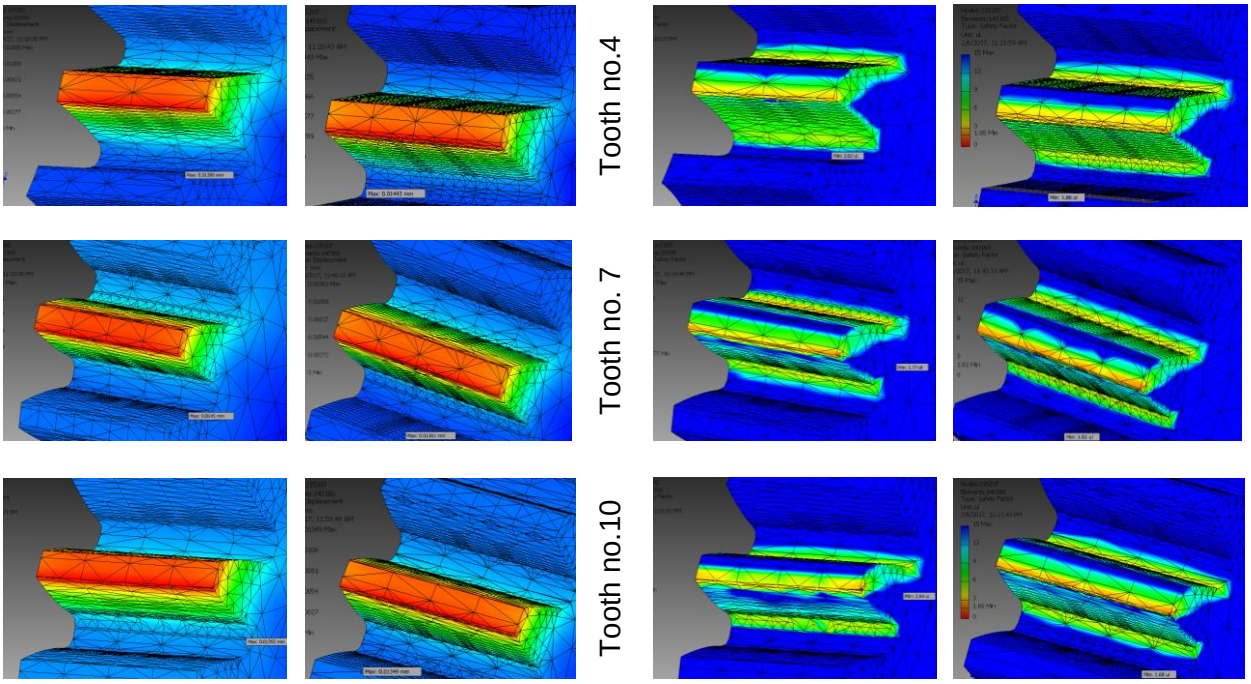

Fig. 3.23. Displacement distribution, for $\varphi_v - \varphi_u = 50°$ (a) and $\varphi_v - \varphi_u = 80°$ (b)

Fig. 3.24. Safety factor distribution, for $\varphi_v - \varphi_u = 50°$ (a) and $\varphi_v - \varphi_u = 80°$ (b)

In order to be able to compare the analyzed cases in Fig. 3.25 ÷ 3.27 are shown the graphs of the maximum values of the analyzed parameters, according to Tab. 3.2.

Tabelul 3.2 *Maximum values of analyzed parameters resulting from static analysis*

$\varphi_v - \varphi_u$	**The analyzed tooth**	**Maximum Von Mises stress, MPa**	**Maximum displacement, mm**	**Minimum safety factor**
50°	Tooth no. 4	173,7	0,01385	2,02
	Tooth no. 7	197,7	0,01450	1,77
	Tooth no. 10	171,8	0,01392	2,04
80°	Tooth no. 4	186,1	0,01443	1,88
	Tooth no. 7	217,0	0,01361	1,61
	Tooth no. 10	208,6	0,01349	1,68

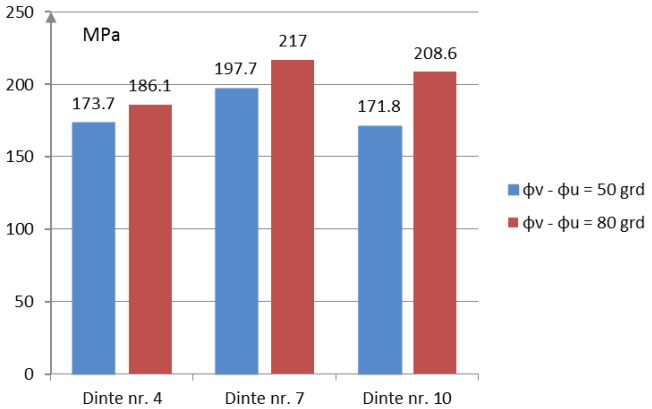

Fig. 3.25. Comparison of the maximum Von Misses equivalent stress (static analysis)

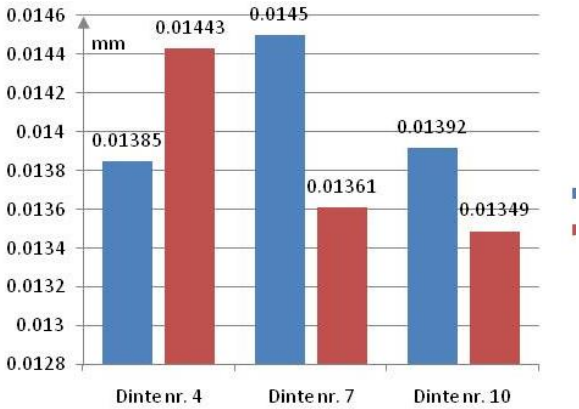

Fig. 3.26. Comparison of the maximum displacements (static analysis)

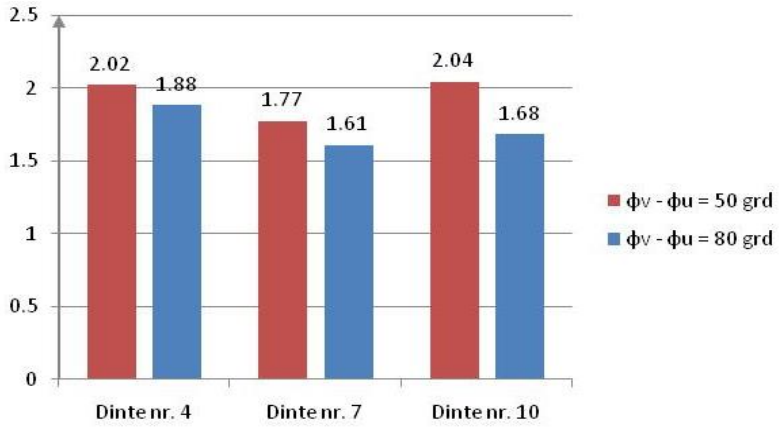

Fig. 3.27. Comparison of the minimum safety factor (static analysis)

Comparing the cases $\varphi_v - \varphi_u = 50°$, respectively $\varphi_v - \varphi_u = 80°$ it can observe that the maximum stresses have higher values, respectively lower safety factors, in the second case. Since the applied moment is constant, the forces applied on the tooth decrease with the increase in the radius of the centroid, which explains higher maximum stresses in the case $\varphi_v - \varphi_u = 80°$.

3.3.3.3. Dynamic analysis of the stress and strain distribution

The analysis of the non-circular gears meshing performance by dynamic simulation is carried out using the same algorithm as in chapter 2.3.3.3

Dynamic simulation resulted in the output data graphs specific to the movement: the gears position (Fig.3.31), the variation of the rotation speeds (Fig.3.29) and the variation of the two gears accelerations (Figure 3.30);

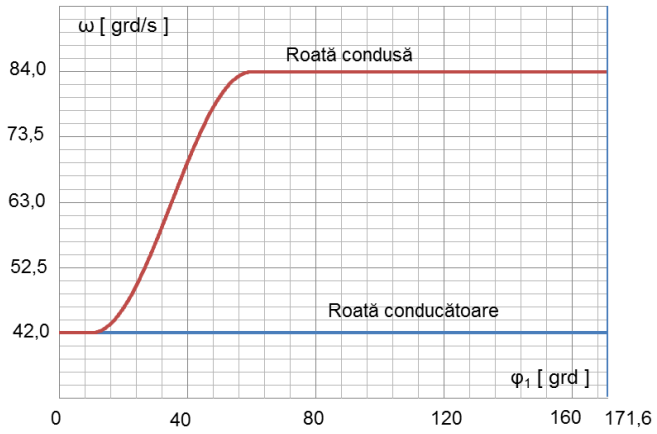

Fig. 3.29. Angular speed variation, for gear with $\varphi_v - \varphi_u = 50°$ (dynamic simulation)

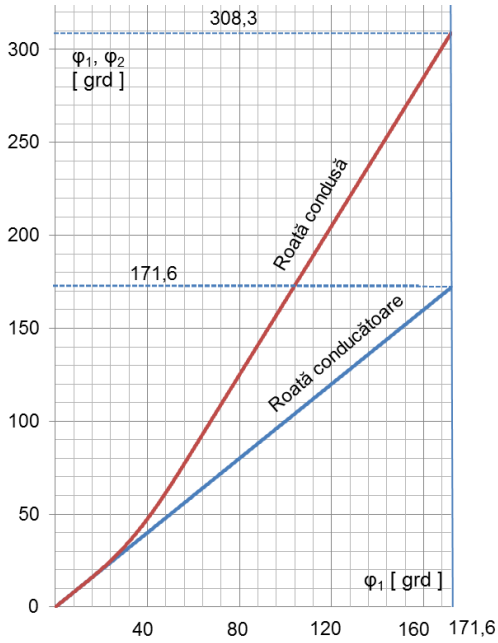

Fig. 3.31. Rotation angle variation, for gear with $\varphi_v - \varphi_u = 50°$ (dynamic simulation)

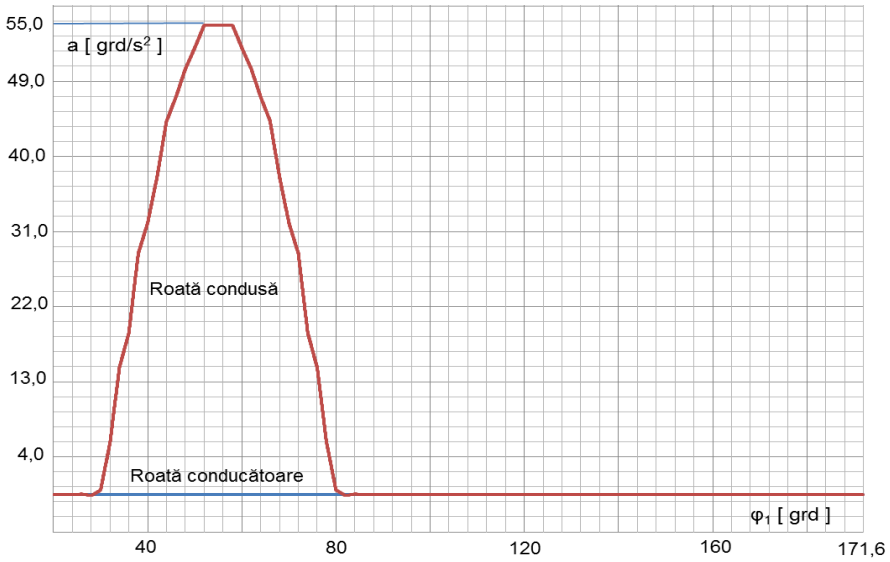

Fig. 3.30. Acceleration variation, for gear with φ_v - φ_u = 50° (dynamic simulation)

Analyzing the graphs obtained from the dynamic simulation, it can be observed that the same kinematics data were obtained with those imposed.

Following the dynamic simulation, for the gear with φ_v - φ_u = 50 °, the output data were exported for the FEM analyze, focused on the teeth no. 4, 7 and 10 (Fig.3.32 - 3.35).

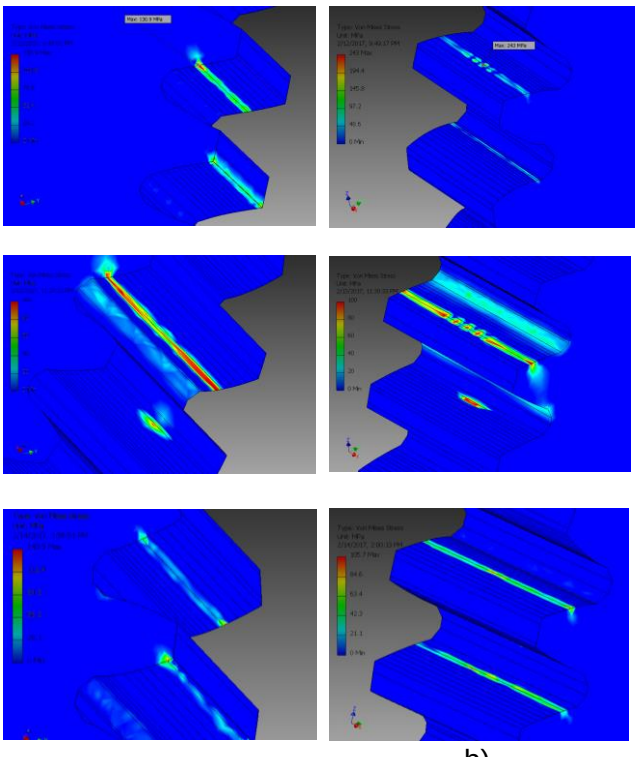

Fig. 3.32. Von Mises equivalent stress distribution, from the driving gear (a), and from the driven gear (b), with meshing on the top of the tooth

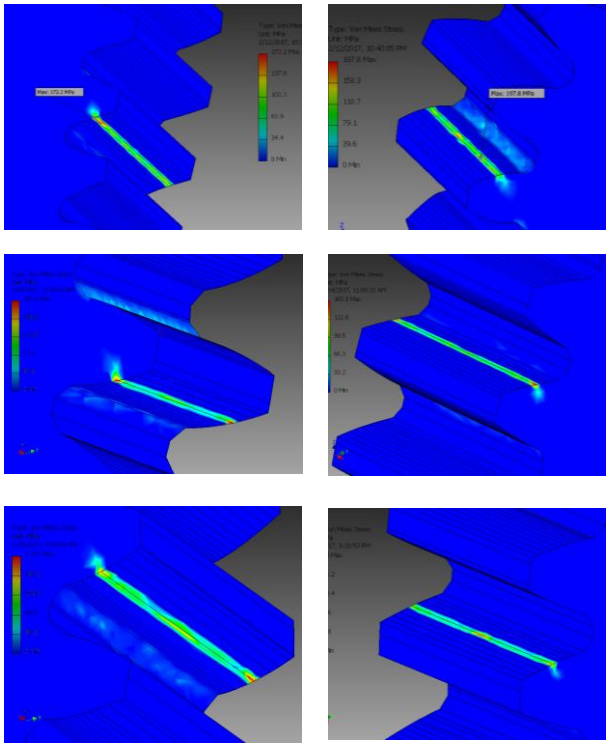

Fig. 3.33. Von Mises equivalent stress distribution, from the driving gear (a), and from the driven gear (b), with meshing on the middle of the tooth

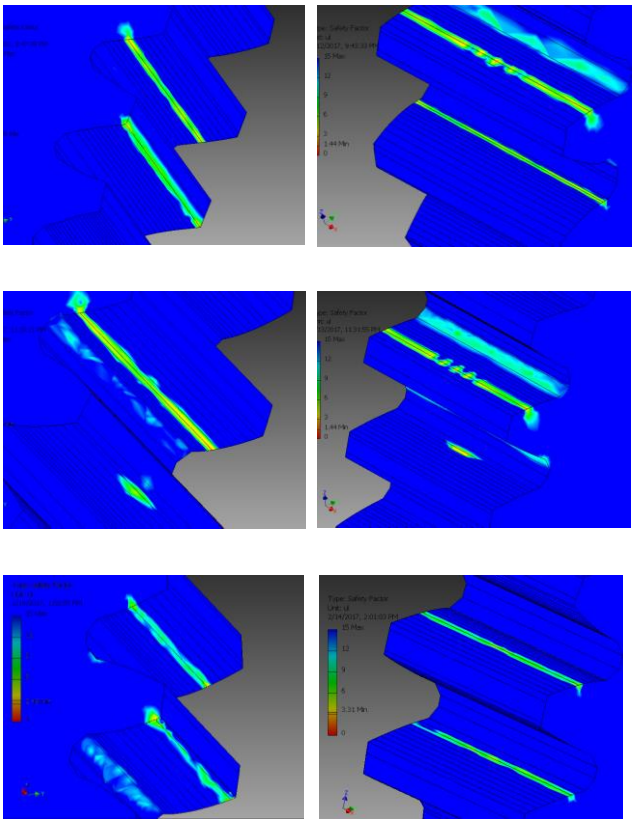

a) b)

Fig. 3.34. Safety factor distribution, from the driving gear (a), and from the driven gear (b), with meshing on the top of the tooth

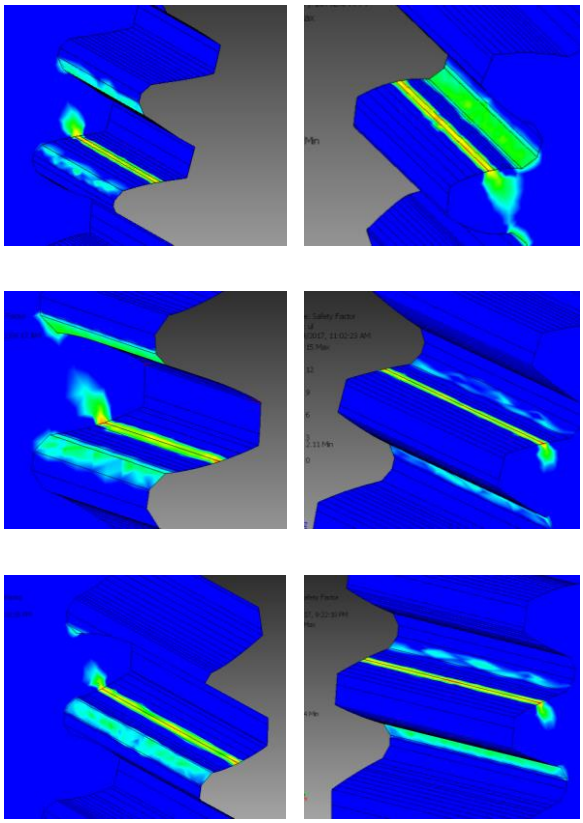

a) b)

Fig. 3.35. Safety factor distribution, from the driving gear (a), and from the driven gear (b), with meshing on the middle of the tooth

Analysing the graphs from Figure. 3.32 ÷ 3.35, conclusions can be drawn, regarding both the quality of the meshing and the level of stresses and displacements. Regarding the meshing quality, it can see the contact patch during the gears meshing and the number of meshing teeth. Thus, it can be verified that, when the meshing is made in the middle of the tooth, there is only one pair of meshing teeth, and when the contact moves towards the top, there are two pairs of meshing teeth.

Figures 3.36 and 3.37 present a comparative study of the maximum equivalent stresses and minimum safety factor in the analyzed cases.

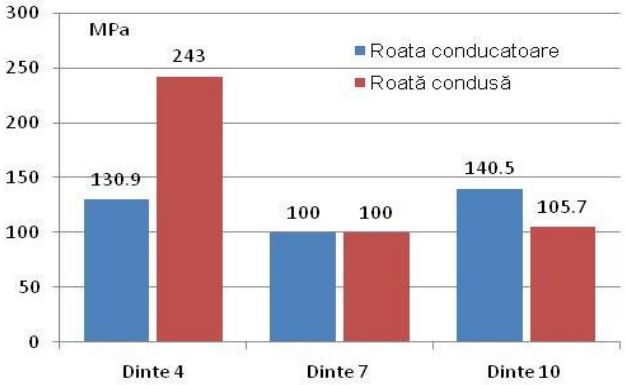

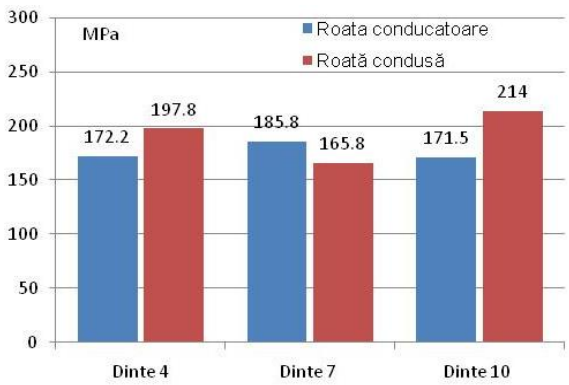

a) b)

Fig. 3.36. Comparison of the maximum Von Mises equivalent stress, in case of meshing on the top of the tooth (a), and on the middle of the tooth (b)

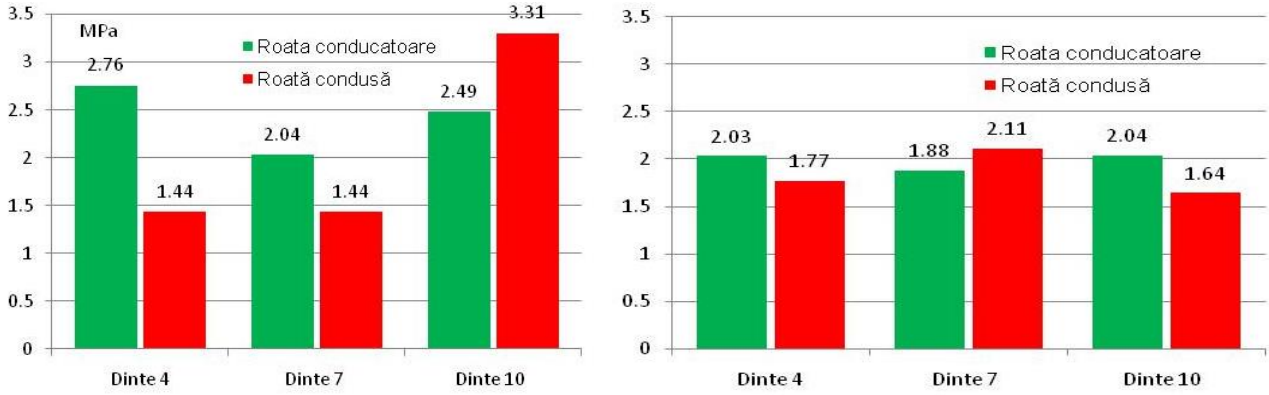

a) b)

Fig. 3.37. Comparison of the minimum safety factor, in case of meshing on the top of the tooth (a), and on the middle of the tooth (b)

3.4. CONCLUSIONS

Chapter 3 presents the results of the research on the modification of the door driving mechanism kinematics of a billets heating furnace within a hot rolling mill, using a non-circular gear. The purpose of modifying kinematics is to reduce heat loss by decreasing the time when the door is opened, by increasing the angular speed of the door, respectively.

In order to modify the kinematics, it was proposed to insert a non-circular gear in the door driving kinematics, that divides the working cycle into two and three phases, respectively, at different variable speeds. The gear is designed based on a transmission ratio defined as a hybrid function: constant for small durations, at the opening and closing of the door, and variable, according to a cosinusoidal law, for the rest of the cycle.

For each of the two hypotheses, the two and three phases working cycle, respectively, starting from the proposed definition laws of the transmission ratio, significant parameters influencing the kinematics of the mechanism were established: the angles of the driving gear that split the phases, φ_u (for the two-phases working cycle) respectively φ_v and φ_u, (for the three-phases working cycle) as well as the maximum transmission ratio i_{max}. Studying the influence of these parameters on the transmission ratio i_{21}, on the angle of the driven gear φ_2 and on the door speed v_u, it was found that the transmission ratio and the variation of the door speed are mainly influenced by the difference $\varphi_v - \varphi_u$, this having convenient values in the range [50°, 80°]. The value of the angle φ_u and the maximum transmission ratio i_{max} , do not significantly influence the transmission ratio, however, it is desirable, as small as possible values for the angle φ_u, in order, for the gear, to operate with an i_{max} ratio, as long as possible..

Following the analysis, it has been established that the three-phases working cycle is more advantageous for both, motion kinematics and subsequent teeth generation and the following convenient values of the transmission ratio defining parameters have been established: φ_u **=** 10°; $\varphi_v \in$ [60°, 90°]; $\boldsymbol{i_{max}}$ **=** 2. The parameters have been chosen so that, to meet the technological condition of reducing the door opening / closing time, and don't introduce additional overloads of the door drive mechanism.

The comparative analysis of the centrodes generated for various values of the defining parameters confirmed the above conclusions. Also, centrodes geometry is favorable to subsequent generation of the teeth flank, being generally composed of convex arches, except

for a concave portion, where the curvature is significantly influenced by the difference φ_v-φ_u. The pitch curves for each gear were modeled using the AutoCAD program and the AutoLISP programming language.

To generate the flanks of the driving gear teeth, the rolling method was applied and an analytical method developed, to track the rolling of a generating rack tooth on the non-circular centrode. The positioning and rolling movements required to generate the tooth flank were transferred to the rack tooth with standard geometry. The mated flanks of the driven gear teeth were generated by the coordinate transformation method, following the meshimg of the teeth. The automatic generation of the teeth flank profiles was based on an original AutoLISP codes, and the completion of the gears representation was accomplished by additional editing operations in AutoCAD. The solid models of the driving and driven gears were generated for the values of the defining parameters, chosen conveniently in two variants: $i_{max} = 2$, $\varphi_u = 10°$, $\varphi_v = 60°$ and $i_{max} = 2$, $\varphi_u = 10°$, $\varphi_v = 90°$.

For the analysis of the stress and strain distribution, that occur in the gear, the Finite Element Method (FEA) was developed using the Autodesk Inventor work environment. The analysis was performed both, statically and dynamically, a situation very close to the real operating conditions. The analysis was performed for three pairs of teeth, located in the concave zone of the centrode and, respectively, in the areas where the centrode geometry changes the definition law, in the two mentioned hypotheses. The dynamic analysis of stress and strain distribution, revealed a correct tooth meshing, without interference, the stress and displacement, ranging within acceptable tolerances, with coverage safety coefficients.

Capitolul 4

GENERAL CONCLUSIONS, PERSONAL CONTRIBUTIONS AND PERSPECTIVES

4.1. CONCLUSIONS

The main objective of this paper was to identify and solve concrete industrial applications using non-circular gears; based on the author's practical experience, two applications were proposed from the metallurgical industry: 1 - modified kinematics of the crank-slider mechanism from a nails machine, in order to improve the cold plastic forming process during the nail head phase, and 2 - modified kinematics of the billets heating furnace discharge doors, from the section hot rolling mill, in order to reduce the heat loss while the unloading door is open.

In order to carry out the proposed researches, it was necessary to study the current state of research and achievements in the field. This study highlighted that the non-circular gears design algorithm is not a standardized one, and is specific to each application, depending on the initial data required / imposed by the application. Also, the analysis of similar applications in the field has encouraged research, suggesting solutions to solving the problems formulated in the paper, and outlining the research algorithm, respectively to chose the designing data, in order to obtain the desired variable kinematics, gears designing under certain hypothesis, for a constructive comparative analysis, the generation of gears in the variant considered to be convenient and the theoretical study of the designed non-circular gear performance by the meshing simulation.

Practical, the design of the non-circular gear for each of the two proposed applications required the following steps: **i)** defining the variation law of the transmission ratio, dividing the working cycle into two or three phases, respectively; **ii)** establishing the defining parameters of the transmission ratio, that influence the kinematics of the mechanism, and studying their influence on kinematics; **iii)** selecting the appropriate values of the defining parameters, so that the proposed objective is met, values that constituted the input data in the subsequent design of the non-circular gear; **iv)** generating the centrode / pitch curve for each gear; **v)** generation of the non-circular gears teeth flanks; **vi)** generating the cross sections of the gears by means additional editing operations, and generating solid models of non-circular gears; **vii)** analysis of meshing quality, by analysis of teeth contact and by analysis of the stress and strain distribution. Graphics generation for analyzing the influence of defining parameters on the kinematics of the mechanism, the centrodes and teeth flanks generation of non-circular gears and the study of teeth contact were made in the AutoCAD work environment using the original AutoLISP codes. The stress and strain distribution analysis was done by the Finite Element Method (FEM) in the AutoDESK Inventor work environment.

In order to modify the kinematics of the crank-slider mechanism that interferes in the process of nail head forming, on the classical nails machine MC337, two laws of transmission ratio variation, trigonometric and polynomial, respectively, were proposed, dividing the working cycle into two, respectively three phases. Starting from these variation laws, the transmission ratio was defined by a hybrid function, with two and three definition laws, respectively, with several parameters. Following the transmission ratio to be positive, monotone, continuous, derivable and periodic, and, under the condition of closing the non-circular centrodes (the working cycle being defined by a complete rotation of the gears), the significant parameters that

influence the kinematics of the crank-slider mechanism, were defined: the rotation angles of the driving gear, that split the working phases (φ_0 – for the two-phases working cycle, φ_{1a}, φ_{1r} – for the three-phases working cycle) and the extreme values of the transmission ratio (*a* – minimum value, *b* – maximum value). After analyzing the influence of these parameters on the displacement and on the relative speed of the mechanism, in the four cases, the following convenient values were set for the parameters: $\varphi_0 = 8\pi/9$; $\varphi_{1a} = 8\pi/9$; $\varphi_{1r} = 3\pi/2$; $a = 0{,}4$; $b = 1{,}6$. It is also noted that the two proposed laws for the transmission ratio variation, trigonometric and polynomial law, respectively, are similar, as respects their influence on the kinematics of the crank-slider mechanism, a slight advantage obtained in case of trigonometric law, otherwise easier to analytically handling.. As a result, the designing of the non-circular gear has further considered the trigonometric variation of the transmission ratio, as defined by the above mentioned parameters, in the two working cycle dividing hypotheses.

Starting from the definition of the transmission ratio and considering the fundamental principle of rolling, the polar equations of the mated non-circular gears were determined. The centrodes modeling, involved the writing of AutoLISP codes, that automated the graphical representation process. The generated centrodes are closed curves, consisting of convex arches, except for a small concave portion on the driving centrode; the comparison of the centrodes, in the two analyzed cases, revealed a more "friendly" geometry, with larger radii, in case of working cycle dividing into three phases.

The generation of the teeth flanks, was based on the rolling method, developing an analytical method, to track the tooth of the generating rack on the non-circular centrode. The generation hypotheses considered a constant pressure angle at a standard value of 20 °, and a constant curvilinear pitch, resulting from dividing the length of the pitch curves into the number of teeth chosen $z_1 = z_2 = 36$. The coordinate transformations allowed the mated flanks of the driven gear teeeth to be defined, following the instantaneous rotation center, variable along the centers line. The chosen analytical method allowed automatic teeth flanks generation, using original AutoLISP codes in the AutoCAD graphical environment. A comparison of the gear teeth profiles, generated in the two hypotheses, revealed that, the teeth are similar as respect to the profile shape, differences being recorded in the quadrant 4 of the driving gear, where, the slide returning kinematics and centrodes geometry, differ.

Subsequent generation of solid models in AutoCAD allowed the meshing quality analysis to be performed, based on the Static Contact Patcht criterion as a first qualitative parameter of the meshing. The contact patch and its distribution was made using the AutoCAD program, in the areas adjacent to the "transition" teeth, where the variation law of the transmission ratio and the geometry of the centrode are modifying.The analysis of the static contact patch, showed that its evolution was appropriate, and there was no interference on the inactive flanks. Differences between the characteristics of the contact patch appear on the transition teeth, in the two hypotheses, under discussion; in case of the three-phases working cycle, patch distribution is not as favorable as in the two-phases working cycle, but dividing the working cycle into three phases is usefull, as respect to crank-slider mechanism kinematics.

For the analysis of the stress and strain distribution, that appear in the gear, the Finite Element Method (FEA) was developed, using the Autodesk Inventor application. The FEA simulation was done on the 18-18' teeth pair, located in the area corresponding to the nail-heading phase, an area where the meshing forces are maximum. The analysis was performed both, statically and using the data obtained from the dynamic simulation, a situation very close to the real operating conditions. The study highlighted the fact that, the equivalent stresses fall

within the permissible limits, with coverage safety coefficients, as well as, the fact that, the gear kinematics complies with the required initial conditions.

In order to modify the kinematics of the heating furnace unloading doors kinematics, the same steps presented in the first application were accomplished. The transmission ratio was defined by a hybrid, multiparametric function, with trigonometric variation, corresponding to the division of the working cycle into two and three phases, respectively. In order to ensure a positive, monotonous, continuous, derivable and periodic transmission ratio, and provided that the working cycle is defined by an incomplete rotation imposed on the driven gear, in accordance with the opening angle of the furnace door, it determined, as defining parameters, the rotation angles of the driving gear, which delimit the working phases (φ_u – for the two-phases workimg cycle, respectively φ_v și φ_u – for three-phases working cycle), and maximum value of the transmission ratio (i_{max}). Studying further, in the two hypotheses, the influence of the defining parameters, on the transmission ratio, the rotation angle of the driven gear and the speed of the furnace door, it was found that the transmission ratio and the variation of the door speed are mainly influenced by the difference $\varphi_v - \varphi_u$. It has also been found that the three-phases working cycle is more advantageous for both, motion kinematics and subsequent teeth generation, and the following convenient values of the defining parameters have been setted: $\varphi_u = 10°$; $\varphi_v \in [60°, 90°]$;$i_{max} = 2$.

The generation of centrodes and teeth flanks were based on the same principles and methods used in the first application, in two variants: $i_{max} = 2$, $\varphi_u = 10°$, $\varphi_v = 60°$ and, respectively, $i_{max} = 2$, $\varphi_u = 10°$, $\varphi_v = 90°$. The resulting centrodes are open curves, since the imposed rotation angle of the gears is less than 360 °. The solid models generated in AutoCAD and imported into Inventor allowed the analysis of stress and strain distribution to teeth contact by Finite Element method (FEM). The analysis of the three teeth in the area with ascending radius of the centroid, corresponding to the second phase, both static and dynamic, in the two hypotheses, revealed that the equivalent stresses fall within the permissible limits, with coverage coefficients. At the same time, it was possible to analyze the distribution of the contact patch, in the mentioned cases, the quality of the meshing being satisfactory.

. This papesr, through the two new applications proposed for use of non-circular gears, completes the research in the field and, at the same time, creates new perspectives for developing the applicability of non-circular gears whose design and generation are facilitated by current software tools and unconventional technologies.

4.2. PERSONAL CONTRIBUTIONS

The fulfillment of the research objectives proposed in this paper, was based on the following original personal contributions:

- Synthesis of research and achievements in the field of non-circular gears, highlighting the applications that lead to the modification of the classic cycle of the crank-slider mechanism and speed variation solutions of some closing and regulation elements;
- Achievement of an original classification of non-circular gear, following the application domain;
- Study of the nail machine kinematics and the proposal of introducing a non-circular gear to modify the kinematics of the crank-slider mechanism in order to improve the plastic deformation process of the material, during the nail head forming;
- Dividing of the crank-slider mechanism working cycle in two or three phases in order to modify its kinematics during the nail head forming working cycle of the process;

- The kinematics study of the furnace discharge door driving mechanism and the proposal to introduce a non-circular gear to modify the kinematics of the mechanism in order to vary the angular speed of the door so that, to reduce heat losses;
- Dividing the working cycle of the billets heating furnace door driving mechanism into two or three phases, in order to modify the kinematics of the door;
- Defining the non-circular gears transmission ratio as a multiparametric function with multiple variation laws, corresponding to the two proposed applications*;*
- Study of the influence of the transmission ratio defining parameters, on the kinematics of the proposed mechanisms ;
- Creating the original AutoLISP codes (Appendix 5) to generate graphs for the transmission ratio definition, angle of driven gear rotation, displacement of the crank-slider mechanism and furnace discharge door speed;
- Creating original AutoLISP codes for modeling non-circular mated centrodes (Appendix 1 and Appendix 3);
- Development of an analytical method for defining the flanks of the non-circular gears teeth;
- Creating original AutoLISP codes to generate gears teeth (Annex 2 and Appendix 4);
- Developing a method of studying the meshing quality using the static contact patch in the AutoCAD work environment;
- Verifying the meshing quality by analyzing the stress and stain distribution on the teeth contact area using the Finite Element Method (FEM) in INVENTOR environement;
- Verifying of the required initial kinematic conditions, by dynamic simulation in INVENTOR, and of the real loadings during the meshing time.

4.3. RESEARCHE PERSPECTIVES

The papers proposes two practical applications, by which, the technological processes can be partially improved by using non-circular gears. These applications can be completed or can be approached from an extended perspective, relative to the possibilities of improving the technological processes. Thus, at the nail machine, besides the main movement of the nail head forming, the kinematics of the other movements, that occur on the machine, can be modified (see Chapter 2.1). This can be done either by using a non-circular gear for each movement or by using a single gear (or a gear assembly) to modify the all kinematics. In the case of the second application, the proposed non-circular gearing modifies the closing-opening speed of the billet heater furnace door, using the same toothed part of the gear, both when closing and opening the door (the inactive flanks become active flanks) by reversing the direction of rotation of the motor. By using a rotary reversing mechanism with non-circular gears, it will no longer be necessary to change the direction of rotation at each door opening / closing cycle, taking place at a complete rotation of the gears.

Also, non-circular gears could be used in many other applications in the metallurgical industry. Thus, some applications, such as classic drawing machine, require frequent start-ups of electric drive motors in load (with very high torque) and shocks. The use of a non-circular gear, that works only when the electric motor is started, would significantly reduce starting torque and mechanical shocks. In other applications whitin the section hot rolling mills, where variable speed electric motors are currently used, it is necessary that, in certain short zones of the rolling line (e.g., in the billets descaling area), the transfer rate of the billets or laminates has to be reduced, and then return to the initial value. Non-circular gears (simple or tandem) used in

the driving mechanism kinematics of the transport roller, can successfully solve this requirement in a simple and inexpensive way.

Examples can continue because, due to their flexibility, non-circular gears offer unlimited research perspectives, both in the metallurgy and other industries.

LIST OF PUBLISHED PAPERS

A. Scientific papers published in a volume of a scientific event indexed in ISI Proceedings

[1] Niculescu M., Andrei L., Cristescu A., *Generation of non-circular gears for variable motion of the crank-slider mechanism*, 7TH International Conference on Advanced Concepts In Mechanical Engineering, IOP Conf. Series: Materials and Engineering, Volume 147, Number 1, 2016, ISSN: 1757-8981.

B. Scientific papers published in magazines indexed by BDI

[2] Niculescu M., Andrei L. *Meshing analysis in case of non-circular gears designed for the nails forming kinematics optimization* , Annals of ”Dunărea de Jos ” University of Galați, Fascicle V, Technologies In Machine Building, 2016, Galati University Press, ISSN 1221-4566;
[3] Niculescu M., Andrei L., *Non-circular gears with transmission ratio as hybrid function*, Bulletin of the Transilvania University of Braşov, Vol. 9 (58), Series I, No.2, 2016, pag. 181-189, Transilvania University Press, ISSN 2065-2119;
[4] Cristescu A., Niculescu M., Andrei L.,*The Influence of Kinematics Variation on multispeed gears meshing*, Innovative Manufacturing Engineering 2015, Applied Mechanics and Materials Vols. 809-810, 2015, pag. 962-967, ISSN: 1662-7482.

C. Scientific papers published in the volumes of international conferences

[5] Niculescu M., Andrei L., *Using non-circular gears for the unloading door kinematics modification*, 21st Innovative Manufacturing Engineering & Energy International Conference (IManE&E 2017), Matec Web Conf., Volume 112, 2017.

D. Patent applications

[6] Niculescu M., Andrei L., *Angrenaj necircular pentru modificarea cinematicii maşinii de confecţionat cuie* –patent invention request in national A/00586/22.08.2017;
[7] Niculescu M., Andrei L., *Angrenaj necircular pentru modificarea cinematicii uşilor de descărcare ale cuptorului de încălzit ţagle* – patent invention request in national A/00585/22.08.2017.

REFERENCES

[1] *,** http**://**www.universalleonardo.org
[2] Burmester L., *Lehrbuch der Kinematik,* 1888, , Leipzig, Arthur Felix Verlag;
[3] Glober C., Hyman E., *Rollcurve Gears*, Transactions of ASME, 1939,61, 223-231;
[4] Boyd W., *Elliptical gears provide feed control*, Machine Design, 1940,12;
[5] Fellows E.R., Edwin R., *Gear generating cutting machine*, United States patent 1516524, 1924;
[6] Bopp & Reuther Gmbh, *Improvements in or relating to milling toothed gears*, Patent No. DE668897, also published as GB 531563, 1938;
[7] Litvin F., Ketov C. F., *Planetary reducer*, USSR Certificate of Invention, 1949;
[8] Litvin F., et. al., *Generation of Noncircular Gear by Enveloping Proces*, USSR Certificate of Ivention,1949 to 1951;
[9] Litvin F., Noncircular Gears: Design, Theory of Gearing and Manufacture, 2nd edn., Gos Tech Isdat, Leningrad, Moscow (in Russian), 1956;
[10] *,** http**://**www.gearshub.com
[11] *,** http**://** www.cunningham-ind.com
[12] *,** http**://**www.maplesoft.com
[13] Litvin F., Alfonso Fuentes Aznar, et. al., *Noncircular Gears Design and generation,* Cambridge University Press, 2009;
[14] Riaza Q., ş.a., *The synthesis of an N-Lobe noncircular gear using Bézier and B-Spline nonparametric curves in the design of its displacement law*, Journal of Mechanical Design, Vol. 12;
[15] Tsay Ming-Feng, Fong Zhang-Hua, *Study on the generalized mathematical model of noncircular gears,* "Mathematical and computer modelling", Vol. 41, 2005;
[16] Mundo D., *Geometric design of a planetary gear train with noncircular gears,* Mechanism and machine teory, Vol 42, 456-472, 2006 ;
[17] Ceccarelli M., et.al., *Numerical and experimental analysis of non-circular gears and cam-follower systems as function generators*, Mechanism and Machine Theory, Vol. 43, 2008, 996-1008;
[18] Mundo D., Gatti G., Dooner D.B., *Combined syntesis of five-bar linkages and non-circular gears for pieces path generation*, 12th IFToMM World Congress, Besancon (France), June 18-21, 2007;
[19] Liu, J-Y, et.al., *Study on the use of a noncircular gear train for the generation of figure-8 patterns*, Proc. IMechE, Vol. 220, part C, 2006;
[20] Mckinley J.R., ș.a. *Planar motion generation incorporating a 6-link mechanism and non-circular elements*, ASME 29th Mechanism and Robotics Conference, 2005;
[21] Bair B., et.al., *Mathematical model and characteristic analysis of elliptical gears manufactured by circular-arc shaper cutters*, Journal of mechanical design, Vol. 129/211, 2007;
[22] Bair B., et.al.,*Tooth profile generation and analysis of oval gears with circular - arc teeth*, Mechanism and machine theory, Vol. 44, 1306-1317, 2009;
[23] Yan Jia et. al., *On the generation of analytical noncircular multilobe internal pitch curves*, Journal of mechanical design, Vol 130, 2008;
[24] Vasie M., Andrei L., *Noncircular Gear Design and Generation by Rack Cutter,* The Annals of "DUNĂREA DE JOS" University of Galați, Fascicle V, Technologies in Machine Building, ISSN 1221-4566, 2011;

[25] Vasie M., Andrei L., *Analysis of Noncircular Gears Meshing,* Mechanical Testing and Diagnosis, ISSN 2247 – 9635, Volume 4, 70-78, 2012;
[26] Vasie M., Andrei L., *Technologies for Non-Circular Gear Generation and Manufacture,* The Annals "Dunărea de Jos" of Galați, Fascicle V, Technologies in Machine Building, ISSN 1221-4566, 2010, 167;
[27] Figliolini G., Angeles J., *Synthesis of the Base Curves For N-Lobed Elliptical Gears*, Journal of mechanical design, 125 (2005) 997-1005.
[28] Lozzi A., *Non-circular gears-graphic generation involutes and base outlines*, Proceedings of the Institution of Mechanical Engineers, 214 (2006).
[29] Litvin F., ș.a., *Generation of planar and helical elliptical gears by application of rack-cutter, hob, and shaper*, Comput. Methods Appl. Mech. Eng., 196 (2007) 4321–4336.
[30] Litvin F. et.al., *Design and investigation of gear drives with non-circular gears applied for speed variation and generation of functions*, Comput. Methods Appl. Mech. Eng., 197 (2008) 3783–3802.
[31] Chang L., Tsay C.B., *Computerized Tooth Profile Generation and Undercut Analysis of Gears Manufactured With Pre-Shaving Hobs*, Appl. Mech. Mater., 16–19 (1996) 1278–1282.
[32] Figliolini G., Angeles J., *The Synthesis of Elliptical Gears Generated by Shaper-Cutters*, Journal of mechanical design, 125 (2003) 793-801.
[33] Quintero H. F., et.al., A*n analytical model for the tooth profile generation of noncircular gear*, *12th IFToMM World Congress*, 2007.
[34] Xia J., et.al., *Noncircular Bevel Gear Transmission With Intersecting Axes*, Journal Mech. Des., 130 (2008) 545-551.
[35] Bair B.W., et.al., *Mathematical Model and Characteristic Analysis of Elliptical Gears Manufactured by Circular-Arc Shaper Cutters,* Journal of mechanical design, 129 (2007) 210-214.
[36] Bair B. W., *Computer aided design of elliptical gears with circular-arc teeth*, Mechanism and Machine Theory, 39 (2004) 153–168.
[37] Bair B. W. et. al., *Tooth profile generation and analysis of oval gears with circular-arc teeth*, *Mech. Mach. Theory*, 44 (2009) 1306–1317.
[38] Jian Gang Li, et.al., *Numerical computing method of noncircular gear tooth profiles generated by shaper cutters,* "Int. J. Manuf. Technol", Vol. 33, 1098-1105, 2007.
[39] Vasie M., *Cercetări privind roțile dințate cu transmitere variabilă a mișcării*, Universitatea "Dunărea de Jos" Galați, 2012
[40] Vasie M., Andrei L., *Design And Generation Of Noncircular Gears With Convex-Concave Pitch Curves,* The Annals of Dunarea Jos University of Galati, Fascicle V (2012) 55–60..
[41] Danieli G. A., *Analytical Description of Meshing of Constant Pressure Angle Teeth Profiles on a Variable Radius Gear and its Applications*, Journal of mechanical design, 122 (2000) 203-217.
[42] Danieli G. A., Mundo D., *New developments in variable radius gears using constant pressure angle teeth*, Mechanism and machine theory, 40 (2005) 203–217.
[43] Laczik B., et.al., *A New Approach for Designing Gear Profiles using Closed Complex Equations The Method of Gear Profile Generation*, Acta Polytechnica Hungarica, 11 (6) (2014) 159–172.
[44] Gao S., et.al., *Design and analysis of shapes of elliptic gears*, 12th International Conference on Geometry and Graphics, 2006.
[45] Zarebski I., Salacinski T., *Designing of non-circular gears*, The archive of mechanical engineering, LV (2008) 275–292.
[46] Lin C., *Design and Manufacture of Noncircular Bevel Gears*, 13th World Congress in Mechanism ans Machine Science, Guanajuato, Mexico, 2011;

[47] Jing L., *A Pressure Angle Function Method for Describing Tooth Profiles of Planar Gears*, Journal of mechanical design, 131 (2009) 051005-1 - 051005-8.
[48] Zhao Y., *Planar unfolding algorithm of noncircular bevel gears*, China Mech. Eng., 19 (17) (2008) 2046–2049.
[49] Li S., *Effects of machining errors, assembly errors and tooth modifications on loading capacity, load-sharing ratio and transmission error of a pair of spur gears*, Mechanism and Machine Theory, 42 (2007) 88–114.
[50] Li S., *Effect of addendum on contact strength, bending strength and basic performance parameters of a pair of spur gears*, Mechanism and Machine Theory, 43 (2008) 1557–1584.
[51] Mundo D., Danieli G. A., *Use of the Non-Circular Gear in Pressing Machine Driving Systems,* Mechanical Department, University of Calabria, Italy;
[52] Doege E., Bohnsach R., *Press Concept forthe Future in Precision Forging*, Advanced Technology of Plasticity, Proceedings of the 6thICTP, Nurenberg, 1999, pp.203-210;
[53] Doege E., Hindersmann M., *Optimize Kinematics of Mechanical Presses with Non-Circular Gears*, Annals of the CIRP, Vol. 46/1, 1997, pp.213-216;
[54] Yokoyama T., Takahashi K., *Driving apparatus for powder compacting* press US Patent 4662234,1987;
[55] Quintero H. F., Romero C. A. and Vanegas Useche L. V., *Thermodynamic and dynamic analysis of an internal combustion engine with a noncircular-gear based modified crank-slider mechanism*, 12th IFToMM World Congres Besançon (France), June 18-21 2007;
[56] Mundo D., Danieli G.A., ș.a. *Generation of Variable Radius Elliptical Helical Gears and Experimental Results*, The 11th World Congress in Mechanism and Machine Science, 2004;
[57] Figlioni G., et.al., *Synthesis of Non-Circular Gears*, Proceedings of the International Conference on Gearing, Transmission, and Mechanical Systems*,* Professional Engineering Publishing, 2000;
[58] Takahiro Yamada, et. al., *Vehicle window regulator*, United States Patent 4998379*;* Mar 12 1991;
[59] Nolta J.P., *Constant to variable gear pitch for temperature door rotation*, United States Patent US 2014/0000397 A1, Ian 2 2014;
[60] Vonhausen G., *Valve actuator*, United States Patent 4638977*,* Jan 27 1987*;*
[61] Sugiyama T., *Engine starter apparatus*, United States Patent 5111707, May 12 1992;
[62]. Infanger A. W., Brownlie A. W.,*Steering System,* US Patent 3823617, 16.07.1974;
[63] Emura T., Arakawa A., *A new steering mechanism using noncircular gears*, The Japan Society of Mechanical Engineers International Journal Series III Vol. 35 No. 4, 1992, 604-610;
[64] Johnson K. M., *Power transmission assembly*, United States Patent 4262233, Apr.14 1981;
[65] Freudenstein F, *Intermittent motion mechanism employing non-circular gears,* US Patent 3424021, 28.01.1969;
[66] Matsuda Yasuhiko, *Intermittent drive mechanism* , US Patent 4756203, 12.07.1988;
[67] Russell F. S., Simonelli R. J, *Wire coiling machine*, US Patent 4372141, 08.02.1983*;*
[68] Yazar Mehmet, Ozdemir Ahmet, *Comparative analysis of the pressure variations and the flow rates of a hydraulic pump made of a pair of elliptical and cylindrical spur gear,* Technology, Volume 14(1), 1-10 (2011), Gazi University, Institute of science and technology, Department of mechanical education, Ankara;
[69] Kowalczyk L., Urbanek S. *The Geometry and Kinematics of a Toothed Gear of Variable Motion,* FIBRES & TEXTILES in Eastern Europe July / September 2003, Vol. 11, No. 3 (42);
[70] Urbanek S.,*Geometrical analysis of the rolling lines of non-circular pinions of the elliptical type with consideration of selected kinematic and design demands*, Technical University of Łódź, 1967, Ph.D. Dissertation (in Polish);
[71] Proiect nr. MCC337, CCCPFTT Câmpia Turzii, *Mașina de confeționat cuie MCC 337;*

[72] Cristescu A., Niculescu M., Andrei L., 2015, *The Influence of Kinematics Variation on Multispeed Gears Meshing*, Trans Tech Publications, Switzerland Applied Mechanics and Materials Vols. 809-810 (2015) pp 962-967,

[73] Cristescu B., Andrei L., Cristescu A., *Analytical generation of involute flanks of noncircular gear tooth,* The Annals of "Dunarea Jos" University of Galati, Mathematics, Physics, Theoretical Mechanics, Fascicle II Year VI (XXXVII), 2014, v 1 pp 36-43 104–110;,

[74] Cristescu A., Andrei L., Cristescu B., *Influence of tooth profile on the noncircular gear tooth contact*, 13TH International Conference on Tribology (ROTRIB'16), IOP Conference Series – Materials Science and Engineering, vol. 174, 2017, ISSN: 1757-8981

[75] Stăncescu C., *Modelare parametrică și adaptivă cu Inventor*, Efitura Fast , 2014;

[76] Stăncescu C., et.al., *Proiectare Asistată cu Autodesk Inventor* – Îndrumar de laborator, Editura Fast , 2012;

[77] Man &Machine, *Autodesk Inventor* - Note de curs , 2016;

[78] Finkelstein E., *AutoCAD 2004*, Editura Teora, 2004 ;

[79] Stăncescu C., *AutoLISP Manual de programare*, Editura Fast 2000, București , 1996;

[80] G. Rădulescu, et.al., *Îndrumar de proiectare în construcția de mașini*. București: Editura Tehnică, 1986;

[81] G. Buicliu, et.al.., *Manualul inginerului*. București: Editura Tehnică, 1955;

[82] Tabără V., Tureac I., *Mașini pentru prelucrări prin deformare* , Editura didactică și pedagocică, București, 1984;

[83] Ciocârdia C., et.al., *Tehnologia presării la rece*, Editura didactică și pedagocică, București, 1991;

[84] Teodorescu M., et.al., *Elemente de proiectare a ștanțelor și matrițelor*, Editura didactică și pedagocică, București, 1983;

[85] Iliescu C., *Tehnologia presării la rece*, Editura didactică și pedagocică, București, 1984;

[86] Tschaetsch H., *Metal Forming Practice – Processes*, Machines, Tools, *Springer-Verlag Berlin Heidelberg*, 2006;

[87] Cristescu B., *Studii privind elemente de proiectare și generare a angrenajelor necirculare*, Teza de doctorat, Galați, 2016;

[88] Proiect IPROLAM nr. 505.30-012, *Dispozitiv de ridicare a ușilor de descarcare,* 1977.

[89] Ghiţă E., *Teoria şi tehnologia suprafeţelor poliforme*, Published by BREN, Bucureşti, 2001, ISBN 973–8143–07–1.